Chemical Engineering Journal 480 (2024) 147963

Contents lists available at ScienceDirect

Chemical Engineering Journal

journal homepage: www.elsevier.com/locate/cej

Review

Recent progress in molybdenum disulfide (MoS_2) based flexible nanogenerators: An inclusive review

Mayuri Srivastava [a], Swagata Banerjee [b], Satyaranjan Bairagi [d,*], Preeti Singh [b,e], Bipin Kumar [a,b], Pushpapraj Singh [a,c], Ravindra D. Kale [e], Daniel M. Mulvihill [d,*], S. Wazed Ali [a,b,*]

[a] School of Interdisciplinary Research, Indian Institute of Technology Delhi, Hauz Khas, New Delhi 110016, India
[b] Department of Textile and Fibre Engineering, Indian Institute of Technology Delhi, Hauz Khas, New Delhi 110016, India
[c] Centre for Applied Research in Electronics, Indian Institute of Technology Delhi, New Delhi, India
[d] Materials and Manufacturing Research Group, James Watt School of Engineering, University of Glasgow, Glasgow G12 8QQ, UK
[e] Fibres & Textile Processing Technology, Institute of Chemical Technology, Mumbai, India

ARTICLE INFO

Keywords:
Flexible nanogenerators
MoS_2
Piezoelectric nanogenerators
Triboelectric nanogenerators
Thermoelectric nanogenerators
Renewable energy

ABSTRACT

Energy consumption and structure have changed in the new era along with the growth of the Internet of Things (IoT) and artificial intelligence, and the power sources for billions of dispersed gadgets and sensors have sparked attention globally to protect the environment. Due to the rising usage of non-renewable energy sources and the resulting environmental damage, researchers are investigating alternative energy systems that can harness energy from the environment. Therefore, self-sufficient small-scale electronic systems will be possible through the use of underutilised natural waste energy sources collected in nanogenerators (NGs). The features of the materials used have a significant impact on how well NGs work. In this regard Molybdenum disulfide (MoS_2), a 2D material, is one of the compounds that is discussed vastly nowadays due to its exceptional characteristics that made it useful in a variety of applications. Many research papers on the advancement and implementation of MoS_2 materials have been published, but this article will give an in-depth overview. It offers an introduction and interpretation of the main properties of 2D MoS_2 nanomaterials, starting with their current state, properties, and various synthesis processes. Later, the review concentrates on MoS_2 applications and energy-harvesting capabilities and gives a comprehensive study of piezoelectric, triboelectric and thermometrical nanogenerators based on 2D MoS_2 nanocomposite materials.

Abbreviations: 2D, 2 Dimensions; MoS_2, Molybdenum disulphide; IoT, Internet of Things; NGs, Nanogenerators; ZnO, Zinc Oxide; GaN, Gallium Nitrate; PbZrTiO3, Lead Zirconate Titanate; BaTiO3, Barium Titanate; GO, Graphene Oxide; *g*-C_3N_4, Graphitic Carbon Nitride; *h*-BN, Hexagonal Boron Nitride; TMDCs, Transition metal di-chalcogenides; $SLMoS_2$, Single-layer molybdenum disulphide; S, Sulphur; Mo, Molybdenum; PL, Photoluminescence; eV, Electron volts; PDMS, polydimethylsiloxane; PI, Polyimide; UTS, Ultimate tensile strength; $MoSe_2$, Molybdenum diselenide; WS_2, Tungsten disulphide; TiS_2, Titanium (IV) Sulfide; $TaSe_2$, Tanatlum diselenide; NMP, N-methyl-pyrrolidone; n-BuLi, n-Butullithuim; Li, Lithium; RF, Radio-frequency; C60, Fullerene; VPD, Vapor deposition; PVD, Physical vapor; CVD, Chemical vapor deposition; ALD, Atomic layer deposition (ALD); MoO_3, Molybdenum trioxide; HER, Hydrogen Evolution Reaction; ALD, Atomic layer deposition; $MoCl_5$, Molybdenum(V) chloride; H2S, Hydrogen Sulfide; $Mo(NMe_2)_4$, Molebdenum Nucleoside diphodphate kinase B; Si, Silicon; Al_2O_3, Aluminium oxide; TENGs, Triboelectric nanogenerators; TEG, Thermoelectric nanogenerator; PENGs, Piezoelectric nanogenerators; NW, Nanowire; LEDs, Light-emitting hydroxides; TMDOs, Transition metal dioxides (TMDOs); PVDF, Poly(vinylidene fluoride); $ZnSnO_3$-, Zinc Tin oxide; ET, Ethidium bromide; Y, Eosin Y; P(VDF-TrFE, Polyvinylidene fluoride-trifluoro ethylene; TOCN, TEMPO-oxidized cellulose nanofibril; PZT, Lead Zirconate Titanatee; LiNbO3, Lithium Niobate; DFT, Density Functional Theory; PET, Polyethylene Terephthalate; TOCN, (2,2,6,6-tetramethylpiperidine-1-oxyl)TEMPO-oxidized cellulose nanofibril; BTO, Barium Titanatee; VOC, Open-circuit voltage; PU, Polyurethane; CNT, Carbon nanotube; LPE, liquid phase exfoliation; PS, Polystyrene; PPy, Polypyrrole; AFM, Atomic force microscope; QSs, Quantum sheets; TFTs, Thin-film transistors; FETs, Field-effect Transistor; LOP, Low operating power; PDMS, Polydimethylsiloxane; PTENG, Photo thermoelectric nanogenerator.

* Corresponding authors at: Materials and Manufacturing Research Group, James Watt School of Engineering, University of Glasgow, Glasgow, G12 8QQ, UK. (Satyaranjan Bairagi and Daniel M. Mulvihill); Department of Textile and Fibre Engineering, Indian Institute of Technology Delhi, Hauz Khas, New Delhi-110016, India (S. Wazed Ali).

E-mail addresses: Satyaranjan.Bairagi@glasgow.ac.uk (S. Bairagi), Daniel.Mulvihill@glasgow.ac (D.M. Mulvihill), wazed@iitd.ac.in (S.W. Ali).

https://doi.org/10.1016/j.cej.2023.147963
Received 6 October 2023; Received in revised form 2 December 2023; Accepted 6 December 2023
Available online 12 December 2023

1. Introduction

The energy, resource, and environmental concerns that people face is becoming increasingly significant as modern civilization grows [1]. Traditional non-renewable energy sources have limited supply and damage the environment when they are used [2]. The environment is emitting more carbon as a result of rising energy demand, and the scarcity of fossil fuels has increased demand for green and renewable energy production. Harvesting renewable energy is a fantastic way to meet the energy needs of future generations and mitigate climate change [3]. The advancement of renewable energy-generating technologies is essential for promoting sustainable economic growth and safeguarding the environment. The majority of electronic devices use batteries, which must occasionally be recharged or replaced [4].

Although batteries are the most established and effective technology, they are not appropriate for Internet of Things (IoT) applications due to their weight and price and also it would be difficult to track, replace, and recycle every one of the billions of batteries that are in use globally and have a limited lifespan. To make the Internet of Things (IoT) a reality, it is thus necessary to incorporate a nanogenerator that converts mechanical energy from human motions into electrical energy [5]. Nanogenerators have been created to harvest ambient mechanical energies, which are thought of as waste energies (e.g., turbulence, human motion, vibration, etc.), and use them for self-sufficient power systems that can do away with batteries and can eliminate harmful harvesting equipment with little to no maintenance [6]. The process of turning friction into electricity allowed for the beginning of mechanical energy harvesting in the late 1700 s.Through the creation of the electromagnetic generator, Wimshurst machine (static electricity), and Van de Graaff generator, these findings were later commercialized in the 19th century. However, throughout the past century, mechanical energies have not been the focus of energy-scavenging technology. The development of nanogenerators has only recently witnessed a spike due to the appearance of highly specialized nanotechnologies and methodologies. Through the

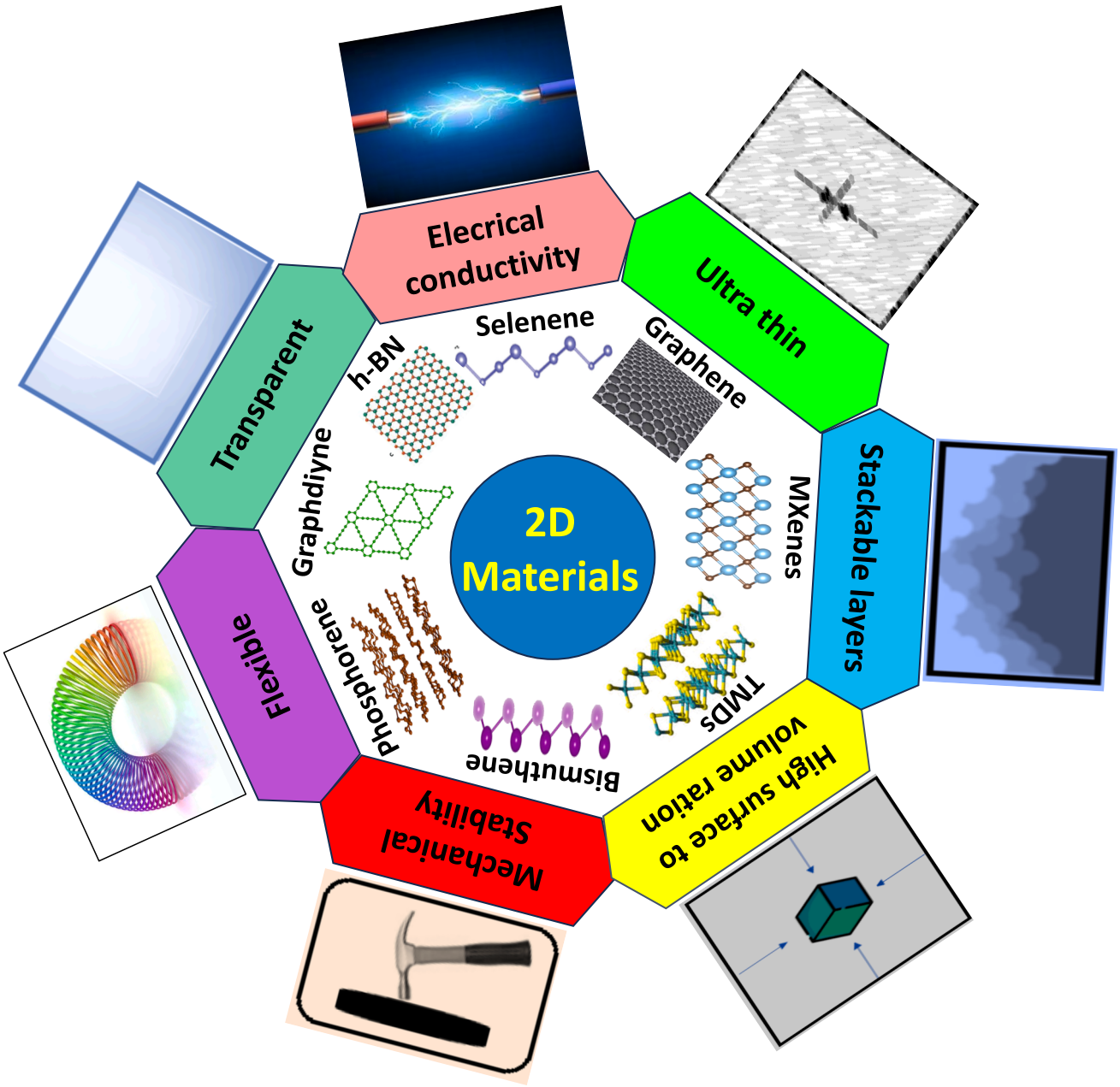

Fig. 1. Schematic representation of 2D materials with their characteristics.

use of pyroelectric, triboelectric, and piezoelectric processes, nanogenerators transform mechanical forces into electrical energy. Vibration, solar, and thermal sources are among the environmental energy harvesting sources that have grown significantly. This is mostly because they are more reliable, efficient, and stable overall in the system [7,8].

Several semiconductor nanostructured materials, including ZnO [9], GaN [10], and insulating materials, like PbZrTiO3 [11] and BaTiO3 [12] have been created to replace conventional batteries. These materials have high piezoelectric charge coefficients, which equate to high output voltage. Due to their electronic structures, chemical, electrical, and optical properties, 2D materials have also piqued a lot of interest in this respect [13]. Materials with an exceptionally thin layered crystalline structure that exhibit Van der Waals bonding in the interlayer and covalent bonding in the intralayer are referred to as two-dimensional nanomaterials. Owing to quantum confinement, 2D nanomaterials have a high surface area to volume ratio, atomically thin structure, and unique properties that distinguish them from their bulk form. These materials offer excellent performance in energy conversion and storage, and potential environmental applications for graphene-based materials include membrane-based dissociation, adsorptive pollutant removal, photocatalytic oxidation, sensors. Attributed to their significant precise surface area and riveting characteristics (Fig. 1) that are usually inaccessible in high volume or bulk forms, two-dimensional (2D) such as graphene-based nanomaterials, particularly immaculate graphene and graphene oxide (GO), as well as reduced GO, has piqued the interest of researchers. Environmental applications for graphene-based nanomaterials include adsorptive pollutant removal, photocatalytic oxidation, sensors, and membrane-based dissociation [14,15].

Driven by graphene, a wide range of 2D nanomaterials, including monoelemental and multicomponent objects like transition metal dichalcogenides, have been discovered in exponential growth [16], graphene-analogous graphitic carbon nitride (*g*-C_3N_4) [17], hexagonal boron nitride (*h*-BN) [18], phosphorene [19], perovskites [20], transition metal carbides/nitrides (MXenes); [21–23], group IVA and group VA monoelements Xenes [24,25] such as graphdiyne [26–28], bismuthine [29,30] Selenene [31–33] and so on are highly sought-after for a variety of fascinating uses that stem from their distinctive optical, electrical, and catalytic characteristics.[34] for example, recycling solar power (photovoltaic cells, perovskites, photocatalysis) [35], energy recovery via mechanical means (triboelectric and piezoelectric devices) [36], process of recovering heat (thermoelectric and pyroelectric systems) [37] and recycling chemical energy, for example, producing electricity through osmosis [38]. In order to generate power for handheld electronic devices that can harness human energy for a variety of practical uses, including as motion detection and code transmission. 2D nanomaterial-based nanogenerators may prove to be an appealing option [39].

Since the article's main application section is based on the research about fabrication of (piezo-, tribo-, and thermo-eletcric) nanogenerators, we have concentrated on molybdenum disulfide (MoS_2) because of its exceptional combination of properties. It is superior to other 2D materials, such as graphene, MXene, Xene, and hexagonal boron nitride (h-BN), among others, for the creation of nanogenerators. Its ability to convert mechanical stress into electrical energy, a necessary quality for effective nanogenerator performance, is one of its main advantages. The direct bandgap and semiconducting characteristics of MoS_2 are essential for managing the electrical charge flow in nanogenerator devices. Its layered nature also makes it simple to exfoliate into thin layers, which makes it easier to create the thin films and nanostructures that are essential for designing nanogenerators. MoS_2 must possess both mechanical strength and flexibility in order to endure mechanical deformations that occur during energy conversion operations. MoS_2′s tunable characteristics, which can be adjusted for thickness, flaws, and doping, give the material flexibility in meeting different nanogenerator needs. Additionally, MoS_2 shows compatibility with other materials that are frequently utilised in nanogenerator devices, guaranteeing efficient integration with substrates and electrodes [40]. The article then goes on to describe in full the introduction, characteristics, development, and range of uses of molybdenum disulfide nanoparticles.

Molybdenum disulfide (MoS_2), a 2D transition metal dichalcogenide, stands as an attractive and promising 2D material with numerous phenomenal physical, chemical, physiological, and photoelectronic transistors and photodetectors, that vary considerably from those of graphene-based nanomaterials, conceivably paving the means for new ecologically aware factors and applications [41,42]. MoS_2 nanosheets, which have previously been shown to have been used in the disciplines of electronics, enzymes, biomedicine like patchable and implantable devices, and energy, are anticipated to have a variety of uses in the environment [43,44]. Indeed, bulk MoS_2 has long been thought to be useful as environmental catalysts and adsorbents because it occurs naturally as the abundant mineral molybdenite [45]. Methodology for disassociating MoS_2 monolayer or very few constituents from bulk quantities and generating mass amounts of MoS_2 nanosheets with distinctive attributes to nanosized materials become accessible. Since then, Molybdenum disulfide (MoS_2) has been one of the transitions metal di-chalcogenides (TMDCs) that has demonstrated remarkable behaviour in terms of synthesis, properties, functionalization, and tuning [46]. Single-layer molybdenum disulfide ($SLMoS_2$) displays superior properties when it reaches the nanoscale. The direct band gap implies a faster rate of electron and hole generation/recombination and, as a result, high mobility of electrons exists [47]. It has a high refractive index, $n = 4.7739$, according to Beal and Huges (1979) [48]. As a result, it can be used as a solid lubricant in optical electronics and chemical coating materials. It is widely used as a drought-stricken lubricating oil due to its low coefficient of friction and ruggedness. $SLMoS_2$ has a low reactivity. Dilute acids and oxygen have no effect on it [49,50]. It has high elasticity and a low pretension. Furthermore, the very flimsy framework of MoS_2 presents some difficulties in optoelectronics applications, as single-layer sheets reflect 100 % of incident photons [51,52].

In this review, we present a thorough overview of MoS_2 (in both bulk and single-layer form), reviewing significant previous literature focusing on their structure, characteristics, fabrication techniques, and MoS_2 applications as a flexible piezoelectric, triboelectric and thermoelectric nanogenerators for energy harvesting [53]. In order to better understand their architectures, we first categorize the MoS_2 nanostructures into three different forms or polytypes. The crystalline anisotropy of individual sandwiched S-Mo-S layers and their many properties, such as activity, resistance, catalytic, photosensitive, and electrical properties, are investigated. Wide-ranging synthesis methodologies employing physical and chemical techniques are then described. Additionally, a focus is placed on their techniques of manufacture, as well as their varied chemical and physical characteristics and applicability. Then, several significant recent advancements and future research directions for materials based on MoS_2 employed in energy harvesting applications are also emphasized. We anticipate that this analysis will aid and motivate the future research and development of MoS_2-based materials and devices. Fig. 2 represents MoS_2 materials based piezoelectric, triboelectrically and thermoelectrical nanogenerators.

2. Properties of MoS_2

Molybdenum disulfide (or moly) is a molybdenum and sulphur inorganic compound with a chemical formula denoted as 'MoS_2'. The compound belongs to the transition metal dichalcogenide class. Molybdenum is a transition metal with a partly filled 'd-shell', that accounts for its chemical stability and versatility in compound synthesis [56]. Metal-disulfide compounds and nanocomposites are identically enticing for an extensive range of mechanical, electrical, and other applications because disulfides have strong S-S bonds [57].

It can also be used as a potential replacement for graphite in high-vacuum application fields, but it has a lower maximum operating

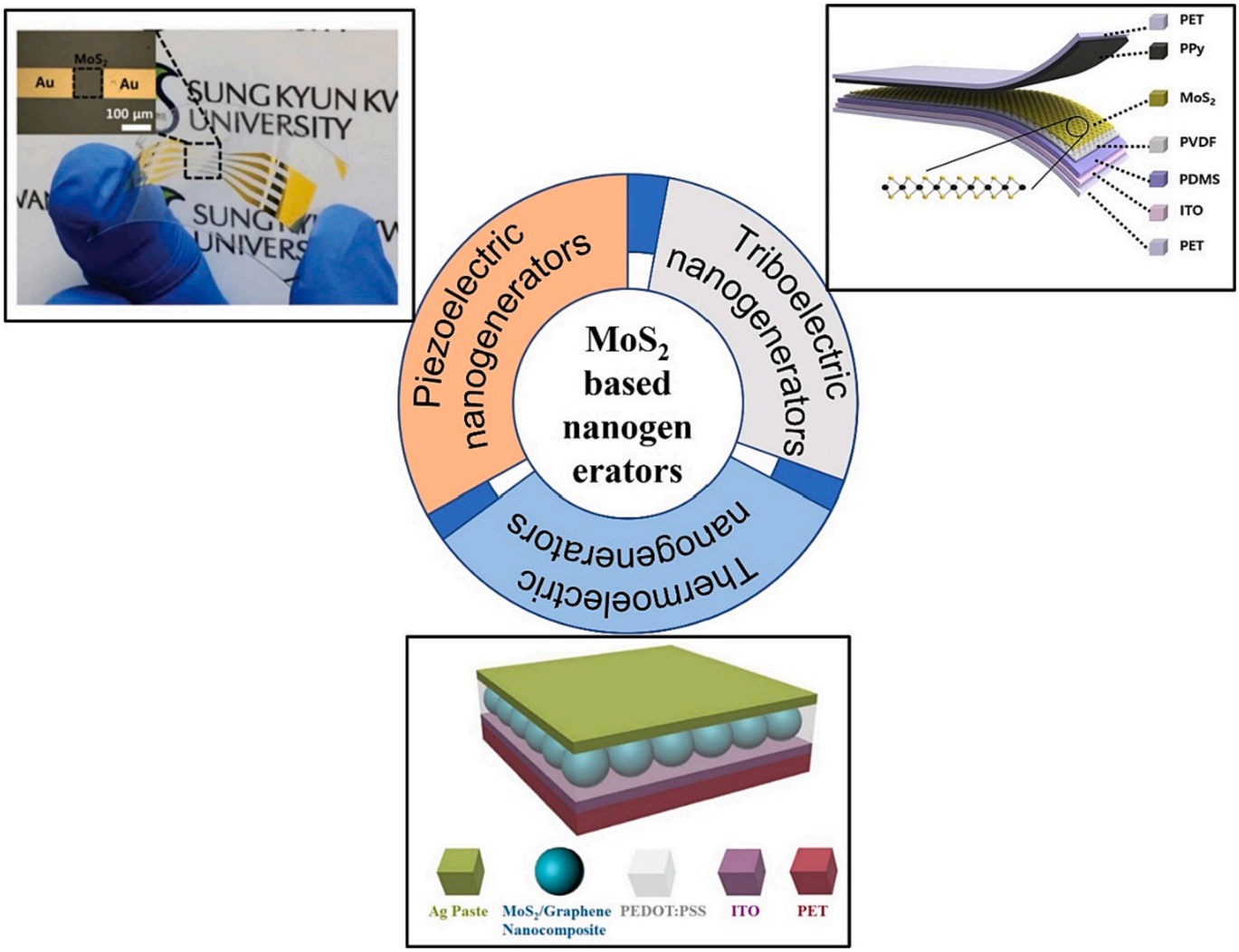

Fig. 2. MoS_2 based flexible nanogenerators [54,55]. All essential copyrights and permissions received.

temperature than graphite [58,59]. The physical appearance, structure, optical and electrical, chemical, thermal, and mechanical properties of MoS_2 are discussed below.

2.1. Physical appearance and structural properties

Molybdenum disulfide (MoS_2), a bright-coloured black solid, which is the primary molybdenum ore, consists of a crystal structure of a hexagonal plane of Sulphur (S) atoms on either side of a hexagonal plane of Molybdenum (Mo) atoms. To create the two-dimensional sheets of MoS_2, the three planes stack up on top of one another, locked together by solid covalent connections existing in-between the Mo and S atoms [60 61]. The crystal phases of bulk MoS_2 crystal can be found in a variety of forms depending on the different synchronisation of the Mo atom, such as 1 T MoS_2, 2H MoS_2, and 3R MoS_2 and the structure of the 3 polymorphs is shown in Fig. 3**.** [62,63]. In these polymorphs, the first digit represents the number of monolayers in a unit cell, while the last three letters, T, H, and R, stand for trigonal, hexagonal, and rhombohedral, respectively, to denote structural symmetry [64,65]. These phases are distinguished by their own features that result from changes in layer symmetry. With its deformed octahedral symmetry, the 1 T triagonal phase is known for its metallic behaviour, which promotes effective electrical conductivity. On the other hand, the hexagonal 2H phase features a band gap that affects its electrical characteristics and is semiconducting. With its rhombohedral symmetry and rotational stacking, the 3R phase similarly demonstrates semiconductor capabilities; but, because of the unique layer arrangement, its specific properties differ. These structural variations affect piezoelectric characteristics in addition to electrical conductivity. The unique layer symmetries connected to each phase affect MoS_2's capacity to produce electric charge in response to mechanical stress [66].A material's band structure can be significantly altered by reducing its thickness to one or even a few atomic layers. Based on the thickness it is demonstrated by some research groups that band gap of 1 T phase of MoS_2 exist with 1.8 to 2.1 eV while 2H and 3R phase consist of 1.2–1.3 eV and 1.416 eV respectively [67]. Monolayer MoS_2, for instance, differs from its bulk form in that it has a direct band gap, which makes it potentially valuable for applications in piezoelectric electronics and optoelectronics. Thus, surface alterations, such as the addition of atoms and defects that result in surface ferroelectricity and piezoelectricity, can significantly change the piezoelectric characteristics of 2D materials [68]. For electronics and energy-based reactions, most of the studies are done in 2H and 1 T MoS_2 phases [69]. Table 1 represents the contrast among the three polytype structure of MoS_2.

2.2. Optical properties

This includes band gap, reflectance, transmittance, emittance, absorptance, and index of refraction [70,71]. $SLMoS_2$ has a direct band gap of about 1.8 eV with a very high sensitivity in photon detection

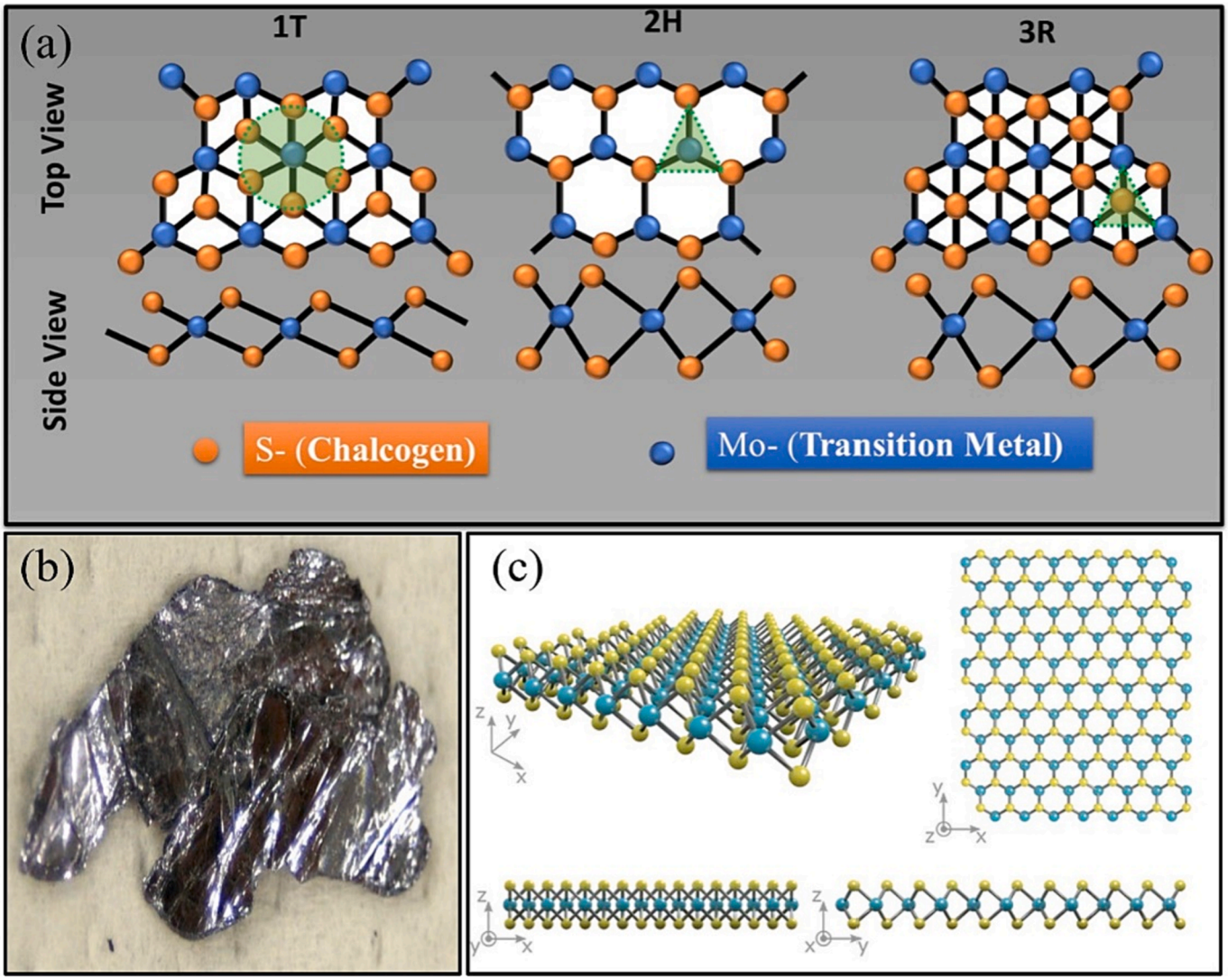

Fig. 3. (a) Representation of the 3 polytype structures 1 T, 2H and 3R MoS_2 from both (Top and side view), (b) Shiny silver black and grey sheet like structure of MoS_2, and (c) A layer of molybdenum atoms (in blue colour) is sandwiched between two layers of sulphur atoms (in yellow colour) in the crystal structure of monolayer MoS_2 [images reproduced from Molybdenum Disulfide (MoS_2): Theory & Applications]. All essential copyrights and permissions received. (For interpretation of the references to colour in this figure legend, the reader is referred to the web version of this article.)

Table 1
Represents the Contrast among the three Polytype structures of Molybdenum Disulfide.

MoS_2 Properties	MoS_2 Polytypes		
	1 T	2-H	3-R
Coordination	Octahedral	Trigonal Prismatic	Trigonal Prismatic
Space Group	P3m1	$P6_3/mmc$	R3m
Lattice Parameters	a = 5.60 A, c = 5.99 A & edge sharing octahedral	a = 3.15 A, c = 12.30 A	a = 3.17 Å, c = 18.38 A
Property	Paramagnetic & Metallic	Semiconducting	Semiconducting
Electrical Conductivity	10^5 times higher than the 2H phase	Low (~0.1 S m^{-1})	Low (~0.1 S m^{-1})
Band Gap	1.8–2.1 eV	1.2–1.3 eV	1.416
Absorption Peak	No peaks at 604 nm & 667 nm	Showed peaks at 604 nm & 667 nm	Showed peaks at 604 nm & 667 nm
Symmetry	Octahedral	Hexagonal	Rhombohedral
Stacking	AbC	AbABaB	AbABcBCaC
Application	Intercalation Chemistry	Dry lubricants	Dry lubricants & non-linear optical devices

resulting in higher penetration efficiency for incident light with high absorption coefficient. According to Lopez-Sanchez et al, the photo-responsivity of single layered MoS_2 can reach as high as 880 A/W for incident light at 561 nm, and the photo-response exists throughout the 400–680 nm range [72]. The electron-hole pair is effectively produced by photoexcited in doped $SLMoS_2$, which combines the doping-induced charges to generate two electrons and one-hole bonded states [73]. MoS_2 monolayers can absorb about 10 percent of the overall of incident light to photon energies just above the bandgap [74].

In direct band gap semiconductor material, Wannier-Mott excitons

(or, more correctly, excitonic polaritons) recombine to form the photoluminescence (PL) band, and the wavelength of irradiation is related to the band gap while taking the exciton binding energy into consideration [75,76]. The indirect band gap of a bulk MoS_2 crystal is observed as 1.29 eV [77].

Most notably, it is noted as a distinct characteristic of MoS_2, with variations in the MoS_2 layer's thickness resulting in variations in its bandgap. Because MoS_2 is a semiconductor, its electrical and optical properties are affected by the minimal energy needed for an electron to transit from the valence band to the conduction band. This energy difference occurs at a moment that is roughly 1.2 to 1.3 electron volts (eV) in bulk form. On the other hand, it changes from a bulk to a monolayer or few-layer semiconductor by decreasing its thickness. When MoS_2 is in monolayer form, it displays a direct band gap. Monolayer MoS_2 has a band gap value of between 1.8 and 2.1 eV. As the number of layers drops, the indirect to direct band gap steadily changes. The local levels, or localized states, within the band gap likewise decrease with decreasing thin film thickness. The energy band gap then rises as a result of this. MoS_2′s direct band gap considerably enhances its light-emitting characteristics, making it more advantageous for use in optoelectronics [69].

2.3. Electrical properties

For electronic operations like transistor performance, the electronic band structure is crucial. The electronic band gap specifies whether the material is having a zero-band gap (conductor), a moderate band gap (semiconductor), or having a large band gap (insulator) [78]. Owing to a small band gap, single layered MoS_2 is well-suited for transistor applications. It is well known that band gap plays a crucial role in electronic applications. Thus MoS_2′s band gap, like graphene's, can be modified by straining the material. A few research groups have reported that the increment of 300 meV and 1.2 eV in bandgap observed when 1 % biaxial and 1.5 % uniaxial tensile mechanical strain is applied in layered and bulk MoS_2 material respectively [7980].

Apart from that, this band gap is also influenced by the lateral electric field (can convert semiconducting structure to the metallic structure)[81]. MoS_2 is a non-direct band gap semiconductor in the bulk (and bilayer), it becomes a direct band gap semiconductor in the monolayer [82]. It should also be observed that the absence of inversion symmetry causes the symmetry of the monolayer (D3h point group) to be different from that of the bulk (D6h), encouraging investigation into the significant applications of MoS_2 to be used to produce piezoelectricity [83].

2.4. Mechanical properties

In structural applications of MoS_2, the mechanical properties play an important role. Having a good stiffness comparable with steel and a greater breakage toughness than adaptable polymers like polydimethylsiloxane (PDMS) and polyimide (PI) [84], make it suitable for flexible electronics MoS_2 is a sturdy semi-conducting material that can withstand up to 25 % elastic deformation before getting ruptured completely. Besides this, it has a larger intrinsic energy band gap and Seebeck coefficient than graphene [85,86]. Turning to Young's modulus and yield stress, MoS_2 has a reported Young's modulus of 270 ± 100 GPa and yield stress of 15 ± 3 N/m (23 GPa), which is similar to steel in the Bertolazzi et al. [87] study and E = 16.5 N/m, or E^{3D} = 210 GPa measured by another research group (Cooper et al. [88]). Recently Liu et al. [89] in his nano-indentation studies observed Young's modulus of around 170Nm^{-1}on chemical-vapor-deposited single layered MoS_2 while based on SW potential theory, it is predicted that the effective Young's modulus for single layered MoS_2 will be 139.5 Nm^{-1}. The in-plane stiffness of monolayer MoS_2 is 180 ± 60 Nm^{-1}. The MoS_2 breaking occurs at an effective strain of 6–11 % with a regular breaking strength of 15 ± 3Nm^{-1} (23GPa) [90]. M.B. Khan et.al. 2017, [91] studied the breaking strength of MoS_2 nanosheet disseminated in a polystyrene matrix and observed strength of around 48 GPa - twice the ultimate tensile strength (UTS) of MoS_2 nanosheets and enhanced substantially (∼×3) with a small addition of MoS_2 nanosheets (0.00002). The delocalized electrons of Mo are believed to be responsible for this unique behaviour [92]. Next the bending modulus (D) of $SLMoS_2$ is 9.61 eV, seven times that of graphene due to more interaction effects that restrict bending movement [93]. Another research group observed that a single layer of S atoms has a bending modulus of 1.75 eV. Using the 'geometric method' or 'thin shell theory' with the SW potential, it was determined to be 9.61 eV [94].

2.4.1. Buckling phenomenon

Buckling under uniaxial compression is important for nanodevices. It is frequently evaluated using phonon analysis and molecular dynamics simulation [95,9697]. The buckling critical strain is proportional to the layer length, as calculated by $c = L = 43.522$, and is comparable to theoretical values. The critical strain is temperature independent up to 50 K, it changes with the increase due to a thermally facilitated healing process like the one found in carbon materials [98]. Single-layered MoS_2 has a buckling critical strain twenty times that of graphene (19.7 in length is approximately 0.0068)[99].whereas the buckling critical strain for $SLMoS_2$ of the same length is 0.0094, which is one order higher than graphene, according to Jiang 2014′s simulation results. It implies that $SLMoS_2$ is more compressible than graphene due to a higher buckling critical strain, making it a better choice [100] for nanodevice applications.

2.5. Thermal properties

The thermal properties of a substance are those that relate to how effectively it transmits heat or in another way, they are the properties of a material when heated. Thermal energy can be transmitted by phonons or electrons in a material when there is a temperature gradient. Additionally, electronic thermal conductivity is crucial for metals [101]. Few-layer MoS_2 has a thermal conductivity of about 52 $Wm^{-1}K^{-1}$, lesser than thick graphene (1000 $Wm^{-1}K^{-1}$) layers, according to research by Sahoo et al. (2013)[102]. It is also observed that the thermal conductivity of MoS_2 has been measured to be 18.06 $Wm^{-1}K^{-1}$ measured along its plane and in the out of plane direction, it reduces to 4.17 $Wm^{-1}K^{-1}$ [103]. Layer exfoliation and restacking result in lattice mismatch, which lowers heat conductivity and increases phonon dispersion [104]. The exfoliated MoX_2 group make excellent candidates for thermally insulating solid lubricants due to their low heat conductivity [105]. A summary of the aforementioned properties of $SLMoS_2$ is tabulated below (Table 2).

3. MoS_2 synthesis

MoS_2 nanostructures have been synthesised by using a variety of techniques [Fig. 4], which can be split into two main groups: physical and chemical techniques. High-energy techniques such as microwave plasma, laser ablation, arc discharge, sputtering, pulsed-laser deposition, mechanical exfoliation, sputtering, epitaxy, plasma, etc. are commonly used in physical methods [111]. The MoS_2 nanostructures that were produced, however, are patchy and prone to aggregation, which could limit their surface areas and prevent further functionalization or dispersal. The disadvantage of this process is that it requires a high-purity raw material and it is difficult to destroy its original lattice structure. A variety of chemical routes have been reported, including metal–organic chemical vapor deposition, high-temperature transport, hydrothermal method, decomposition or annealing strategies, and solvothermal and sonochemical synthesis [112,113].

Table 2
The summary of $SLMoS_2$ properties.

SI. No.	Property (Reported)	Unit (S.I.)	Obtained Value	Reference
1.	Young's modulus	$N{\cdot}m^{-1}$	$E^{2D} = 180 \pm 60$ $E^{2D} = 335.0$ $E^{2D} = 120 \pm 30$ $E^{2D} = 170$ $E^{2D} = 139.5$	[87–89,106]
2.	Yield stress	$N{\cdot}m^{-1}$	$\sigma_{int} = 15 \pm 3$ $\sigma_{int} = 42.4$ $\sigma_{int} = 16.5$ $\sigma_{int} = 44.4$ $\sigma_{int} = 17.5$	[87,88,92,107,108]
4.	Bending modulus	eV	$D = 9.61$	[93]
5.	Buckling strain	$1/L^2$	−43.52	[100]
6.	ThermalConductivity	$W{\cdot}m^{-1}{\cdot}K^{-1}$	6 (L = 4 nm)2 (L = 120 nm)	[109,110]
7.	Electronic band	ev	parabolic; Band Gap(monolayer),Egap ≈ 1.87 (direct)Band gap (Bulk) 1.23	[98,99]
8.	Optical absorption	$A{\cdot}W^{-1}$	high photoresponsivity 880	[72]

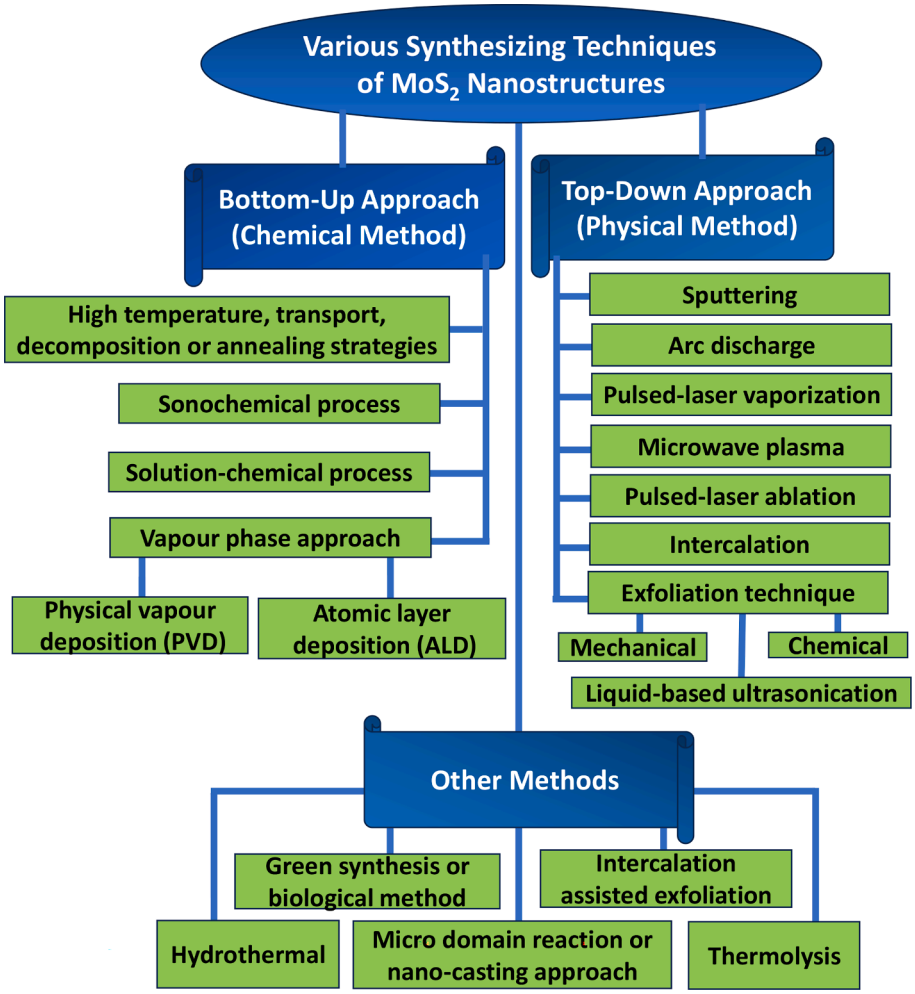

Fig. 4. Various synthesizing techniques of MoS_2 nanostructures.

3.1. *Physical methods or top-down approach*

The physical method is used in top-down approaches to nanomaterial synthesis. The bulk quantity of material is reduced in the top-down approach, or we can say that in other words "a giant crystal is exfoliated''. The top-down approach's fundamental drawback is that it can only be used with 2D materials, regardless of its benefits in terms of affordability and easiness of use [114].

3.1.1. *Exfoliation technique*

Exfoliation or intercalation is complete material separation. It is an easier and more scalable technique. Exfoliation became the most popular method for preparing monolayer materials after Novoselov and Geim discovered exfoliated graphene in 2004 and were awarded a Noble Prize in 2010 [115]. This method was later applied to many other 2D materials, including some $MoSe_2$, WS_2, MoS_2, $MoTe_2$, TiS_2, $TaSe_2$, and h-BN-type transition metal dichalcogenides (TMDCs) [116].

3.1.1.1. Mechanical exfoliation. The very first single or few layered graphene with significant adhesive characteristic was synthesized by Novoselov's group by using Scotch tape method [117]. Although many researchers have used this scotch tape method to synthesize the MoS_2 layered structure, its main disadvantage is that it produces a low yield. This method's alternative, anodic bonding, has a higher yield and is an easy and simple method [118].

3.1.1.2. Liquid based ultrasonic exfoliation. Liquid phase exfoliation involves three steps in its mechanism: dissolution, sonication by adding surfactants as a reinforcing material [119], and the third one is separation centrifugation. Although the liquid exfoliation process is not so expensive, quality is deficient in overcoming the low yield; the technique is used for graphene preparation by using a variety of surfactant solution, ionic liquids and organic solvents by some researchers [120].

The technique of sonication of bulk MoS_2 materials in chemical reagents with transitional polarities, such as by use of N-methyl-pyrrolidone (NMP)), provides an efficient method for exfoliating other layered materials bound by van der Waals forces with low consumption energy (e.g., graphite, TMD, and hexagonal boron nitride) [121] but the primary drawback of ultrasonic exfoliation is that raw materials are frequently multi-layered [122]. Thus, it is necessary to remove surface-bound organic solvents or surfactants (like NMP) because of toxicity issues and practical requirements in unique applications [123]. A diphase structural combination of 1 T MoS_2 phase and 2H semiconducting phase by MoS_2 exfoliation is developed by the Ambrosi. et al. [124] group by using n-BuLi but a long reaction time, low yield, and uncontrolled nature are some of the drawbacks of this ion intercalation method [125]. From this liquid exfoliation technique, researchers not only developed powders and wet suspensions but also a few researchers developed a thin film to study its optical and electrical properties [126,127].

3.1.1.3. Chemical exfoliation. To enhance the yield, MoS monolayers were made via chemical exfoliation and lithium-ion intercalation [128]. In particular, Li-intercalated MoS_2 with weaker interlayer attractions is produced when bulk MoS_2 is incubated in an organic solvent that contains Li (for instance, n-butyllithium in hexane). An ultrasonically reacting Li_xMoS_2 with water creates a colloidally stable dispersion of MoS_2 nanosheets. The charge transfer to MoS_2 nanosheets during Li intercalation produces a zeta-potential l of 45 to 50 mV at neutral pH. [129,130]. The lateral measurements of 200 to 800 nm and a cross-sectional area of 1 to 1.2 nm, depicting that atom-thin monolayer MoS_2 was generally achieved with a yield rate of almost 100 % [131]. The large-scale manufacture of MoS_2 nanosheets by this innovative chemical exfoliation technique, opens the door to real-world uses for these nanosheets in industries like power generation and anti-corrosion [132].

3.1.2. Sputtering

Sputtering is useful to synthesize MoS_2 thin films with low coefficients of friction. Sputtering conditions and parameters influence the compositional and morphological structure of thin films [133]. Vacuum and magnetron sputtering are two sputtering techniques commonly used by researchers [134]. End mills, drills, and cemented-carbide inserts can all be sprayed with solid lubricants using the closed-field magnetrons sputtering approach. [135–137]. Bichsel, Buffat, and Lévy prepared MoS_2 films in a planar magnetron system using radio-frequency (RF) sputtering in 1986, and they also comprehensively examined the impact of sputter processing parameters on the morphological features of MoS_2 films with a focus on fine substrate temperature control. The coatings created by pulsed magnetron sputtering of loosely packed powder targets made of chromium and boron powder alloyed with 12.8, 18.9, and 24.0 atom percent MoS_2 were described in a 2008 paper by Audronis et al. A simple dip technique was also used to create a thin film of molybdenum disulfide (MoS_2)[138].

3.1.3. Arc discharge

One method for synthesizing nanomaterials in an inert atmosphere is the arc discharge method, a continuous plasma discharge caused by an electrical breakdown of gas [139]. Similar to how carbon onions and nanotubes are made, the MoS_2 particles were created using arc discharge equipment [140–142]. In 2000, Chhowalla [140] synthesized IF-MoS_2 films using a high-pressure arc-discharge technique. Later, Alexandrou et al. 2003, [143] created MoS_2 core–shell particles and in 2003, Sano [144] demonstrated that 2H MoS_2 powder can be used to produce closed caged MoS_2 nanoparticles with a considerably homogeneous size distribution.

3.1.4. Pulsed-laser vaporization

This process can be done in a sealed chamber or with a background gas like oxygen, which is prevalently used when dispersing oxides to completely oxygenate the deposited films [145]. In 2004, Parella et al. testified the synthesis of nano-octahedra of MoS_2 nesting up to five layers with high symmetry and discrete size of close nano octahedra which make them the most analogous inorganic structure to carbon fullerenes (C60) that have been identified so far [146]. Serena et al. [147] and Sahu et al. 2019, [148] also achieved better thickness and improved the growing conditions to establish a polycrystalline film. Apart from that, microwave plasma [149–151], pulse Laser ablation [152–154], intercalation [155] and a few other top-down approaches [156–159] are useful to successfully synthesise MoS_2 nanostructures such as nanosheets, nanocubes, nanorods hollow-cage fullerene-like particles, fibrous floccus, spherical nanovesicles and some of the layered structure.

3.2. Chemical method or Bottom-Up approach

The 'bottom-up' approach has the probability of producing a lesser amount of waste and is more economical [160]. There is a large variety of methods involved in bottom-up approaches but only a few are used in the synthesis of the nanostructure of tri-chalcogenides family such as vapour phase deposition, solvothermal process, solution chemical process, etc. which are briefly described as below.

3.2.1. Vapor phase deposition

Vapor deposition (VPD) is a commonly used procedure in the semiconductor and biotechnology industries for depositing a thin film of various materials in order to accomplish precise surface modification. It is one such possible method that has drawn a lot of interest. Physical vapor (PVD), chemical vapor (CVD), and atomic layer deposition (ALD) are all methods for synthesizing MoS_2. Wang et al. (2013) used chemical vapor deposition (CVD) to create MoS_2 flakes with regular structure, huge size, precise number of layers, and high crystallinity [161] providing new opportunities for high-performance nano-electronics. Later Yui. et al., 2019 [162] grew single-layer MoS_2 films on sapphire substrates from molybdenum trioxide (MoO_3) sulfide using the same CVD process and analysed that when the substrate is angled 30° and positioned 9.5 cm downstream of the molybdenum source, the dimensions of the prepared single-layer MoS_2 are roughly 100 m - found to be bigger than MoS_2 prepared on a horizontal face-up substrate.

3.2.1.1. Physical vapour deposition (PVD). A thin film can be formed by the condensation of solid material and the condensed vapor is collected and nucleated on the exterior of the substrate to form a stable and solid film [163]. Among the various PVD synthesis techniques, thermal evaporation is the most widely used by many researchers. [164]. A high-optical-quality monolayer of MoS_2 on an insulating substrate of SiO_2, glass, and sapphire was synthesized by Wu et al. with excellent optical quality and high crystallinity [165]. Later Zhang and coworkers (2015) [166] developed amorphous MoS_2 nanosheet with improved catalytic activity h firmness for the Hydrogen Evolution Reaction (HER) in acidic

solutions because of its three-dimensional nanostructure, unstructured nature, and availability of uncovered edge sites.

3.2.1.2. The atomic layer deposition (ALD). Method is generally useful for fabricating both thick and thin films with fewer impurities and higher uniformity for use in various electronic and sensor-based applications. Loh et al [167] grew a highly crystalline and thin MoS_2 film on a sapphire wafer using $MoCl_5$ and H2S precursors at 300 °C. while Jurca et al. used a volatile $Mo(NMe_2)_4$ precursor (to avoid toxic and corrosive by-products) with H_2S at a very low temperature of 60 °C, followed by an annealing process to crystallize the amorphous film and photolithography compatibility for device fabrication [168]. Huang. et.al. [169] proposed a one-step ALD method for high crystalline MoS_2 film growth on Si and Al_2O_3 substrates. They discovered that film grain sizes may be controlled from 20 nm to 100 nm at 420 °C to 480 °C, and that an Al_2O_3 substrate generates thicker film growth than a Si substrate.

3.2.1.3. Solution chemical process. When using hydrothermal and solvothermal synthesis techniques, a series of physicochemical reactions typically occurs in a stainless-steel autoclave for several hours or more at a relatively high temperature (e.g., 200 °C) and high pressure. As a result, a variety of MoS_2 powders with different morphological structures are produced. Various structures like nano cubes, nanowires, nanoribbon, nanobelts different types of nanotubes like capped, T-shaped nanotube and twisted nanotube are also reported during investigation and experiments by using different precursors like sulfurization of $Mo_6S_2I_8$, MoO_3, $(NH_4)_2MoS_4$ and etc [170–174]. Electrochemical deposition and photo-assisted deposition are sometimes employed [175–178] in this technique. Among different nanostructures, it is observed that MoS_2 nanoribbons are perfect for fabricating devices since they can be oriented in parallel arrays and can reach lengths of 50 m [179]. The hydrothermal route has been widely used in many hydrogens evolution reactions (HER) and energy storage device-based applications in recent years [180,181]. Although most MoS structures are synthesized by normal hydrothermal route, a few studies have used magnetic fields [182] or microwave assisted hydrothermal route [183]. Luo et al. studied the morphological structure under different conditions, such as different molar conc. ratios, in one of their research studies. As the hydrothermal temperature and time increased, he found a variety of morphological formations, including coral-like collected particles, flower-like spheres, and wrapped nano-sheet structures. In another study, Wang et al. demonstrated a change in the morphology of MoS_2 from nano to micro (rods-spheres-flakes to flowers) with changing the pressure values ranging from 0.1 MPa to 3.5 MPa, [184]. The solvothermal process [185–191] was widely used to create various nanoparticle morphologies [190,192–194] and nanostructures, as well as metal–organic frameworks [195–198]. Numerous publications have also been made on the various MoS_2 nanostructures created using the solvothermal procedure, which has been shown to be an easy and effective way to create MoS_2/C nanocomposites [199,200]. Apart from that, high-temperature transport, decomposition or annealing strategies [170,201–205] and sonochemical synthesis [206–213] are some of the techniques used by many research groups. The summary of MoS_2 synthesis discussed above is presented in Table 3:

Other methods also include micromechanical exfoliation (Scotch tape-based), intercalation exfoliation, hydrothermal synthesis, micro-

Table 3
Summary of MoS_2 synthesis.

Sl. No	Method of synthesis	Precursor	Nanostructure developed	Advantage	Disadvantage	Reference
1	Sonochemical reaction	$(NH_4)_6Mo_7O_{24}$ and CH_3COSH	Hollow MoS_2microspheres	Homogenous size distribu-tion, quick reaction time, high phase purity, controlled growth rate of crystals		[188]
2	Low temperature thermal reaction	$Mo(CO)_6$ with S	circular bodies with flakes/rods			[189]
3	Simple annealing process	$(NH_4)_6Mo_7O_{24}{\cdot}4H_2O$, $Na_2S{\cdot}9H_2O$ HCl and $NH_2OH{\cdot}HCl$	MoS_2nanoparticle to nanorod structure	Facile technique	Requires high temperature	[192]
4	Simple method followed by annealing	Pollen grains, $(NH_4)_6Mo_7O_{24}{\cdot}4H_2O$ and $Na_2S{\cdot}9H_2O$	MoS_2 microspheres			[194]
5	Arc Simple method followed by annealing discharge	MoS_2 Powder	fullerene type structure			[132]
6	Pulsed Laser Vaporization	MoS_2 Powder	nanooctahedra of MoS_2	Number of layers can be controlled by laser pulses		[134]
7	high-temperature annealing	$(NH_4)_2MoS_4$ with S	MoS_2 thin layer			[159]
8	Hydrothermal Reaction	ammonium molybdate and thiourea @200 °C	Flower like microsphere	Morphology can be tuned by varying the reaction condition of hydrothermal synthesis	Long duration of time	[168]
9	Hydrothermal Reaction	$Na_2MoO_4{\cdot}2H_2O$, (NH_2CSNH_2) and PEG-1000@200 °C for 24 hrs.	Nanoflakes			[169]
10	Microwave Hydrothermal Synthesis	$((NH_4)_6Mo_7O_{24}{\cdot}H2O$ and NH_2CSNH_2 @200–220 °C for4-10 min.	1 T@2H MoS_2 nanosphere	Quick process		[170]
11	CVD method	MoO_3,S powder and MMT @ 400–750 °C for 20 min @10 °C/min	Thin layer sheet	Layers can be deposited on large area	Inferior quality with lot of defects, low carrier mobility	[214]
12	hydrothermal intercalation and exfoliation route	LiOH, ethylene glycol and MoS_2 bulk crystals	ultrathin MoS_2 nanosheets			[215]
13	Ball–milled method	Elemental molybdenum and sulfur powders @ 400 rpm for 10 h	Uniform MoS_2 microspheres	Facile, scalable	Chances of contamination	[216]
14	Co-precipitation method	$((NH_4)_6Mo7O_{24}{\cdot}H_2O$, ammonium sulfide and citric acid at 150 °C under magnetic stirring	MoS_2 nanorods	Quick, low temperature method	Chances of contamination due to precipitation of impurities	[217]

domain reaction or nano-casting approach, green synthesis and thermolysis of a single precursor containing Mo and S have all been used in the preparation of 2D thin-layer MoS_2 [218–227].

4. MoS_2 for green energy harvesting source (as nanogenerator)

Given the present energy crisis, energy harvesting is not an unfamiliar term today. The immense demand for energy has made it difficult to strike a balance between the supply and demand of energy. Hence, there is a need to opt out of the conventional dominant fossil fuel-based energy sources, which are polluting and exhaustive in nature. Harvesting energy from wasted mechanical sources is gaining attention owing to its abundance and easy availability [228]. Scavenging for energy from surrounding sources, and adapting it into suitable electrical energy for powering of electronic gadgets, is what is meant by the term "energy harvesting". Some of the non-conventional energy harvesting technologies that have potential to cater to the energy demands of upcoming generations includes piezoelectric [229], triboelectric, and thermoelectric energy harvesting techniques. These are cleaner alternatives compared to fossil fuel-based energy sources, as they do not give out any polluting by-products during their energy production process. Some of these technologies being based on material property, open avenues for synthesis of novel substances with superior energy conversion efficiencies. Further, they being inexhaustive in nature, serve as a continuous source of energy. Such kind of technologies, outshine batteries in terms of lifespan and performance stability. The sections to follow provide an idea about the potential of MoS_2 as a piezoelectric, triboelectric and thermoelectric material. It has been used in the form of flexible nanogenerators to act as a power source for fulfilling energy requirements for various applications.

With its remarkable mechanical and electrical capabilities (section 2), molybdenum disulfide (MoS_2) is an intriguing material that can work wonders at the nanoscale, particularly in the field of nanogenerators. Regarding a nanogenerator, a device meant to transform tiny mechanical or thermal energies into electrical power [230], When used with several kinds of nanogenerators, such as piezoelectric, triboelectric, and thermoelectric nanogenerators, the adaptability of MoS_2 is evident. MoS_2's two-dimensional (2D) structure is made up of thin layers with increased flexibility and surface area. This makes it perfect for absorbing and transforming mechanical and electrical energy (like pressure or vibrations) into electrical energy or other forms [231].

MoS_2 is a good material for harvesting energy from motions or vibrations and can function as an excellent piezoelectric material in a piezo nanogenerator because of its ability to respond to mechanical deformations and generate electric charges. MoS_2's surface characteristics make it an appealing material for use in triboelectric nanogenerators (TENGs). MoS_2's distinct two-dimensional structure, which is made up of stacked sheets of molybdenum atoms encased in sulphur atoms, is essential to understanding its tribological properties. Because MoS_2 is two-dimensional, it has a high surface area, which makes it easier for it to interact with other materials in frictional processes. This characteristic is essential for triboelectric applications, in which materials exchange charges because of mechanical contact and separation to produce energy. MoS_2 also has outstanding frictional characteristics, functioning as a solid lubricant to lessen wear and improve the energy conversion efficiency in TENGs. MoS_2's chemical reactivity, especially along the edges of its layers, improves its capacity to participate in charge transfer during friction, which helps explain why triboelectric applications find use for it. Overall, MoS_2's customised surface qualities make it a viable option for the creation of effective and long-lasting triboelectric nanogenerators for energy harvesting [232].

A specific kind of nanogenerator called a thermoelectric nanogenerator (TEG) uses the principles of nanotechnology and thermoelectricity to transform minute temperature variations into electrical energy at the nanoscale [233]. MoS_2's thermal characteristics make it an extremely promising material for thermoelectric nanogenerator applications (TEGs). Because of its modest thermal conductivity, MoS_2 is a good fit for gadgets that use temperature differences to generate electricity. The excellent conductivity and thermal management of MoS_2 are critical in thermoelectric nanogenerators. MoS_2's layered structure makes it possible for it to sustain a temperature gradient, which is necessary to induce a voltage across the substance. This characteristic makes it possible to transform thermal energy into electrical energy, which has potential uses in situations where temperature swings are common. Moreover, the 2D form of MoS_2 gives it a high surface area, which can improve its contact with heat sources and maximise the effectiveness of thermal energy harvesting. MoS_2 has a lot of potential to help develop small, effective thermoelectric nanogenerators for low-power, sustainable electronic applications by utilising these thermal properties [234].

By combining these characteristics, MoS_2 shows versatility with various kinds of nanogenerators, highlighting its potential in multipurpose energy collecting apparatuses. MoS_2 is a versatile material in the field of green energy harvesting since it contributes specifically to each form of nanogenerator, whether it is exploiting temperature differentials, responding to mechanical stress, or producing electricity through friction. We can harness a renewable energy source and lessen the environmental damage caused by traditional power producing techniques by utilising MoS_2 for green energy gathering. It's a step in the direction of developing greener and more sustainable technologies. An overview of MoS_2's potential as a thermoelectric, triboelectric, and piezoelectric material can be found in the sections further follows in the article. MoS_2 has been employed as a power source to meet the energy needs of numerous applications in the form of flexible nanogenerators.

4.1. *MoS_2-based flexible piezoelectric nanogenerators (PENGs)*

The adoption of efficient compact sources of energy is essential due to the limited supply of fossil resources, environmental damage, difficulties with chemical batteries, and the numerous practical advantages of wearable gadgets. The piezoelectric effect was brought to light in 1880 by Pierre and Jacques Curie. When the core symmetry of bulk or nanostructured semiconductor crystals is disturbed by an outside force, a piezoelectric potential is then produced. Piezoelectric nanogenerators are nano-electronic devices that convert mechanical or potential energy into electrical or automated energy (PENGs). They have the potential to be used in place of traditional chemical batteries. Mechanical energy can be transformed into electricity by piezoelectric nanogenerators [3]. Fig. 5 indicates the different types of fabricated piezoelectric nanogenerators.

Wang et al. [9] invented the first PENG in 2006. In this case, piezoelectric ZnO nanowire (NW) arrays converted mechanical energy into electric energy. Since the first PENG was claimed, numerous minisized electronic devices such as marketable light-emitting diodes (LEDs) and liquid crystal screens, and numerous piezoelectric energy harvesting devices have been created and examined [239]. PENGs can therefore be used to power handheld gadgets, wireless devices, and futuristic sensor networks as both mechanical energy harvesters and cutting-edge power sources. To date, the nanogenerator device has been built using a variety of piezoelectric/ferroelectric nanostructures [231,240] such as GaN, ZnO nanorods/nanodots, PZT, BaTiO3, LiNbO3, and others [241–245]. Piezotronics and piezo-photonic sensors are frequently made using inorganic nanostructures with semiconducting-piezoelectric multifunctional characteristics as self-powered nanosystems [246–248]. However, nanostructured materials with dual characteristics are quite uncommon, yet their use in the design of nanogenerator devices is crucial. Due to their superior qualities like good stability at ambient temperature, excellent mechanical strength, chemical inertness, and exemplary physicochemical characteristics, 2D layered materials like graphene, layered double hydroxides, transition metal dichalcogenides (TMDCs), and transition metal dioxides (TMDOs) have also gained popularity as their material properties are most suitable for designing

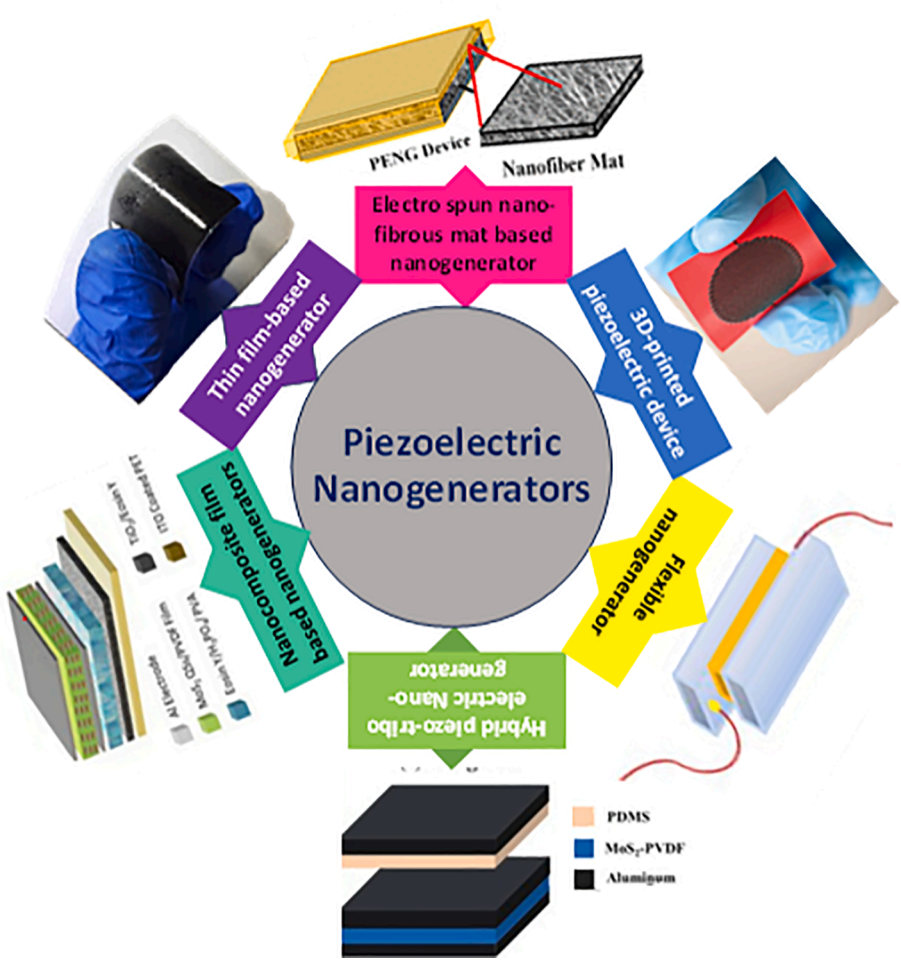

Fig. 5. Represents the different types of fabricated piezoelectric nanogenerators [3,235–238] All essential copyrights and permissions received.

and fabricating nano-electronic sensors [249–254]. Due to its three atomic layer structure, direct band gap, light absorption, and non-centrosymmetric properties, 2D MoS_2 has been extensively investigated in comparison to other TMDCs materials, making it a strong contender for the upcoming generation of optoelectronic and power generation devices. Furthermore, DFT simulations revealed that even-layer MoS_2 lacks piezoelectricity due to the breakdown of its centrosymmetric structure, whereas MoS_2 nanosheets had a high piezoelectric charge coefficient [255].

The center symmetry of the odd-layer MoS_2′s symmetrical structure contributes to its strong piezoelectricity. Single-layer MoS_2 is a piezoelectric material for energy harvesting because of its high piezoelectric coefficient and remarkable mechanical attributes [256–258]. Wu et al. (2014) [231] explored, for the first time, the experimental investigation of the piezoelectric characteristics of two-dimensional MoS_2 suitable for the generation of an efficient nanogenerator for powering electronic devices. They predicted that high-performance piezoelectric materials would be very interesting in two-dimensional materials with high crystallinity and the capacity to sustain tremendous strain. Theoretically, monolayer MoS_2 is projected to be substantially piezoelectric due to the strain-induced lattice distortion and the related charge polarisation; however, this effect is lost in the bulk equivalents due to their centrosymmetric structures. Based on this, Wu and colleagues have created a transparent and flexible PENG and achieved the first experimental observation of piezoelectricity in a monolayer MoS_2 flake. Monolayer MoS_2 is anticipated to be a good piezoelectric material due to the opposite orientations of neighbouring atomic layers, an effect that vanishes in the bulk. With a peak output of 15 mV and 20 pA, a single monolayer flake that is 0.53 % has a mechanical-to-electrical energy conversion efficiency of 5.08 % and a power density of 2 mW m^{-2}. Additionally, with a greater atomic layer (n) in the MoS_2 flakes, the development of the output performance was examined. Thin MoS_2 flakes with an odd number of atomic layers are repeatedly stretched and released, resulting in oscillating piezoelectric voltage and current outputs. In contrast, flakes with an even number of layers do not produce anything. These findings show that centrosymmetric bilayers and bulk crystals are nonpiezoelectric, but monolayer MoS_2 with broken inversion symmetry exhibits a high intrinsic piezoelectric response. Piezoelectricity and semi-conductivity in two-dimensional nanomaterials may be coupled to create applications for tunable /stretchable electronics and optoelectronics, adaptive bio probes, and nanodevice powering. Later, atomic force microscopy analysis has also demonstrated the existence of piezoelectricity in free-standing monolayer MoS_2, where the results display that monolayer MoS_2 shows a piezoelectric effect with a coefficient of 2.9×10^{-10}C/m, which is in good accord with the predicted value and similar to widely piezoelectric materials with wurtzite structure (e.g., ZnO) [235]. A few of the piezoelectric nanogenerators, their operational representation, output voltage and some of the energy harvesting techniques from different locations are schematically represented in Fig. 6.

The first ultrasensitive piezoelectric nanogenerator (PNG) composed of electrospun two-dimensional (2D) molybdenum disulfide (MoS_2) integrated poly(vinylidene fluoride (PVDF) nanofiber webs was discovered by Maitey et al. in 2017. They showed that PNG can charge a capacitor in a very short span of time and has an acoustic sensor that is 70 times more than that of tidy PVDF NFW-produced nanosensors (e.g.,

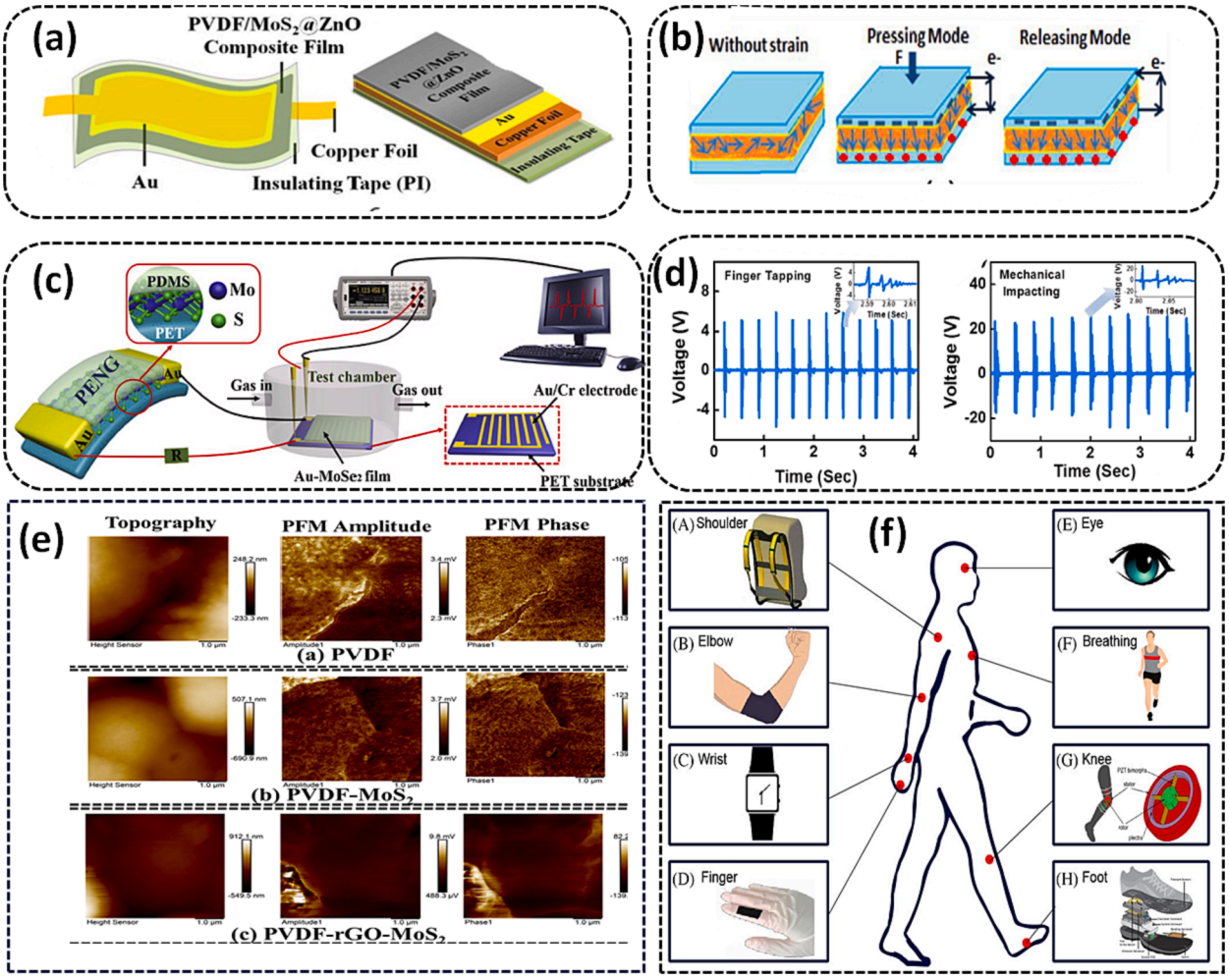

Fig. 6. (a) Schematic pictorial of PVDF/MoS_2@ZnO PENG [266] (b) schematic representation of the operation of a self-poled piezoelectric nanogenerator [238] (c) MoS_2 -flake-equipped self-powered gas sensor (PENG) with testing setup [267] (d) Results of output voltages PVDF − MoS_2 nanocomposite based device using by (f) finger tapping and (g) mechanical impact (~10.6 kPa) (insets representing the magnified views of voltage waveforms) [238] (e) PFM results of (a) PVDF, (b) PVDF-MoS_2 and (c) PVDF-rGO-MoS_2 composite films [265] (f) Innumerable piezoelectric energy harvesting procedures from the various parts of the humanoid body including (A) The shoulder, (B) Elbows, (C) The wrist, (D) Fingers, (E) Eyes, (F) Chest, (G) Knees, and (H) Feet [268]. All essential copyrights and permissions received.

within 44 s, 9 V is charged up). The path is paved for designing affordable self-powered wearable electronics, fabricating biomedical nanosensors for in-house analysis such as heart bit observing, compression tracking from footsteps, and vocal tract aberration, as well as robotic applications. This is due to the 2D-MoS_2 modulated PNG's superfast charging performance and exterior low-impact detection functionality [259] while later in an observation the higher output voltage was observed with a PVDF-$ZnSnO_3$-MoS_2 nanofiber web. The research group of Muduli et al. 2021, created a lead-free, inexpensive, bendable, and loose PENG based on PVDF-$ZnSnO_3$-MoS_2 electrospun nanofiber using a hydrothermal technique for synthesising $ZnSnO_3$ and MoS_2, as well as their composite PVDF-$ZnSnO_3$-MoS_2 nanofiber via the electrospinning process. The fabricated piezoelectric device has open-circuit voltage, short-circuit current, and instantaneous power density of 26 V, 0.5 A, and 28.9 mWm^{-2}, respectively. The calculated power density is predicted to be 18 times superior to that of pristine PVDF PENG. The synergistic effect of piezoceramic ($ZnSnO_3$) and MoS_2 interfacial action in the PVDF matrix leads to an upsurge in the fraction of the -phase of PVDF performance. Additionally, the constancy and resilience test were run for more than 3000 cycles and for 50 days without any degradation in efficiency. This reliable performance and durability of the device make the PVDF-ZnSnO3-MoS_2 based electrospun nanofiber mat an excellent contender for bio-mechanical energy harvesting and sensing applications useful for human body movements, and practical uses for the nanogenerator, including powering calculators and charging capacitors, were shown in [235]. To study the impact of (Sulphur) S vacancy passivation, Han et al. (2018) [260] constructed a monolayer MoS_2 piezoelectric nanogenerator (PNG) and compared its characteristics prior to and following S treatment. On the MoS_2 surface, native S vacancies are known to occur, giving rise to MoS_2's n-type property. The output of PNGs is reported to be significantly impacted by a relatively high free-carrier density hence, it is necessary to passivate S vacancies to reduce the concentration of electrons. The author successfully passivated the S vacancies using this S-treatment method on the unblemished MoS_2 surface. S atom will chemisorb with the S vacancy site of MoS_2 by engulfing free electrons because the S vacancy site forms covalent connections with S functional groups. S-treatment significantly reduces the monolayer MoS_2 surface's charge-carrier density, which significantly minimizes the piezoelectric polarisation charges' ability to be screened by free carriers. The result is that the S-treated monolayer MoS_2 nanosheet PNG's output peak current and voltage are more than three times as high (100 pA) and twice as high (22 mV), respectively. Furthermore, the maximum power was about ten times higher after the S-treatment. The results show that S-treatment can effectively limit the screening effect by reducing free-charge carriers by S passivation. As a result, as compared to virgin MoS_2, the maximum

power, voltage, and current production peaks of the piezoelectric material were all much higher.

Stretchable/wearable electronics are one example of a practical application that unavoidably calls for CVD-based large-area MoS_2. The maximum power, voltage, and current peaks of the piezoelectric output are significantly higher than those of pure MoS_2. This research's conclusions, therefore, point to a fresh technique for raising the piezoelectric output of CVD-grown MoS_2, which might be used as a capable power source for stretchable/wearable electronics. Biswajoy et al. [261]. presented a novel multifunctional piezoelectric nanogenerator to deal with environmental pollution and the energy crisis in 2020. The authors created a free-standing film for this sustainable technology by uniting piezoelectric molybdenum sulfide (MoS_2) nanoflower with polyvinylidene fluoride (PVDF) polymer via a simple solution casting method, which can be used to generate useful energy by capturing alternatively untapped mechanical energy. Under human finger tapping, this self-poled piezoelectric nanogenerator produced $>$ 80 V with a notable power density of 47.14 $mWcm^3$. Finger tapping can power up to 25 commercial LEDs. Under dark conditions, this MoS_2-PVDF piezoelectric nanogenerator demonstrates catalytic degradation efficiency against four different toxic and carcinogenic dyes, namely Ethidium bromide (ET), Eosin Y, and Acridine Orange. Ethidium bromide (ET) had the highest rate constant (0.32 min), followed by Eosin Y (0.26 min), Rhodamine B (0.21 min), and Acridine Orange (0.127 min). As a result, the nanocomposite has a clear use in systems for water purification as well as self-powered sensors and energy harvesters. Additionally, it could be applied as a surface-mounted film or coating in systems for medical device manufacturing, industrial effluent control, and process engineering. Overall, the development of unique, energy-efficient water remediation technologies and intelligent self-powered electronic gadgets is made possible by the construction of such sophisticated and adaptable piezoelectric nanocomposite materials. At the same time in 2021, Arunguvai and Lakshmi [262] observed the performance of MoS_2 with the copolymer of PVDF material and found very small output voltages by synthesizing a PVDF's copolymer (PVDF-TrFE) based nanocomposite with MoS_2 by inserting nano-MoS_2 into polyvinylidene fluoride-trifluoro ethylene P(VDF-TrFE) by solution cast followed by annealing method. Microscopic and structural transformation analysis were used to confirm the existence of nano-MoS_2 particles in the polymer chain and elemental molecular binding energy. MoS_2 nanoparticles embedded in a polymer composite enhance the conductivity of the Polymer thrice times as compared to its pure. The natural resonance frequency and output voltage performance of four different types of energy harvesting devices-P(VDF-TrFE) with and without substrate, and MoS_2/P(VDF-TrFE) with and without substrate are fabricated based on the substrate effect. MoS_2/P(VDFTrFE) with PET substrate piezoelectric cantilever generates greater AC output voltage 2.96 V in the dimensions of (1 cm x 0.5 cm) in measurements. Due to its high-phase intensity, dielectric constant, and superior mechanical features, the MoS_2/P(VDF-TrFE) with PET substrate piezoelectric vibration energy harvester generates 2.96 V AC voltage at the resonance frequency of 82.6 Hz. Sathiya et al. 2018, [263] address the issue of conventional batteries' limited lifetime, monitoring, and replacement in electronic devices. Thus, he created for the first time an advanced multi-mechanism-based nanogenerator employing both piezoelectric and triboelectric nanogenerators for miniaturization with the goal of achieving high output voltages to generate electricity in a wide range of devices. They created a piezo-triboelectric hybrid nanogenerator by hydrothermally growing a few layers of MoS_2 over cellulose paper and electrospinning in-situ poled PVDF nanofibers so that it can generate power from everyday activities like writing by hand and touching objects. The output was increased by measuring the mutual production of a parallel-connected piezo and triboelectric nanogenerator using two independent bridge rectifiers. This hybrid nanogenerator's maximum voltage was 50 V, its maximum short circuit current was 30nA, and its average power was 0.18 mW/cm^2. The author's study extends beyond energy harvesting and offers up opportunities for the creation of affordable paper-based nanogenerators that produce electricity from daily chores, making it a great replacement for using physical labour to power wearable electronic devices. Smart paper for signature verification, sensors, residential and commercial security, and other potential applications are all mentioned. In order to promote the more effective dispersion of additional ingredients in water and the composite for making flexible films, some oxidizing agent is used later like Xu et al., in 2021 [264] presented environmentally friendly biomass-based piezoelectric nanocomposites as an alternative to conventional rigid piezoelectric materials, adding to the more environmentally based nanogenerators. By uniformly constructing MoS_2 nanosheets and tetragonal $BaTiO_3$ nanoparticles in a TEMPO-oxidized cellulose nanofibril (TOCN) matrix, the author employed a quick, affordable, and sustainable method to produce composite piezoelectric films. This TOCN/MoS_2/BaTiO3 ternary composite film's highest longitudinal piezoelectric constant (d33) was 45 pC N1, which is much greater than that of previous cellulose-based piezoelectric materials. Additionally, they provide extremely stable piezoelectric output signals with maximum open-circuit voltages of 8.2 V and 0.48 A for short-circuit currents. In addition, the PENG's electricity directly powered an LED or charged a 10F capacitor from zero to 3.1 V in 110 s. To detect minor forces in the environment, such as leaf fall, this novel flexible gadget with excellent sensitivity can be utilised as a self-powered motion sensor. Likewise, it could be utilized in human movements like finger bending and wrist pulse, as well as an electronic skin with better pyroelectric properties for monitoring of temperature. As a result, the study advances our knowledge of the design and construction of flexible, ultralight PENGs with remarkable piezoelectric performance, which has enormous potential for the development of effective mechanical energy harvesters, dynamic sensor networks, and wearable electronics that are simple to manufacture on a large scale.

To see the mechanical impact of these oxidized nanofibril for sensors application, Wu Tao et al. 2021 [2] successfully prepared a TOCN/MoS_2 nanocomposite piezoelectric film by integrating 2,2,6,6-tetramethylpiperidine-1-oxyl (TEMPO)-oxidized cellulose nanofibril (TOCN) with a sole layer MoS_2 nanosheets exfoliated by tri-ethanolamine via an aqueous dispersion technique. The TOCN/MoS_2 nanocomposite films had exceptional mechanical characteristics, with the estimated Young's modulus of 8.2 GPa (max), a peak tensile strength of 307 MPa, and the lowest elongation at break of 13.9 %. The highest open-circuit output voltage (4.1 V) and short-circuit current (0.21A) of the nanogenerator made with TOCN/MoS_2 composite films were both about three times greater than those of the perfect TOCN PENG. Additionally, the nanogenerator's electric current was controlled and converted to a straight current. It was shown that a 10F commercial capacitor can absorb mechanical energy produced by the environment by charging it to 1.6 V in 120 s. The electrical energy that is kept in the capacitor can be used to power a number of LED lights. The TOCN/MoS_2 composite films are hence promising. Apart from these, a few recently amendable fillers like BTO, ZnO, rGO and their heterostructures with MoS_2 are attracting more interest by many researchers. Faraz Mohd. et al. 2022 [265] proposed a novel MoS_2-rGO strategy to enhance the piezoelectric property of PVDF. They investigated the piezoelectric characteristics of flexible PVDF, PVDF-MoS_2, and PVDF-rGO-MoS_2 thin films using the polymer solution casting technique. They found that the produced voltage is much greater in the flexible thin film of PVDF-rGO-MoS_2, which is 5 times higher than the flexible film of PVDF and 2 times higher than the flexible film of PVDF-MoS_2. The measured short circuit current for PENGs based on rGO filled composite film was 0.68A, 0.37A for PENGs based on PVDF-MoS_2 films, and just 0.15A for PENGs based PVDF. The maximum output open-circuit voltages for PVDF-rGO-MoS_2, PVDF-MoS_2, and bare PVDF films-based PENG, respectively, were measured to be 2.4 V, 1.5 V, and 0.5 V. After testing the piezoelectric coefficient, the PVDF-rGO-MoS_2 film based piezoelectric nanogenerator produced 0.81 W of power, while the PVDF-MoS_2 film based piezoelectric nanogenerator produced 0.44 W of power. The piezoelectric coefficients for

PVDF, PVDF-MoS_2, and PVDF-rGO-MoS_2 thin films were found to be 53 pm/V, 68 pm/V, and 72 pm/V, respectively. The PVDF-rGO-MoS_2 nanocomposite film-based PENG performs better based on all of the observed values. The mechanism behind the improved performance of PVDF, in the author's opinion, is an increase in the piezoelectric property of PVDF with a surge in the -phase content of PVDF and, as well as this, the intrinsic piezoelectric property of PVDF plays a significant role in uplifting the performance parameters of PVDF-rGO-MoS_2 nanocomposite film-based PENG. By increasing the phase content as a result of free -electrons interacting with PVDF CH2 dipoles, the existence of rGO also contributes to stimulate polarisation of the PVDF matrix. As a result, changing the PVDF content from α to β phase can enhance the output performance. Later by hot pressing technique, Cao Shuoang et al. 2022 [266] created a PVDF/MoS_2@ZnO piezoelectric fused film by incorporating MoS_2@ZnO nanocomposites material grown by solely growing ZnO on the exterior surface of highly porous MoS_2 nanosheets using in situ polymerization in PVDF. They noticed how heterostructure (MoS_2@ZnO) successfully encourages the transition from one phase to another in PVDF, raising the phase content from 6.2 2.5 % to 54.3 2.7 %. The computed longitudinal piezoelectric constant (d33) for the composite film peaked at 31 4 pCN-1. The open-circuit voltage (VOC) and short-circuit current of the PVDF/MoS_2@ZnO piezoelectric composite film are 6.22 V and 528nA, respectively, under 100 KPa acting force. This nanogenerator can charge a 1.0 F commercial capacitor to 1.81 V in 400 s. An agile piezoelectric sensor was developed to record pressure signals generated by human motor control like bending of forearms, shoulders, and finger joints. A supple piezoelectric sensor was developed as a result to capture pressure signals brought on by humanoid body

Table 4
Comparative summary of the piezoelectric nanogenerator based on MoS_2 nano and composite materials.

SI.	Materials	Method	Dimensions	Force/ Pressure	Frequency	Voltage (V)	Isc (μA)	Power density mW/ cm^2	Application	Ref.
1.	$_2$/Palladium		5 μm × 5 μm × (0.6–100 nm)		0.5 Hz	15 mV	20pA	2 mW/ m^2	Nanodevices, bioprobes, stretchable/ tunableelectronics	[231]
2.	MoS_2/PVDF	Electrospinning	11 cm x 8.5 cm x 150 μm	Finger touch ~ 7 N	100–150 Hz	Charge up to 9 V a capacitor within a very short time span 44 s/9V	–	–	self-powered wearable electronics and robotics	[259]
3.	MoS_2	liquid-phase exfoliatedCVD				22	100	73	sretchable/wearable electronics	[260]
4.	MoS_2 nanosheetsembedded in poly(vinylidenefluoride) (PVDF) polymers	Spin coated (at 1000 rpm, 10 s)	Three dimensions of 1X1 cm^2, 2X2 cm^2. 3x3 cm^2			50	30	0.18	self-powered sensors for IoT, security,	[263]
5.	MoS_2/PVDF	Solution cast	1 cm × 1 cm × 50 μm	27.5 N	Hz	>80 and Remanant pol. is 3.38 μC cm^{-2}	3.05	47.14	Self-powered sensor, energy harvester,and water remediation systems	[261]
7	MoS_2/P(VDF-TrFE) & MoS_2/PVD with PET	Solution castfollowed byannealing	1 cm * 0.5 cm		29 Hz 82.6 Hz	1.72.96	–	–	Energy harvesting	[269]
8.	2,2,6,6-tetra methylpiperidine-1-oxyl (TEMPO) -oxidizedcellulose nanofibril Nanosheet (TOCN) /molybdenumdisulfide (MoS_2)	Aqueous dispersion				4.1	0.21	–	nanogenerators for energy harvestcan be utilized for lighting several LEDs.	[2]
9.	(PVDF)–$ZnSnO_3$–MoS_2	Electrospinning	2 × 2 cm^2	Finger tapping with~1kgf	3 Hz	26	0.5	28.9	Biomechanical field, sensing of body parts movements, and real-timeapplication	[235]
10.	Cellulose(RC) /MoS_2 nanosheetnanocomposite	Solution cast	20–30 μm	0.88 kPa		2	150	–	Sensors and electronics.	[270]
11.	2,2,6,6-tetra methylpiperidine-1-oxyl (TEMPO) -oxidizedcellulose nanofibril Nanosheet (TOCN)/ (MoS_2)/BaTiO3	Solution cast	1.5 × 3 cm^2	50 N		8.2	0.48μA	–	Stress and temperature sensing, energyharvesting,	[264]
12.	PVDF-MoS_2, and PVDF-rGO-MoS_2	Solution cast	50 μm	~15 kPa		0.5 1.52.4	0.15 0.370.68		Piezoelectric nanogenerator application	[265]
13.	PVDF/MoS_2@ZnO piezoelectric composite film	in situ polymerization	2 cm × 3 cm x 0.109 ± 0.005	100 KPa		6.22	528nA	1.15 mA·m^{-2}	wearable intelligentdevices.	[266]

drive (the elbow joints, bending of fingers, and wrists). The PVDF/MoS_2@ZnO piezoelectric nanogenerator has demonstrated performance that suggests mechanical energy harvesting in the environment showing that it can be used in wearable intelligent devices. As a result, we can draw the conclusion that MoS_2 can considerably assist to easing the global energy crisis by offering a green energy option. Piezoelectric power generation might be a good substitute for traditional power sources for low powered electronic devices given the present rise in microscale gadgets. A comparative study of the piezoelectric nanogenerator of 2D MoS_2 nano-composites materials in tabular form is given in Table 4.

4.2. MoS_2-based flexible thermoelectric nanogenerators (TEGs)

The thermoelectric effect has been a familiar phenomenon since the discoveries of Seebeck, Peltier, and Thomson. Thermoelectric materials are potential candidates for transferring heat energy into electrical energy and vice versa (Fig. 7) [271]. The material properties like thermal conductivity, electrical conductivity, and Seebeck coefficient govern the conversion efficiency of thermoelectric materials. A figure of merit also helps to assess the quality of thermoelectric materials. It is dimensionless and evaluated using the following formula:

$$zT = \frac{S^2\sigma}{\kappa}T$$

where S is the Seebeck coefficient, σ is the electrical conductivity, κ is the thermal conductivity, and T is the absolute temperature. A thermoelectric module may be used as a cooler or as a power generator. The cooler implements the Peltier effect while the power generator requires the implementation of Seebeck effect. Raising the figure of merit, zT, of a thermoelectric generator is typically the primary emphasis for enhancing its efficiency (Fig. 8a) [272].

Energy is harvested using thermoelectric materials, primarily through the use of nanogenerators. Materials having low thermal conductivity, high conductivity, and high dissipation factors are mandatory to upsurge the zT of the nanogenerators. Molybdenum sulfide (MoS_2) is a promising material in this respect. It has the least thermal conductivity and a high Seebeck coefficient. The high band gap of MoS_2 imparts electrically insulating behavior to the substance until a high external electric field is applied over it. On the other hand, semimetals like graphene, which have high electrical conductivity, when fabricated into nanocomposites with MoS_2, make a good thermoelectric device (Fig. 8b). The higher electron mobility of graphene than MoS_2 helps to provide more electron carrier connections in the nanocomposite which

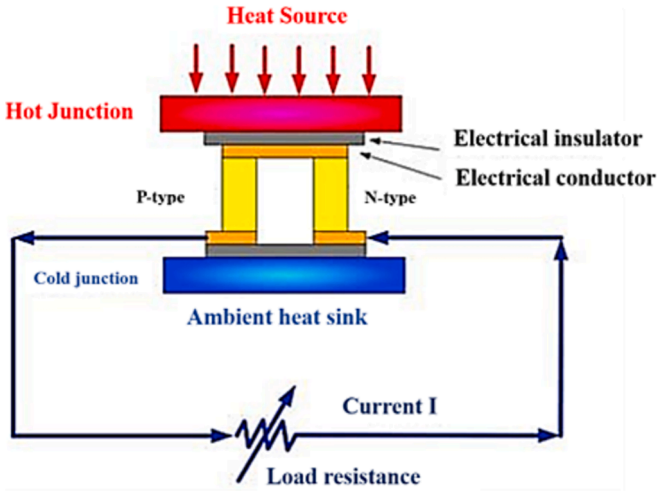

Fig. 7. Schematic illustration of energy conversion by thermoelectric materials [273]. All essential copyrights and permissions received.

enhances the electrical conductivity of the MoS_2/graphene nanocomposite. Thermoelectric nanogenerator (TEG) prepared from pure MoS_2 gave higher output voltage compared to the TEG prepared from pure graphene. This was ascribed to the higher Seebeck coefficient of MoS_2 compared to graphene. The incorporation of graphene in the nanocomposite helped to enhance the electrical conductivity while preserving the inherent nature of MoS_2. This can therefore be used as a self-powering temperature sensor [55]. Energy harvesting from non-conventional renewable sources is drawing attention due to the demand for a sustainable energy supply. A thermoelectric nanogenerator comprising a molybdenum sulfide/ polyurethane (MoS_2/PU) photoelectric layer and a tellurium wire-based thermoelectric device were designed to harvest energy from infrared light (Fig. 8c). The MoS_2 nanoclusters used provided a good surface area-to-mass ratio and contributed to making the photothermal film flexible. The integration of the thermoelectric device in the photothermal film, produced a temperature gradient by absorption of infrared light. This established a potential difference between the electrodes, which was then utilized for energy harvesting. MoS_2 effectively absorbs Infrared energy and transforms it into heat. Hence, higher MoS_2 content samples had a greater surface temperature. This proves the exceptional photothermal properties of MoS_2. The increase in the tellurium content helped to improve the Seebeck coefficient which enhanced the efficiency of the nanogenerator. This demo0nstrates the good thermoelectric properties of tellurium [274].

Monolayer MoS_2 could also serve as an attractive material for thermoelectric nanodevices. The Seebeck coefficient of the monolayer can be tailored by the application of voltage within a suitable range. Monolayer MoS_2 transistors were developed to study the mechanism of photocurrent generation. It was observed that the photo thermoelectric effect influenced the photocurrent generation, rather than the splitting of electron-hole pairs. On exposure to light, a temperature gradient develops between materials of different Seebeck coefficients (material and electrode). Consequently, a photovoltage junction forms and current will flow as an outcome [275]. Further studies on single-layer MoS_2 proves that this material has promising applications beyond optoelectronics (Fig. 8d). Chemical vapor deposited monolayer MoS_2 helps to realize the fabrication of large-area devices for thermoelectric applications. The electron transport mechanism helps to tune the thermopower generated, which reached a maximum of up to 30 mV/K. The temperature's cube root and the Seebeck coefficient were connected. Additionally, understanding the relationship between conductance and thermopower aids in understanding the electrical and thermal properties of such low-dimensional material [276]. A summarized comparative study of MoS_2 material-based thermoelectric nanogenerators are represented in Table 5**.** To further improve the thermoelectric properties of MoS_2, heterostructures of MoS_2-graphene were considered. It was found that the thermoelectric properties changed from p-type for pristine MoS_2 to n-type for heterogenous MoS_2-graphene structures. The Seebeck coefficient and the electrical conductivity of the heterostructures were largely affected by those of MoS_2 and graphene individually which resulted in variations in the electronic structure of MoS_2-graphene heterostructures near the Fermi level [277].

4.3. MoS_2 based flexible triboelectric nanogenerators (TENGs)

The very first flexible triboelectric nanogenerator was explored by Fan et al. [278] in 2012. One of the promising methods for obtaining electrical energy from mechanical sources that are flexible in terms of price and sustainability is triboelectric energy harvesting technology. After that, much research has been examined by the different research groups using different materials. In recent days, the demand for 2D semiconductive materials has increased tremendously in the area of mechanical energy harvesting. Owing to their inborn qualities, which include sufficient transparency, flexibility, and a large surface-to-volume ratio. Among different 2-D materials, dichalcogenide group-

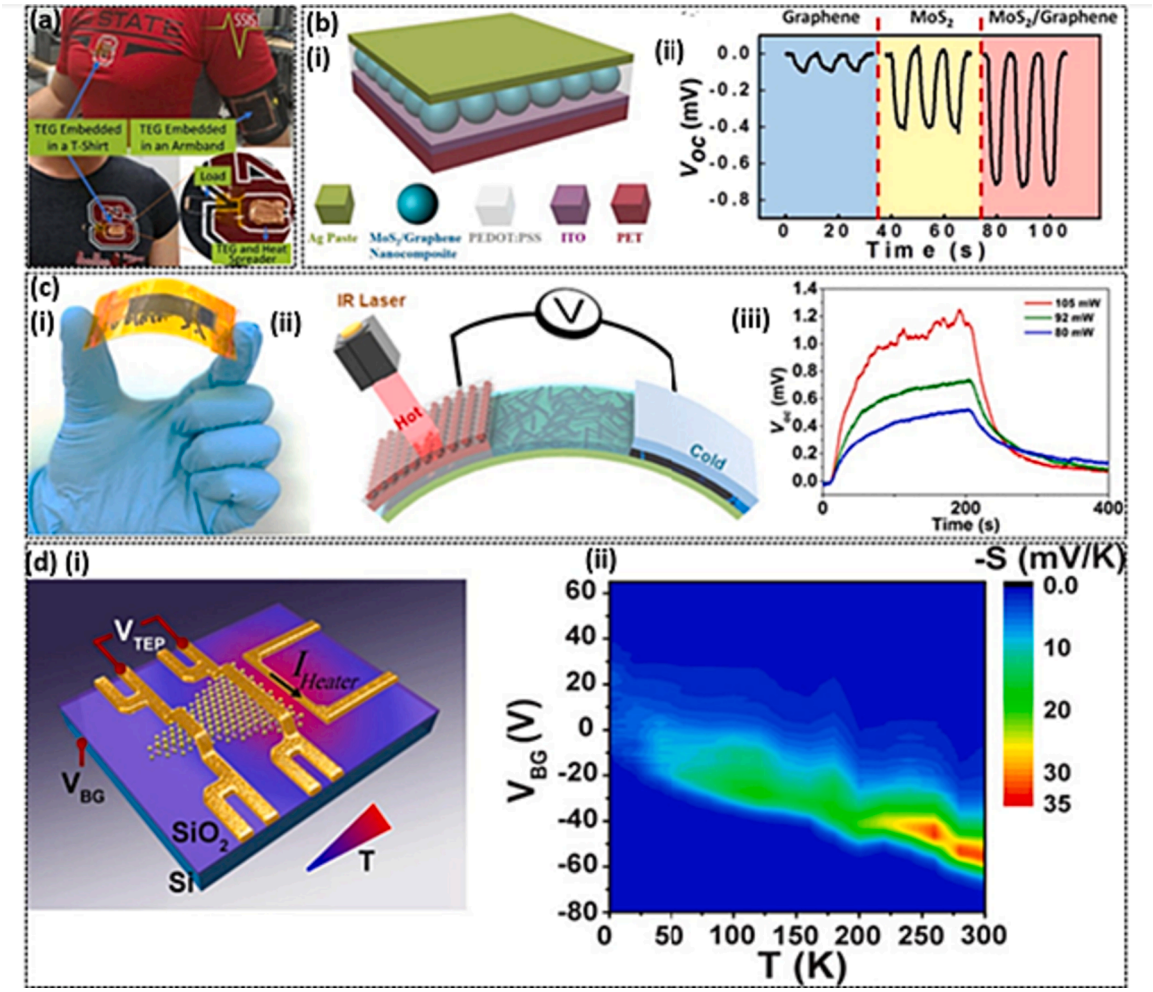

Fig. 8. (a) T-shirt and armband embedded with thermal harvesting unit [272]; (b) (i) Fabrication process of the thermoelectric nanogenerator, (ii) Comparative voltage analysis of pristine graphene, pristine MoS_2 and MoS_2/graphene nanocomposite [55]; (c) (i) Flexible photo-thermoelectric nanogenerator, (ii) Illustration of the working of photo-thermoelectric nanogenerator, (iii) Output performance of photo-thermoelectric nanogenerator [274]; (d) (i) Illustration of fabrication of thermoelectric device, (ii) Conductance measured with respect to back gate voltage and temperature [276] All essential copyrights and permissions received.

Table 5
Summary of some of the prominent works featuring MoS_2 as a thermoelectric material.

Sl. No	Materials	Method of Fabrication	Output voltage	Power density	Application	Ref
1	MoS_2/graphene	Hydrothermal followed by sonication	−0.73 mV	8.8 nW/cm^2	Self-powered temperature sensor	[29]
2	MoS_2/PU	MoS_2 nanostructures and tellurium nanowires prepared through hydrothermal process. MoS_2/PU films prepared through solution coating on PET substrates	1.2 mV		Harvesting energy from outdoor sunlight	[239]
3	Single layer MoS_2	Mechanical exfoliation			MoS_2 based FET	[275]
4	Single layer MoS_2	Chemical vapour deposition				[276]
5	MoS_2 monolayer-graphene heterostructures	Synthesized based on DFT calculations				[277]

based molybdenum disulphide (MoS_2) has drawn massive interest to harvest waste mechanical energy available in our surrounding environment. MoS_2 has shown maximum output voltage (7.48 V) and current (0.82 μA) as associated with other 2D materials such as molybdenum diselenide ($MoSe_2$), tungsten disulphide (WS_2), and tungsten diselenide (WSe_2), as reported by Han et al. [279] in 2019. Further, MoS_2 has suitable electrical, optical and the piezoelectric properties. In each MoS_2, the molybdenum atom plane is squeezed in between two sulphide atom planes by covalent boding and forms S-Mo-S having hexagonal crystal structure [280]. Examples of waste mechanical energies are human body movement, water flow, wind flow and much more. These waste energies can be recycled as useful electrical energy with the assistance of piezoelectric or triboelectric energy harvesting technology. Piezoelectric energy harvesting technology is based on the ability of certain materials to generate an electric charge in response to applied mechanical stress. Triboelectric nanogenerators, on the other hand, operate because of the charge that transfers across an interface during the reciprocating sliding (or tapping) contact of two dissimilar solid surfaces. There are different commercial triboelectric materials such as nylon, cotton, silk, PVDF, rubber (inorganic materials) and MoS_2, molybdenum diselenide ($MoSe_2$), tungsten disulphide (WS_2), tungsten diselenide (WSe_2), titanium dioxide (TiO_2), silicon (Si)

(organic materials). Moreover, some advanced triboelectric materials like graphene, carbon nanotube (CNT), hydrogels, and various biodegradable natural materials have also been explored by different research groups [281] Herein, triboelectric energy harvesting using MoS_2-based material is discussed in detail.

As mono or bilayer of MoS_2 has potential applications in the range of triboelectric energy harvesting, synthesis of thinned MoS_2 nanosheets has been a prominent interest of researchers. The most common method is liquid phase exfoliation (LPE) to synthesize the thinned layer (mono or bilayer) MoS_2 nanosheets. Various studies have already been tried to synthesis MoS_2 thinned layers by LPE method. Here, they have used commercial surfactants such as sodium chlorate, sodium dodecylbenzene sulphonate and so forth as a synthesis medium. However, this existing synthesis medium has environmental issues and hence use of natural surfactants has drawn particular interest for synthesis of MoS_2 thinned layers.

In order to develop MoS_2 thinned layer based triboelectric energy harvesters, Karmakar et al.[282] have synthesized MoS_2 thinned layers (bi-layer and penta layer) using a natural surfactant extracted from Bellyache Bush (*Jatropha gossypifolia*) and Washnut (*Sapindusmokorossi*) juice. For the preparation of the triboelectric nanogenerator, one part has been developed by Al-MoS_2 glued paper and other part by Al- graphene glued paper. The authors have also explained the energy harvesting mechanism as depicted in Fig. 9(a). When pressure is applied on the upper part (dielectric −1), this part contacts with the surface of the lower part (dielctric-2) and therefore, electrons can flow from the lower part to the upper. As a result, the dielectric-1 and dielectric-2 components acquire corresponding negative and positive charges. And when the pressure is released, two dielectric components split, and two metal electrode' surfaces become charged as a result of electrostatic induction (upper and lower). Therefore, a potential difference is taking place between the two dielectric parts and charges are moving from one surface to the other until an equilibrium state is reached. Finally, the authors concluded that the bi-layer MoS_2 based triboelectric nanogenerator shows better energy harvesting performance (~10.20 V) than the multilayer MoS_2 based nanogenerator (~3.82 V). Mono layers of MoS_2 can also be synthesized by the chemical vapour deposition method. Mono layers of MoS_2 2D sheet have more flexibility and higher surface to volume ratio as compared to its bulk form. Therefore, it can be expected that mono layer MoS_2 in the form of a 2D sheet will reveal higher triboelectric characteristics as compared to its other forms (bi-layer, bulk form and so on). In a study, Kim et al. [54] have developed a triboelectric nanogenerator by using 2D mono layer MoS_2. In their study, MoS_2 was synthesized by chemical vapour deposition. The synthesized MoS_2 was mono layer 2D sheet having band gap of 1.8 to 1.9 eV. After synthesising the MoS_2, the triboelectric nanogenerator was fabricated using PVDF/polystyrene (PS)/MoS_2/ITO/PET nanocomposite as a bottom layer and gold (Au)/PET, ITO/PET, and polypyrrole (PPy) as the top layer, respectively (Fig. 9b). The authors have evaluated the triboelectric performance of the MoS_2 based nanogenerator with three different contact modes (an ohmic contact, a schottky contact and pn junction mode). Surprisingly, the MoS_2 based triboelectric nanogenerator showed higher output voltage (4 V to 80 V) and current compared to the case without MoS_2 (2.3 V to 6.9 V). Moreover, Au/MoS_2 and PPy/MoS_2 based triboelectric nanogenerators showed higher output voltage and current as compared to ITO/MoS_2 based nanogenerators. This is due to an ohmic contact taking place in between the MoS_2 and ITO, where a schottky and pn junction contact are

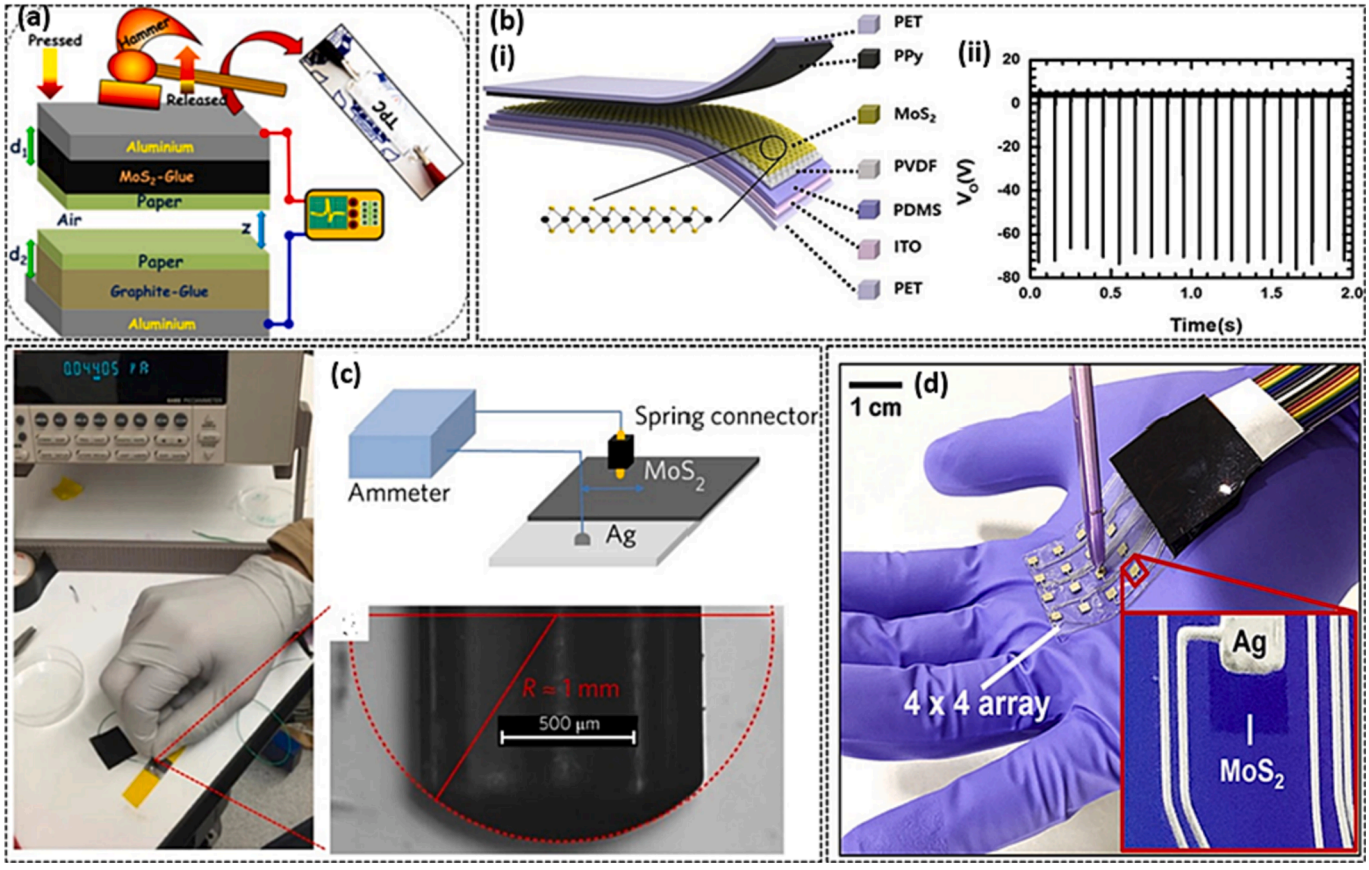

Fig. 9. (a) Schematic illustration of the fabrication of triboelectric power cell [282]; (b) (i) schematic for illustration of TENG based on PVDF/polystyrene (PS)/MoS2/ITO/PET nanocomposite, (ii) output performance of the developed PVDF/polystyrene (PS)/MoS2/ITO/PET nanocomposite based TENG [54]; (c) illustration of MoS2 semiconducting substrate based triboelectric energy harvesting in d.c. mode [283]; (d) MoS_2 based TENG haptic sensor [284] All essential copyrights and permissions received.

taking place between MoS_2 and Au, and MoS_2 and PPy, respectively, since they have work function values of 4.5 to 4.6 (MoS_2), 4.2 (ITO), 5.5 (Au), and 4.6 (PPy).There is no net charge movement at the interface of the MoS_2 and ITO layer in an ohmic contact. Whereas electrons are flowing from one layer to other layer in the case of MoS_2 and Au, PPy combinations. Besides, when pressure is applied on the device, electrons are diffused in the Au and PPy layers and hence negative voltage is generated. Similarly, when pressure is released from the device, the reverse phenomenon has been observed. The authors have also examined the ferroelectric effect of PVDF polymer layers in the MoS_2 based nanogenerator. Here, it has been observed from their experiment that, the MoS_2 based nanogenerator with the ferroelectric PVDF polymer showed higher output voltage 96 V to 80 V) as compared to without PVDF (4 V to 18.4 V). This is due to the concurring effect of the depletion layer (between MoS_2 and Au, PPy) and ferroelectric PVDF polymer layer. The maximum power density was observed as 455 $\mu W/cm^2$ (in the case of nanogenerator composed of PVDF/MoS_2/ITO/PET as bottom layer and PPy/PET as top layer) across the resistance of 10 MΩ and the pressure of ~ 5 kPa at 10 Hz frequency.

On the same concept of metal and semiconducting material junction i.e. existence of schottky barrier during contact between metal and semiconducting material, Liu et al. [283] have verified the triboelectric phenomenon of the MoS_2 based nanogenerator. Here, the authors have executed the triboelectric energy harvesting efficacy by sliding a metal atomic force microscope (AFM) probe on the surface of an MoS_2 semiconducting substrate (Fig. 9c). It has been found that this triboelectric phenomenon can generate higher current density of 10^6 A/m^2 by simple friction between the AFM probe tip and MoS_2 thin film (the film was prepared by pulsed laser deposition technique). This may be due to the collaborative effect of the electronic excitation during friction and schottky barrier between the metal (AFM probe) and semiconducting MoS_2 part. While the conventional triboelectric nanogenerators (TENGs) i.e polymer based TENGs can generate lower current density of 0.1 to 1 A/m^2 since polymer materials have higher impedance values.

Similarly, Park et al. [284] have also developed MoS_2 based triboelectric nanogenerators. For this, MoS_2 mono layer was synthesized by the pulsed laser-directed thermolysis method. The surface–crumpled texture was embedded on the MoS_2 mono layer surface by the pulsed laser-directed synthesis method. As a result, MoS_2 having a crumpled surface resulted in 40 % more power than the equivalent flat surface of MoS_2. Moreover, this nanogenerator shows higher output voltage (~25 V) and current (~1.2 μA) as compared to the flat surface MoS_2 based triboelectric device (output voltage ~ 17 V and current ~ 0.85 μA, respectively). The reason is higher surface roughness was corrugated on the surface of the laser directed MoS_2 layer surface and hence its work function (Φ) value is increased above that of the flat surface based MoS_2 layer. Due to the higher work function value, the crumpled surface based MoS_2 layer can remove electrons easily and therefore charge density on the MoS_2 surface has been increased as compared to the flat surface based MoS_2 layer. Furthermore, MoS_2 and PET based triboelectric nanogenerators were developed by Wu et al. Where, MoS_2 mono layer was used as the friction layer having electron accepting capability and PET was used as the other layer. Since, mono layer of MoS_2 has higher electron acceptance affinity, higher charge density is generated on the surface of same. Therefore, the MoS_2 based triboelectric nanogenerator showed higher charge density i.e. 25.7 W/m^2. which is 120 times higher than the equivalent nanogenerator without MoS_2 [2].

Triboelectricity is built on the principle of contact electrification. However, some recent triboelectric nanogenerators employ contactless interactions for the functioning of these energy harvesters. One such nanogenerator is based on siloxane/eco-flex nanocomposite. Though this idea seems fascinating, the retention of these charges is a challenge in the case of such contactless triboelectric nanogenerators. Hence, in this case, a charge trapping layer namely molybdenum sulphide included with laser induced graphene was introduced. This helped to enhance the surface charge potential many fold. This further improved the triboelectric performance of the nanogenerator. Furthermore, the humidity sensing capability of this nanogenerator was appreciable. The contactless interactions increased the longevity of the device owing to less exposure to wear and tear [285]. Hybrid mechanical sensors based on a combination of triboelectric and flexoelectric effects have also been studied with the help of hollow MoS_2 spheres stacked in multiple layers. The effect of sphere size and layer count on mechanical sensor output performance was also investigated. Because of the difference in electron affinity, triboelectric charges are generated between the hollow spheres and the polymer when pressure is applied. The continuous pressure application further sets up a strain gradient within the layers of the hollow spheres. This strain gradient is responsible for creating an electrical polarization owing to the flexoelectric effect. Thus, when the two phenomena are combined, the mechanical sensor's efficiency increases. Furthermore, as the diameter of the hollow spheres enlarged, the stress gradient also increases with it. This led to an enhancement in the flexoelectric effect and, as a result, in the mechanical sensor's performance [286]. The effect of MoS_2 incorporation in PVDF films was also studied. The insertion of MoS_2 in PVDF films led to the conversion of α to β crystalline phase of the polymer. This resulted in the self-poled nature of the composite film. The effect of annealing on the polymer's crystalline phase content was also explored. Annealing was found to help reduce the crystallite size of the heat-treated pristine polymer film, but with poorly defined structures. Annealed films of MoS2-incorporated PVDF had reduced crystallite size with precisely defined structures. The presence of MoS_2 was confirmed by the evident sponge-like structures in the studies of the nanocomposite carried out [287]. Triboelectric nanogenerators are increasingly being preferred owing to their high-power output. However, the longevity of the device is also dependent on the wear and tear of the contacting surfaces. Sometimes, the electrode or other times the polymer is coated with protective layers to prevent the wearing out of the contacting layers, increasing the device's lifespan. In one such work, the polytetrafluoroethylene film was coated with different coating layers of DLC, MoS_2, and $Ti_3C_2T_x$ (Fig. 10a). It was revealed that the MoS_2-coated films had better output performance as a result of the higher ability of the oxygen and fluorine groups to absorb electrons. This was observed when the triboelectric nanogenerator was operated in contact separation mode. The triboelectric testing films were quite resilient to wear, but as time went on, the output performance of the nanogenerator dropped. This was attributed to the graphitization and potential mass transfer to the mating bodies [288]. Similar work on increasing the lifespan of triboelectric membranes have been carried out on composite membranes of polyvinyl chloride (PVC)/MoS_2 (Fig. 10b). The MoS_2 nanosheets added acted as a solid lubricant that helped to improve the wear resistance of the device while enhancing its output performance at the same time. MoS_2 incorporated PVC membranes generated an output voltage of 398 V, when polyamide membranes were used as their matching pair. MoS_2 helped to increase the surface charge density contributing to the generation of such high output voltage [289].

PVDF has also been doped with MoS_2 in combination with other materials and studied for its triboelectric properties. Triboelectric nanogenerators based on electrospun PVDF incorporated with MoS_2 and carbon nanotubes have generated output voltage above 300 V. Nylon was used as its triboelectric matching pair. The incorporation of carbon nanotubes helped to increase the surface potential. MoS_2 acted as a solid lubricant, that aided in the formation of compact electrospun layers of nanofibers, increasing the longevity of the device. Moreover, the inclusion of MoS_2 and carbon nanotubes synergistically helped to increase the electroactive β phase content of the PVDF polymer. All such types of materials can be used as a source of power for flexible e-wearables [290]. Triboelectric nanogenerators based on p-n junctions generate lower output voltage mostly due to the formation of semiconducting friction layers on the electrode. Recently, a tribodiffusion-based nanogenerator was reported that improved the performance of the nanogenerator manifold. MoS_2 and polypyrrole were used as the triboelectric pair to form the nanogenerator. MoS_2 is n-type material while

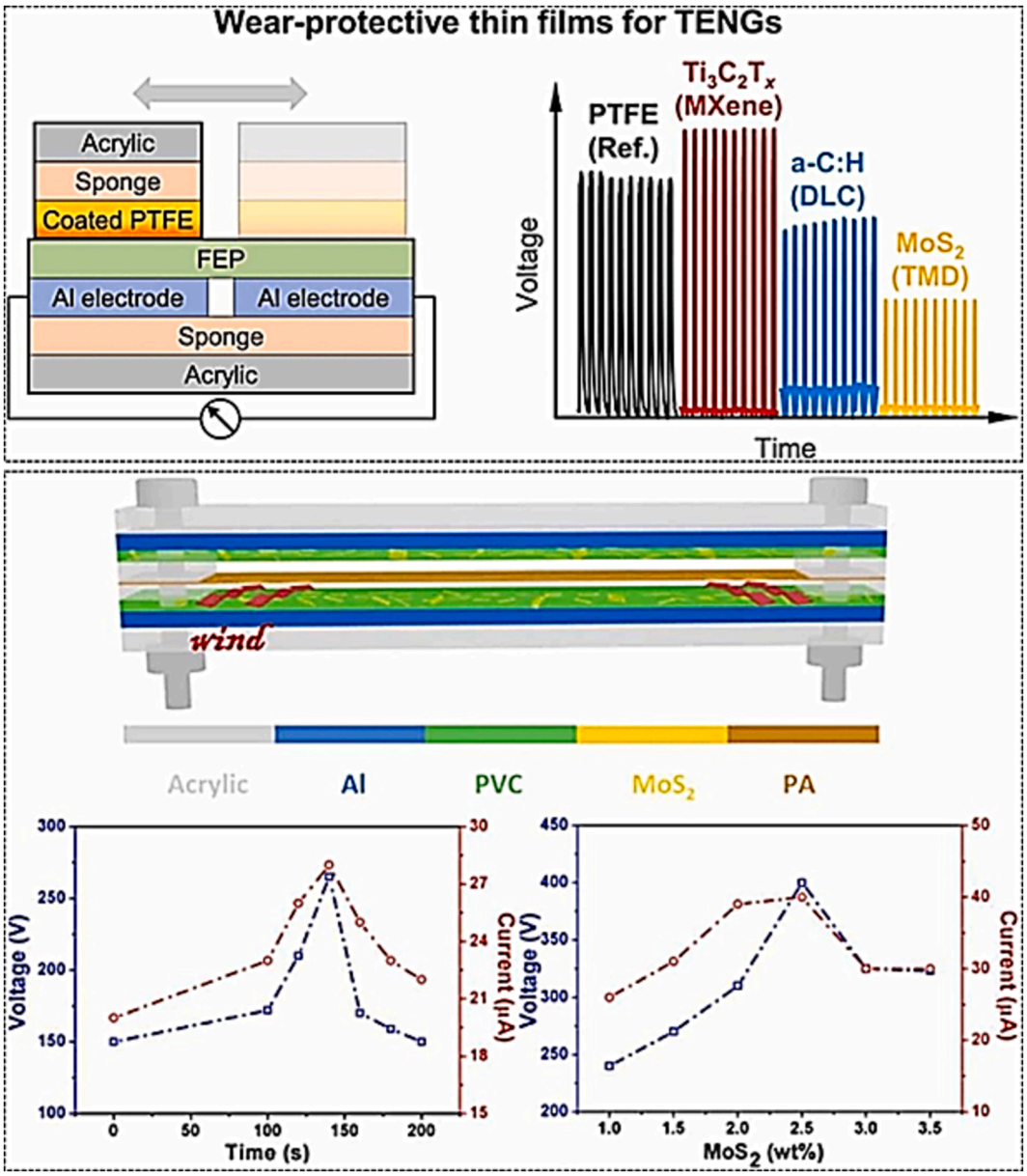

Fig. 10. (a) (i) Thin film based triboelectric energy harvesting, (ii) Triboelectric performance of different thin film materials [288]; (b)(i) Set-up for wind energy harvesting, (ii) Triboelectric performance of the PVC/MoS2 based nanogenerator [289] All essential copyrights and permissions received.

polypyrrole is p-type. When they interact, holes and electrons, repectively disseminate into MoS_2 and polypyrrole, leading to tribodiffusion. This generates an output voltage. The use of silver nanoparticles below the MoS_2 layer helped to improve the output voltage due to increased carrier concentrations. Polypyrrole was also doped with platinum nanoparticles to improve the net voltage output. The use of a piezoelectric material like PVDF-TrFE as one of the layers in the nanogenerator acted as a gate voltage and reduced the overall impedance. A power density of 14.4 mW cm^{-2} was achieved using a load resistance of 1 MΩ [291]. In order to enhance the efficiency of a triboelectric nanogenerator, monolayer MoS_2 was added into the friction layer. It increased the output power density by around 120 times the pristine nanogenerator devoid of monolayer MoS_2. Monolayer MoS_2 basically acts as an electron acceptor layer that captures the electrons and prevents electron-hole pair recombination. Such type of nanogenerator provides insights in the direction of innovating triboelectric nanogenerators with electron trapping sights for improved triboelectric performance [292]. Some of the prominent works featuring MoS_2 as a triboelectric material is represented in Table 6.

5. Applications of MoS_2 based flexible nanogenerators

MoS_2 has been extensively researched for almost a decade, with numerous potential applications being investigated. Fig. 11 shows the applications of MoS_2 based flexible nanogenerators.

5.1. High output energy generation

Direct energy production from fluid motion by low-dimensional raw materials like graphene has garnered a lot of interest due to the abundance of water and the growing demand for clean energy sources. Electricity is created by the movement of a double layer of electrons at the liquid droplet-solid surface interface. Despite efforts to improve graphene nanogenerator performance, the output voltage remains restricted to 100–400 mV [294–297]. The output voltage needs to be raised in order to drive electronic parts and power management circuits.

Table 6
Summary of some of the prominent works featuring MoS_2 as a triboelectric material.

Sl	Material	Method of fabrication	Dimensions	Force/ Pressure	Frequency	Output voltage	Output current	Power density/ power	Application	Ref
1	Bilayer MoS_2 nanosheets	Ultrasonic bath sonication	6.0 cm x 2.0 cm x ~ 100 mm	0.1 kPa-1 kPa	3 Hz	10.20 V	150nA	2.55 mW/ m^2	Capacitor charging and photocatalytic material	[282]
2	MoS_2/Nylon 11 and MoS_2/PVDF-TrFE	Spin coated fims were produced	1 × 1 cm^2	0.15 MPa	–	145 V	NM	50 mW/ cm^2	Capacitor charging and lighting up LEDs	[293]
3	Monolayer MoS_2	Chemical vapour deposition	–	5 kPa	10 Hz	80 V	~7μA	422 μW/ cm2	Lighting up LEDs	[54]
4	Crumpled MoS_2 structure	Laser scribbing onto spin coated films	3 mm × 3 mm	35–160 N	1–10 Hz	25 V	1.2μA	2.25 μW	Haptic sensors	[284]
5	Few layers MoS_2/ PVDF nanofibres	Electrospinning	(1 × 1 cm, 2 × 2 cm^2 and 3 × 3 cm^2)	–	–	50 V	30nA	0.18 mW/ cm2	Lighting up LEDs and energy harvesting from human motion	[263]
6	MoS_2 thin film	Pulse laser depositiom	–	5 nN-30 nN		7–8 mV		l MW/m3	–	[283]
7	Siloxeve/ecoflex nanocomposite with MoS_2/LIG as charge trapping layer	Siloxene prepared by topo-chemical reaction, MoS_2 prepared by prob sonication of MoS_2 powder	3 × 3 cm^2	–	–	31 V at 25 % Rh	–	4.25 μW power	Touchless sensor	[285]
8	Mos_2 hollow spheres	Two step thermal decomposition		0–500 kPa		15 V		6.674 mW/m2 power density	Energy harvesting from human movements	[286]
9	MoS_2/PVDF	Bar-printing	–	10 N	3 Hz	200 V	11.8μA	6.54 μW/ cm2	Power source for smartwatch and smartphone	[287]
10	MoS_2 on PTFE	Sputter coating		2.3 N	1 Hz	31.7 V	88nA	–	Energy harvesting	[288]
11	MoS_2/PVC membranes	Spin coating	120 × 10 × 3 mm			398 V	40μA	1.23mW	Power source to LEDs and water thermometer	[289]
12	MoS_2-Carbon nanotube/PVDF	Electrospinning	~6cm × 6 cm	50 N	1.6 Hz	>300 V	11.5μA	0.484 mV	Harvesting energy from human movements	[290]
13	Monolayer MoS_2 based TENGs	Monolayer MoS_2 prepared by Chemical vapour deposition	1 x 1 cm^2	5 kPa	10 Hz	200 V	–	14.4 mW/ cm2	Capacitor charging	[291]
14	Monolayer MoS_2	Liquid exfoliation	1.5 × 2.5 cm^2	–	–	120 V	–	25.7 W/ m2		[292]

As a result, a 2D semi-metallic graphene substitute may be required. Because MoS_2 is more resistant than graphene, it is anticipated that it will improve output voltage. This idea was abandoned due to difficulties in manufacturing continuous large-area single-layer MoS_2. Li et al. later used sulfurization to produce a multi-layer MoS_2 film with at the centimeter-scale for energy harvesting. However, the output voltage of the resulting film was only 70 V, most likely as a result of the excessive number of MoS_2 layers and the below-par film uniformity [298]. A large-area single-layer MoS_2 film developed by chemical vapor deposition is presented by Aji et al. (2020) [299] as a high energy output nanogenerator (as shown in Fig. 11-high energy output device section) that can generate more than 5 V from the motion of an aqueous NaCl droplet, which increased shunt resistance. They demonstrate how to scale up the MoS_2 nanogenerators by connecting them in series and parallel, producing a three-nanogenerator array with a three-fold boost in output voltage and current. From a larger perspective, the MoS_2 device could be utilized for additional hydrodynamic applications, such as producing electricity from cliffs and rainwater.

5.2. Self-Powered temperature sensor

Mechanical as well as heat energy both exist omnipresent in a nanogenerator (NG) and are typically wasted in our everyday life. It is possible to efficiently capture this waste heat and use it to independently and sustainably power portable electronics while also improving energy efficiency in a variety of other applications. An NG premised on the pyroelectric effect has indeed been developed in order to collect thermal energy and fabricate self-powered sensors [300,301]. The power generated by pyroelectric and NG, on the contrary, is incredibly low and requires improvement for potential implementation. A significant alternative to the pyroelectric effect for waste heat recovery is thermoelectric technology, which has been applied in the arena of space power generation due to its suitable high durability and convenience [302] MoS_2 is a favourable thermoelectric resource, due to its low heat capacity and potentially high Seebeck coefficient and zT [303]. Graphene is a gapless semi-metal with high electrical conductivity, in contrast to MoS_2 [304]. Dollfus et al. created MoS_2 and MoS_2/graphene nanocomposite-based TENGs. The electrical characteristics of those devices were examined using an I-V measurement at ambient conditions. The results showed that MoS_2/graphene nanocomposite has significantly higher electrical conductivity which confirmed that graphene has much higher electron mobility than MoS_2 [305]. Xie et al., 2017 also reported that high-performance thermoelectric devices (as shown in Fig. 11-temperature sensor section) would benefit from a nanocomposite based on the two aforementioned materials because it would combine their positive attributes while avoiding their negative ones [55].

5.3. Photothermal electric generator

Thermal energy harvesting technology has been developed using both the pyroelectric and thermoelectric effects to scavenge thermal

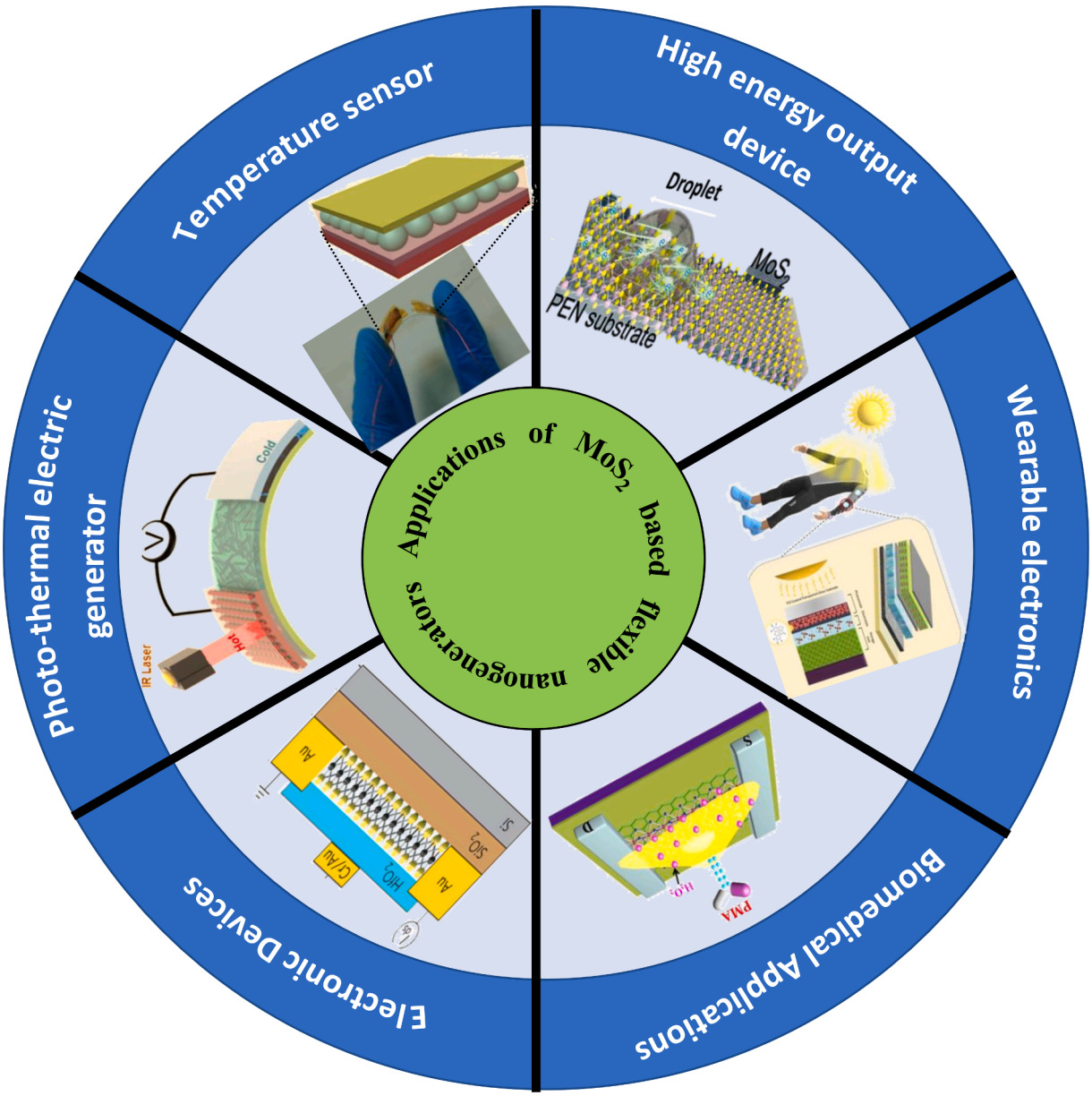

Fig. 11. Applications of MoS_2 based flexible nanogenerators [55,274,299,315,324,335]. All essential copyrights and permissions received.

energy. The thermoelectric energy harvester has been extensively acknowledged as a more operative and well-organized technology than the pyroelectric energy harvester, which generates minute energy [306], but when the ambient temperature is spatially consistent and without variations, there is still a significant issue that needs to be resolved when trying to harvest thermal energy with thermo-electrics [307].

Due to unique photothermal properties of Molybdenum disulfide (MoS_2) is gaining interest for use in photothermal electric generators. These qualities allow for efficient light absorption and subsequent conversion of light into heat. MoS_2 increases light absorption and heat generation by providing a significant surface area through the use of its 2D layered structure components. MoS_2's temperature increases as light is absorbed, creating the conditions for thermoelectric conversion [308]. By means of the Seebeck effect, an electric potential is produced in MoS_2 when the temperature gradient causes charge carriers to migrate. Because MoS_2 may be adjusted for thickness, flaws, and doping, researchers can maximise its performance in photothermal applications [309]. MoS_2-based photothermal generators have potential applications in solar cells and other energy conversion devices and are a promising method of gathering solar energy in practical applications. Although there is still work to be done to improve photothermal energy conversion's overall efficiency, MoS_2 is a strong contender to advance the capabilities of photothermal electric generators due to its special qualities. For instance, MoS_2 has been demonstrated to be a superior photothermal material with greater IR absorbance than graphene oxide and gold nanorods [310,311]. He et al. (2018) present a flexible photo thermoelectric nanogenerator (PTENG) (as shown in Fig. 11-photo thermoelectric generator section) made by combining a MoS_2/PU photothermal layer with tellurium (Te) nanowire-based thermoelectric device for energy harvesting [274].

5.4. Wearable electronics

Molybdenum disulfide (MoS_2) has emerged as a promising material for applications in wearable electronics, offering a unique set of properties conducive to this rapidly evolving field. MoS_2 can be created into a few-layered, 2D material with an atomic thickness thanks to the weak interlayer Van der Waals force, which is adaptable enough for

integration into flexible and stretchable electronic devices [312]. This flexibility allows MoS_2-based components to conform to the contours of wearable surfaces, providing enhanced comfort and adaptability for users. Moreover, MoS_2 exhibits excellent electronic conductivity, which is crucial for ensuring efficient charge transport in wearable devices. Its semiconducting properties further enable the development of thin-film transistors and other electronic components essential for wearable technology [313]. Additionally, MoS_2's compatibility with biological systems is advantageous for applications where the wearable electronics come into direct contact with the human body. The material's biocompatibility, coupled with its mechanical robustness, contributes to its suitability for wearable sensors and health monitoring devices [314]. Researchers are actively exploring MoS_2 for applications ranging from flexible displays and energy storage in smart textiles to sensors for health monitoring, showcasing its potential to drive innovations in the burgeoning field of wearable electronics. For instance, Nardekar et al. 2022 [315] synthesized two-dimensional (2D) dual-functional molybdenum disulfide (MoS_2) quantum sheets (QSs). These have piqued the interest of many researchers because of their potential application in harvesting energy and retrieval for next-generation portable and wearable self-powered electronic goods. His one-of-a-kind MoS_2 QSs-PVDF-based piezoelectric nanogenerator (as shown in Fig. 11-wearable electronics section**)** consistently generates an output voltage of $47V_{pp}$ and a power density of 3.2 mWm^2, both of which are significant compared to pristine PVDF film. Furthermore, the novel PSCPC is united with clothing to directly power wearable electronics by scavenging both natural sunlight and ambient interior light. They were capable of successfully demonstrating the probable use of 1 T-MoS_2 QSs in energy conversion and storage systems. This work directly validates the "Dual-functionality" of 2D MoS_2 QSs, and offers numerous advantageous characteristics such as compact design, stretchability, and economic viability, and can serve as an appropriate platform for constructing battery-free wearable tech.

5.5. Chemical (Re)-activities

Molybdenum disulfide (MoS_2) exhibits noteworthy applications in chemical reactivity, leveraging its unique properties for catalytic processes and other chemical transformations. As a catalyst, MoS_2 has gained attention due to its inherent catalytic activity, especially in hydrogen evolution reactions. Its layered structure provides active sites for catalysis, enabling efficient chemical reactions. MoS_2's catalytic prowess extends beyond hydrogen evolution to include reactions involved in energy storage systems, such as lithium-ion batteries. The material's tunable properties, achieved through modifications in its structure and composition, allow researchers to fine-tune its catalytic performance for specific applications [316]. MoS_2 is also explored for its potential in environmental remediation, acting as a catalyst in processes like photocatalysis for pollutant degradation**.** Beyond catalysis, MoS_2 demonstrates chemical reactivity in sensors, detecting various gases and chemicals due to its sensitivity to surface interactions. The combination of MoS_2's catalytic and sensing capabilities positions it as a versatile material for applications ranging from sustainable energy technologies to environmental monitoring, showcasing its significance in advancing chemical reactivity in diverse fields [317]. For instance here, On the MoS_2 (0 0 0 1) faces, only a sulfuric acid–potassium dichromate solution was observed to induce significant and deep flaws [318]. Additionally, MoS_2 has a high photo corrosion resistance, which could be advantageous in photoelectrochemical applications. The basal plane, which generally has totally synchronized sulphur atoms, was thought to be relatively inert while metallic edge planes with sulphur vacancies were the most active MoS_2 sites [319,320]. The sulphur becomes significantly more reactive after the initial CS bond in thiophene is broken, and the last extrusion may take place at a different location on the cluster to complete the hydrodesulfurization procedure. When desulfurizing oil products, MoS_2 can be utilised to eliminate molecules that contain sulphur [321]**.**

5.6. Electronic devices

MoS_2 has a number of intriguing properties, one of which is that its bandgap is non-zero when it is compared to graphene. Because of its changeable conductivity, MoS_2 serves as a semiconductor and is useful for electrical and logical devices [322]. Because of its atomically thin layers, MoS_2, a semiconductor with a direct bandgap, can be used to create thin-film transistors (TFTs), an essential part of contemporary electronics. Excellent electronic performance is demonstrated by MoS_2-based TFTs, including high carrier mobility, which is essential for effective charge transport in electronic circuits [323]. Furthermore, MoS_2 is a perfect fit for flexible electronics and wearable technology (Fig. 11-wearable electronics section**)** due to its variable conductivity, which makes it compatible with transparent and flexible substrates. The creation of flexible displays, sensors, and other bending electronic components is made possible by the material's mechanical flexibility, which enables it to bend and conform to unusual shapes without compromising its electronic capabilities [324]. Because MoS_2 can absorb and emit light with such efficiency, it has also shown promise in optoelectronic devices like photodetectors and light-emitting diodes (LEDs). It is hence useful for applications in communication, sensing, and imaging technologies [325]. Because of the controllable electrostatic properties of MoS_2, short-channel FETs and minimal power electronic devices are now possible. The performance of a MoS_2 transistor with a 5-nm gate length appears to satisfy the standards of the 2026 Road Map for low operating power (LOP) devices [46]. When compared to ultrathin Si transistors, it possesses a greater driving current, a smaller source-drain current leakage, and a higher operating frequency. With greater stability than silicon transistors, 2D MoS_2 can be used in analogue electronics thanks to its lower tunnelling current and better on/off current ratio. Typically, MoS_2 monolayer transistors exhibit N-type behaviour, and their carrier mobilities are close to 350 $cm^2\ V^{-1}\ s^{-1}$ (or 500 times lower than graphene). However, they can exhibit enormous on/off ratios of 108 when made into field-effect transistors, which makes them effective and desirable for switching and very efficient logic circuits. It was found that the strain and electronic noise effects were crucial for the $SLMoS_2$ transistor [326,327].

5.7. Biomedical applications

Two-dimensional substance molybdenum disulfide (MoS_2) has drawn a lot of interest recently due to its possible uses in biomedical devices. MoS_2's unique properties, such as its biocompatibility, tunable electronic structure, and large surface area, make it a promising candidate for various biomedical applications such as suitable for interfacing with biological systems, minimizing adverse reactions. Because of its special qualities like its huge surface area, changeable electrical structure, and biocompatibility MoS_2 is an attractive option for a number of biomedical uses, including limiting negative reactions and interacting with biological systems. The creation of biosensors is one noteworthy use. Excellent sensitivity and selectivity have been demonstrated by MoS_2-based biosensors in the detection of biomolecules, such as DNA and proteins. Because of the material's large surface area, biomolecules can be immobilised more effectively, improving sensor performance [328]. MoS_2 has also been investigated for use in medication delivery systems. Therapeutic substances can be controllably encapsulated and released by means of its layered structure. This feature is very helpful for focused medication distribution, which lowers adverse effects and increases treatment effectiveness [329]. As MoS_2 monolayers are a bioabsorbable electrical component that can take up to two months to disintegrate in living cells, according to current research [330]. The results were verified in vivo and in vitro (on animals). Due to its biocompatibility, absorbability, and extremely tiny-scale transistor performance, MoS_2 will be used in the diagnosis and treatment of numerous ailments. MoS_2 is thought to be involved in the treatment of tumor and Alzheimer's disease, despite the fact that certain

investigations have found Mo to be harmful [331–333]. The nanosheets can be employed with microfluidic devices built on polydimethylsiloxane (PDMS) microchips. You can utilize the MoS_2 2D layer to find different amino acids [334]. MoS_2 nanosheets are compiled just on a substratum of reduced graphene oxide (RGO), in order to create a MoS_2/RGO FET sensor (as shown in Fig. 11-biomedical applications section) that can recognize hydrogen peroxide H_2O_2, which has recently been discovered as a biomarker for tumor cells [335]. It is renowned for its biocompatibility and function in the diagnosis and treatment of cancer.

6. Challenges and perspectives

Nanogenerators (NGs) have a lot of potential to be utilised as sources of energy or self-sustaining wearable sensors for smart and portable electronics in the future because of their adaptability, durability, and versatility. In such cases, MoS_2 is an outstanding material for energy harvesting applications. It has often been fabricated in the form of a nanogenerator to cater to the power requirements of electronic applications. No wonder, the performance of these nanogenerators based on triboelectric, piezoelectric, or thermoelectric effect has been outstanding; however, the reliability and consistency of its performance need thoughtful attention. Devices made from monolayer MoS_2 face problems of structural stability owing to their brittle nature. To address these issues, MoS_2 has often been engineered in the form of composites [336]. Several methods of composite fabrication like solution casting and electrospinning have been employed to develop MoS_2-based composites. The solution-cast composite film-based nanogenerators should have thickness engineered in such a way that they become conformable to the substrate they are integrated into. Often, thick films have higher rigidity that restricts their flexible movement, rendering them unfit for integration into electronic wearables. Nanogenerators based on them thus would be inefficient in harvesting energy from mechanical movements. The electrospun nanocomposites face issues of structural stability. They have poor abrasion resistance and tend to wear out with an increasing number of performance cycles. Electrospun nanogenerators thus have a limited lifespan. They are often encapsulated with a polymer coating to enhance their longevity. The power output of these nanogenerators is minuscule compared to the humungous demand for energy [337–341]. Research should be focused on directions that help to upscale the power output of these nanogenerators. Further, standardization of the method of assessing the energy harvesting capability of such nanogenerators is necessary. This would help to assess and compare the performance of the nanogenerators on a normalised platform. But, despite the continuous investigations and excellent applications of NGs, some common challenges are faced by NGs and require the critical attention of researchers. There are:

(a) **Synthesis and scalability:** One challenge is the large-scale synthesis of high-quality MoS2 with controlled thickness and defect density. While various synthesis methods exist, such as the CVD process, hydrothermal synthesis, and the exfoliation technique, achieving uniformity and scalability remains an ongoing challenge. Additionally, the MoS2 structure has various faults that, when used in device applications, result in performance degradation and low dependability. For instance, CVD-grown MoS2 layers are highly reactive and feature a lot of dangling bonds. Examining grain boundaries and point defects leads to the application of defect engineering techniques to manage MoS2 faults. While solid-phase precursor (such as MoO_3, MoS_2 or WO_3) -based chemical vapour deposition (CVD) has demonstrated improved thickness control on a large scale, the electrical performance of the resultant material, which is typically reported from a small number of devices in specific areas, does not demonstrate spatially uniform high carrier mobility [342]. Due to its atomically thin structure and lack of surface dangling bonds, ultrathin 2D transition metal dichalcogenide (TMD) overcomes the limitations of short channel effects and reduced mobility. MoS_2 because of the challenges involved in pre-depositing a minuscule amount of Mo. For example, if all the Mo atoms per unit area are totally converted to MoS_2, then either a single MoO_3 layer or a third layer of a Mo thin film is needed to make a precisely regulated 1L MoS_2 film. This is almost difficult to control [343]. As per the literature reported earlier, the best way ahead is to produce epitaxial monolayers using direct growth and environmentally friendly processes like molecular beam epitaxy (MBE) and pulsed laser deposition (PLD), taking into account the difficulties associated with the synthesis of large-area excellent quality low dimensional layers [344]. However, many improvements are still needed concerning large-area deposition of MoS_2 layer.

(b) **Device architecture and optimization:** Designing an efficient and reliable device architecture for flexible nanogenerators requires careful consideration of parameters such as the arrangement of MoS_2 layers, interfacial properties, and electrode configurations. Optimizing these factors to maximize energy conversion efficiency while maintaining flexibility and durability is a complex task.

(c) **Arrangement of MoS_2 layers:** MoS_2 exhibits intrinsic piezoelectric properties at the monolayer level, but the piezoelectric response diminishes when the quantity of layers rises. Maintaining the monolayer structure or enhancing the piezoelectricity in thicker MoS_2 films is a challenge to improving the energy conversion efficiency of nanogenerators.

(d) **Interfacial properties:** Secondly, the interfacial properties of MoS_2-based nanogenerators play a significant influence in device efficiency and dependability. This involves selecting appropriate electrode materials, surface functionalization, interfacial layers, or device architectures to enhance charge transfer, reduce interfacial resistance, and improve overall device performance. Direct sputtering for electrode deposition and also conductive tapes are utilized as an electrode material, which gives higher capacitance values and potential gaps between the piezoelectric substance and electrode, respectively. Therefore, patterned devices using lithographic patterning, shadow masking, or interdigitated electrodes are explored day by day now due to their lower capacitance values.

(e) **Durability and stability:** Next, the durability and stability of MoS_2-based devices can be influenced by various factors in which the effect of the techniques used for the device fabrication has a major effect. While solution casting and electrospinning are versatile techniques for fabricating MoS_2-based materials, here are some limitations of solution casting and electrospinning when working with MoS_2 materials. Achieving uniformity and controlling the thickness and morphology of MoS_2 films or nanofibers can be more difficult with these methods. It often requires optimization of various parameters, such as solvent composition, concentration, casting conditions, or electrospinning parameters, to obtain the desired properties. Solution casting and electrospinning may result in films or fibers with lower homogeneity and quality. The use of solvents and the process of solvent evaporation in solution casting can lead to the formation of defects, non-uniformity, or cracking in the films. Similarly, electrospinning can result in non-uniform fibre diameters, bead formation, agglomeration, or uneven distribution of MoS_2 material within the fibres. Hence the technique of spin-coating is being used extensively. Spin coating is a well-established and scalable technique, allowing for consistent and reproducible fabrication of MoS_2 films. This scalability and reproducibility ensure that the performance and stability of spin coated MoS_2 devices can be reliably achieved across different batches or manufacturing processes. Although the edge effect and edge film quality (like

material tends to accumulate at the edges of the substrate, leading to non-uniform film thickness and poor edge quality) of a spin-coated film is still a challenging task.

(f) **Aging and degradation mechanisms:** MoS_2-based devices may undergo aging or degradation over extended operation periods, leading to changes in electrical properties, decreased performance, or even failure. Investigating the underlying degradation mechanisms and developing strategies to mitigate them, such as optimizing material quality, passivation techniques, or device encapsulation, are essential for enhancing device durability and stability.

Future research should concentrate on creating moderate materials with high outcomes and more stability. Therefore, it is crucial for designers of nanogenerators to take into account the desired power generation, dimensions and weight constraints, operating time, and environmental exposures (such as temperature, resistance, radioactivity, weather, involuntary movements, and relative humidity). They should also take into account green energy acquisition mechanisms, materials that are better suited for nanogenerator electro-mechanical behaviour, the process parameters, the style of packaging, the bare minimum of electronic components, and other elements. It is also difficult to implement appropriate analytical and numerical modelling approaches in the design of nanogenerators in order to determine the appropriate electromechanical configuration and operating principle for these devices under a variety of operating conditions. The development of effective energy storage systems and electrical interfaces that are very effective while using little power is also crucial. Other concerns relate to the integration of energy storage devices, mechanical robustness, chemical stability, reliability of the electromechanical behaviour of nanogenerators, low-cost production methods, and stability [345].

7. Summary

This article provides a conclusive review on the different frontiers of MoS_2 starting from its synthesis, applications, challenges and perspectives. MoS_2 belonging to the TMDC family, is emerging as a promising material of interest due to its lucrative properties. It surpasses the graphene and Si derivative based materials in several aspects as has been highlighted above. The facile and numerous synthesis routes of this material, helps to tailor the material properties as per end use application. The versatility of this material has found its applications in extended domains of piezoelectric, triboelectric and thermoelectric energy harvesting. This semiconducting TMDC has also been used in electronic devices to scale up their energy generation. The pyroelectric properties of MoS_2 are utilized through the conversion of wasted heat to electrical energy. Self-powered temperature sensing is another extended application of this property of the semiconductor. Interestingly, MoS_2 has also found application in the biomedical field: tt has been used for detection of breast cancer. However, there are reports that state the toxicity of Mo as a biocompatible material and research is still being carried out to confirm the same. The inability of monolayer MoS_2 to sustain large strain applications, limits its boundaries in the optoelectronics field. Hence, there exists a wide scope of research in this area. Further tuning of the optical properties of the semiconductor would help to expand its spectrum of application in the electronics field. It is also important to take care of the structural properties of this semiconductor at elevated temperature. The degradation behaviour of its crystals needs to be studied well to tune and manoeuvre its properties. Thus, it is clear that, although this material has been intensively investigated, there still exist plenty of open questions relating to enhancing its properties and expanding its spectrum of application.

CRediT authorship contribution statement

Mayuri Srivastava: Conceptualization, Investigation, Methodology, Software, Writing – original draft. **Swagata Banerjee:** Conceptualization, Investigation, Methodology, Software, Writing – original draft. **Satyaranjan Bairagi:** Conceptualization, Investigation, Methodology, Software, Writing – original draft, Writing – review & editing. **Preeti Singh:** Conceptualization, Investigation, Methodology, Software, Writing – original draft. **Bipin Kumar:** Conceptualization, Investigation, Methodology, Software, Supervision, Validation, Writing – review & editing. **Pushpapraj Singh:** Conceptualization, Funding acquisition, Investigation, Methodology, Project administration, Resources, Software, Supervision, Validation, Writing – review & editing. **Ravindra D. Kale:** Conceptualization, Formal analysis, Investigation, Methodology, Software, Writing – review & editing. **Daniel M. Mulvihill:** Conceptualization, Formal analysis, Funding acquisition, Investigation, Methodology, Project administration, Resources, Software, Validation, Writing – original draft, Writing – review & editing. **S. Wazed Ali:** .

Declaration of competing interest

The authors declare that they have no known competing financial interests or personal relationships that could have appeared to influence the work reported in this paper.

Data availability

Data will be made available on request.

Acknowledgements

Authors are grateful to the Department of Science and Technology and The Government of India for funding the work on piezoelectric device development and as a part of that the authors have prepared this review article (Sanction Letter: DST/TDT/DDP-05/2018 (G)) under Device Development Program). The authors would also like to acknowledge the support of the UK Engineering and Physical Sciences Research Council (EPSRC) through grant Ref. EP/V003380/1: 'Next Generation Energy Autonomous Textile Fabrics based on Triboelectric Nanogenerators'.

References

[1] N. Izadyar, H.C. Ong, W.T. Chong, K.Y. Leong, Resource assessment of the renewable energy potential for a remote area: a review, Renew. Sustain. Energy Rev. 62 (2016) 908–923, https://doi.org/10.1016/J.RSER.2016.05.005.

[2] T. Wu, Y. Song, Z. Shi, D. Liu, S. Chen, C. Xiong, Q. Yang, High-performance nanogenerators based on flexible cellulose nanofibril/MoS2 nanosheet composite piezoelectric films for energy harvesting, Nano Energy 80 (2021), 105541, https://doi.org/10.1016/j.nanoen.2020.105541.

[3] V. Singh, B. Singh, MoS2-PVDF/PDMS based flexible hybrid piezo-triboelectric nanogenerator for harvesting mechanical energy, J Alloys Compd. 941 (2023), 168850, https://doi.org/10.1016/j.jallcom.2023.168850.

[4] I. Dincer, Renewable energy and sustainable development: a crucial review, Renew. Sustain. Energy Rev. 4 (2000) 157–175, https://doi.org/10.1016/S1364-0321(99)00011-8.

[5] Z.L. Wang, Toward self-powered sensor networks, Nano Today 5 (2010) 512–514, https://doi.org/10.1016/J.NANTOD.2010.09.001.

[6] Q. Xu, J. Wen, Y. Qin, Development and outlook of high output piezoelectric nanogenerators, Nano Energy 86 (2021), 106080, https://doi.org/10.1016/J.NANOEN.2021.106080.

[7] S. Sripadmanabhan Indira C. Aravind Vaithilingam K.S.P. Oruganti F. Mohd S. Rahman Nanogenerators as a Sustainable Power Source: State of Art, Applications, and Challenges Nanomaterials 9 5 773.

[8] H. Askari, A. Khajepour, M.B. Khamesee, Z. Saadatnia, Z.L. Wang, Piezoelectric and triboelectric nanogenerators: trends and impacts, Nano Today 22 (2018) 10–13, https://doi.org/10.1016/J.NANTOD.2018.08.001.

[9] Z.L. Wang, J. Song, Piezoelectric nanogenerators based on zinc oxide nanowire arrays, accessed November 25, 2022, Science 312 (2006) (1979) 242–246, https://doi.org/10.1126/science.1124005.

[10] H. Jiang, Y. Su, J. Zhu, H. Lu, X. Meng, Piezoelectric and pyroelectric properties of intrinsic GaN nanowires and nanotubes: Size and shape effects, Nano Energy 45 (2018) 359–367, https://doi.org/10.1016/J.NANOEN.2018.01.010.

[11] Y.J. Ko, D.Y. Kim, S.S. Won, C.W. Ahn, I.W. Kim, A.I. Kingon, S.H. Kim, J.H. Ko, J. H. Jung, Flexible Pb(Zr0.52Ti0.48)O3 films for a hybrid piezoelectric-pyroelectric nanogenerator under harsh environments, ACS Appl Mater Interfaces. 8 (2016)

6504–6511, https://doi.org/10.1021/ACSAMI.6B00054/SUPPL_FILE/AM6B00054_SI_003.AVI.
[12] Y. Zhao, Q. Liao, G. Zhang, Z. Zhang, Q. Liang, X. Liao, Y. Zhang, High output piezoelectric nanocomposite generators composed of oriented BaTiO3 NPs@PVDF, Nano Energy 11 (2015) 719–727, https://doi.org/10.1016/J.NANOEN.2014.11.061.
[13] P. Sahatiya, S.S. Jones, S. Badhulika, 2D MoS2–carbon quantum dot hybrid based large area, flexible UV–vis–NIR photodetector on paper substrate, Appl Mater Today. 10 (2018) 106–114, https://doi.org/10.1016/J.APMT.2017.12.013.
[14] P. Majumder, R. Gangopadhyay, Evolution of graphene oxide (GO)-based nanohybrid materials with diverse compositions: an overview, RSC Adv. 12 (2022) 5686–5719, https://doi.org/10.1039/D1RA06731A.
[15] S. S. Patil, L. Reddy Nagappagari, G. Kamble, D. E. Shinde, K. Lee, Nanocomposite Materials for Biomedical and Energy Storage Applications, IntechOpen, 2022.
[16] X. Duan, C. Wang, A. Pan, R. Yu, X.D.-C.S. Reviews, undefined 2015, Two-dimensional transition metal dichalcogenides as atomically thin semiconductors: opportunities and challenges, Pubs.Rsc.OrgX Duan, C Wang, A Pan, R Yu, X DuanChemical Society Reviews, 2015•pubs.Rsc.Org. (n.d.). https://pubs.rsc.org/en/content/articlehtml/2015/cs/c5cs00507h?casa_token=5fx8d470TtoAAAAA:mYGTv4OOuaFVE6hL3wbMpZIySdEIUg08jRcENzUJUVvJY4YxBV_NjaVUz1dYzkQEKUVr9N4Tju_Vtxw (accessed November 25, 2023).
[17] G. Algara-Siller, N. Severin, S.Y. Chong, T. Björkman, R.G. Palgrave, A. Laybourn, M. Antonietti, Y.Z. Khimyak, A.V. Krasheninnikov, J.P. Rabe, U. Kaiser, A. I. Cooper, A. Thomas, M.J. Bojdys, Triazine-based graphitic carbon nitride: a two-dimensional semiconductor, Angewandte Chemie - International Edition. 53 (2014) 7450–7455, https://doi.org/10.1002/ANIE.201402191.
[18] Q. Weng, X. Wang, X. Wang, … Y.B.-C.S., undefined 2016, Functionalized hexagonal boron nitride nanomaterials: emerging properties and applications, Pubs.Rsc.OrgQ Weng, X Wang, X Wang, Y Bando, D GolbergChemical Society Reviews, 2016•pubs.Rsc.Org. (n.d.). https://pubs.rsc.org/en/content/articlehtml/2016/cs/c5cs00869g (accessed November 25, 2023).
[19] S.C. Dhanabalan, J.S. Ponraj, Z. Guo, S. Li, Q. Bao, H. Zhang, Emerging trends in phosphorene fabrication towards next generation devices, Adv. Sci. 4 (6) (2017).
[20] C. Huo, B. Cai, Z. Yuan, B. Ma, H. Zeng, Two-dimensional metal halide perovskites: theory, synthesis, and optoelectronics, Small Methods. 1 (2017), https://doi.org/10.1002/SMTD.201600018.
[21] W. Huang, L. Hu, Y. Tang, Z. Xie, H. Zhang, Recent advances in functional 2d mxene-based nanostructures for next-generation devices, Adv Funct Mater. 30 (2020), https://doi.org/10.1002/ADFM.202005223.
[22] W. Huang, C. Ma, C. Li, Y. Zhang, L. Hu, T. Chen, Y. Tang, J. Ju, H. Zhang, Highly stable MXene (V2CTx)-based harmonic pulse generation, Nanophotonics. 9 (2020) 2577–2585, https://doi.org/10.1515/NANOPH-2020-0134/HTML.
[23] M. Wang, J. Zhu, Y. Zi, W. Huang, 3D mxene sponge: facile synthesis, excellent hydrophobicity, and high photothermal efficiency for waste oil collection and purification, ACS Appl Mater Interfaces. 13 (2021) 47302–47312, https://doi.org/10.1021/ACSAMI.1C15064.
[24] H. Hu, Z. Shi, K. Khan, R. Cao, W. Liang, A.K. Tareen, Y. Zhang, W. Huang, Z. Guo, X. Luo, H. Zhang, Recent advances in doping engineering of black phosphorus, J Mater Chem A Mater. 8 (2020) 5421–5441, https://doi.org/10.1039/D0TA00416B.
[25] M. Wang, J. Zhu, Y. Zi, Z.G. Wu, H. Hu, Z. Xie, Y. Zhang, L. Hu, W. Huang, Functional two-dimensional black phosphorus nanostructures towards next-generation devices, J Mater Chem A Mater. 9 (2021) 12433–12473, https://doi.org/10.1039/D1TA02027G.
[26] M. Wang Y.i. Hu J. Pu Y. Zi W. Huang Emerging Xene-Based Single-Atom Catalysts: Theory, Synthesis, and Catalytic Applications.
[27] Y.i. Hu, M. Wang, L. Hu, Y. Hu, J. Guo, Z. Xie, S. Wei, Y. Wang, Y. Zi, H. Zhang, Q. Wang, W. Huang, Recent advances in two-dimensional graphdiyne for nanophotonic applications, Chem. Eng. J. 450 (2022) 138228.
[28] Y. Hu, J. Pu, Y. Hu, Y. Zi, H. Chen, M. Wang, W. Huang, Construction of Reinforced Self-Cleaning and Efficient Photothermal PDMS@GDY@Cu Sponges toward Anticorrosion and Antibacterial Applications, Nanomaterials. 13 (2023). https://doi.org/10.3390/NANO13162381.
[29] W. Huang, J. Zhu, M. Wang, L. Hu, Y. Tang, Y. Shu, Z. Xie, H. Zhang, Emerging mono-elemental bismuth nanostructures: controlled synthesis and their versatile applications, Adv Funct Mater. 31 (2021) 2007584, https://doi.org/10.1002/ADFM.202007584.
[30] M. Wang, Y. Hu, Y. Zi, W. Huang, Functionalized hybridization of bismuth nanostructures for highly improved nanophotonics, APL Mater. 10 (2022). https://doi.org/10.1063/5.0091341.
[31] W. Huang, M. Wang, L. Hu, C. Wang, Z. Xie, H. Zhang, Recent advances in semiconducting monoelemental selenium nanostructures for device applications, Adv Funct Materials 30 (42) (2020).
[32] X. Jiang, W. Huang, R. Wang, H. Li, X. Xia, X. Zhao, L. Hu, T. Chen, Y. Tang, H. Zhang, Photocarrier relaxation pathways in selenium quantum dots and their application in UV-Vis photodetection, Nanoscale 12 (2020) 11232–11241, https://doi.org/10.1039/C9NR10235C.
[33] W. Huang, Y.e. Zhang, Q.i. You, P.u. Huang, Y. Wang, Z.N. Huang, Y. Ge, L. Wu, Z. Dong, X. Dai, Y. Xiang, J. Li, X. Zhang, H. Zhang, Enhanced photodetection properties of tellurium@selenium roll-to-roll nanotube heterojunctions, Small 15 (23) (2019).
[34] Z. Xie, B. Zhang, Y. Ge, Y. Zhu, G. Nie, Y.F. Song, C.K. Lim, H. Zhang, P.N. Prasad, Chemistry, functionalization, and applications of recent monoelemental two-dimensional materials and their heterostructures, Chem Rev. 122 (2022) 1127–1207, https://doi.org/10.1021/ACS.CHEMREV.1C00165.
[35] S. Behura, C. Wang, Y. Wen, V.B.-N. Photonics, undefined 2019, Graphene–semiconductor heterojunction sheds light on emerging photovoltaics, Nature.ComSK Behura, C Wang, Y Wen, V BerryNature Photonics, 2019•nature.Com. (n.d.). https://idp.nature.com/authorize/casa?redirect_uri=https://www.nature.com/articles/s41566-019-0391-9&casa_token=fjeTcZ7nuFsAAAAA:UQJV-Ewq6mZqY-WIGQDjNkBnDNVl1Xz9Ri5U4WPASN1nekTYrDLWGUBaUg04dMhnaPi4pYZAybOz5bjhmA (accessed November 25, 2023).
[36] S. Han, J. Lee, J. Lin, S. Kim, J.K.-N. Energy, undefined 2019, Piezo/triboelectric nanogenerators based on 2-dimensional layered structure materials, Elsevier. (n.d.). https://www.sciencedirect.com/science/article/pii/S2211285518309947?casa_token=EgOeHrksdr0AAAAA:-HP06dxuVNKLYcAWn4W0khoEJPa-YLvdBaExU8ffjq5i8JAmbAkKS2WtPEvaUFCckUZ9_p1IEA (accessed November 25, 2023).
[37] M.-J. Lee J.-H. Ahn J.H. Sung H. Heo S.G. Jeon W. Lee J.Y. Song K.-H. Hong B. Choi S.-H. Lee M.-H. Jo Thermoelectric materials by using two-dimensional materials with negative correlation between electrical and thermal conductivity Nat Commun 7 1.
[38] Z. Zhang, S. Yang, P. Zhang, J. Zhang, … G.C.-N., undefined 2019, Mechanically strong MXene/Kevlar nanofiber composite membranes as high-performance nanofluidic osmotic power generators, Nature.ComZ Zhang, S Yang, P Zhang, J Zhang, G Chen, X FengNature Communications, 2019•nature.Com. (n.d.). https://www.nature.com/articles/s41467-019-10885-8 (accessed November 25, 2023).
[39] R. Zhang, M. Hummelgard, J. Örtegren, M. Olsen, H. Andersson, Y. Yang, H. Olin, Human body constituted triboelectric nanogenerators as energy harvestersCode Transmitters, and Motion Sensors, ACS Appl Energy Mater. 1 (2018) 2955–2960, https://doi.org/10.1021/ACSAEM.8B00667/SUPPL_FILE/AE8B00667_SI_003.MOV.
[40] G. Khandelwal, S. Deswal, … D.S.-J. of P., undefined 2023, Recent developments in 2D materials for energy harvesting applications, Iopscience.Iop.OrgG Khandelwal, S Deswal, D Shakthivel, R DahiyaJournal of Physics: Energy, 2023•iopscience.Iop.Org. (n.d.). https://iopscience.iop.org/article/10.1088/2515-7655/acc7c8/meta (accessed November 27, 2023).
[41] N.A. Kumar, M.A. Dar, R. Gul, J.-B. Baek, Graphene and molybdenum disulfide hybrids: synthesis and applications, Mater. Today 18 (2015) 286–298, https://doi.org/10.1016/j.mattod.2015.01.016.
[42] M. Derakhshi, S. Daemi, P. Shahini, A. Habibzadeh, E. Mostafavi, A.A. Ashkarran, Two-dimensional nanomaterials beyond graphene for biomedical applications, J Funct Biomater. 13 (2022) 27, https://doi.org/10.3390/jfb13010027.
[43] S.A. Han, J.-H. Lee, W. Seung, J. Lee, S.-W. Kim, J.H. Kim, Patchable and Implantable 2D Nanogenerator, Small 17 (9) (2021).
[44] N. Thomas, S. Mathew, K.M. Nair, K. O'Dowd, P. Forouzandeh, A. Goswami, G. McGranaghan, S.C. Pillai, 2D MoS2: structure, mechanisms, and photocatalytic applications, Materials Today Sustainability. 13 (2021) 100073.
[45] G. Yi, E. Macha, J. Van Dyke, R. Ed Macha, T. McKay, M.L. Free, Recent progress on research of molybdenite flotation: a review, Adv. Colloid Interface Sci. 295 (2021) 102466.
[46] K. Alam, R.K. Lake, Monolayer MoS2 transistors beyond the technology road map, IEEE Trans Electron Devices. 59 (2012) 3250–3254, https://doi.org/10.1109/TED.2012.2218283.
[47] D. Gupta, V. Chauhan, R. Kumar, A comprehensive review on synthesis and applications of molybdenum disulfide (MoS2) material: Past and recent developments, Inorg Chem Commun. 121 (2020) 108200.
[48] A.R. Beal, H.P. Hughes, Kramers-Kronig analysis of the reflectivity spectra of 2H-MoS 2, 2H-MoSe 2 and 2H-MoTe 2, J. Phys. C Solid State Phys. 12 (1979) 881–890, https://doi.org/10.1088/0022-3719/12/5/017.
[49] K. Kobayashi, J. Yamauchi, Electronic structure and scanning-tunneling-microscopy image of molybdenum dichalcogenide surfaces, Phys Rev b. 51 (23) (1995) 17085–17095.
[50] W. Zhao, J. Pan, Y. Fang, X. Che, D. Wang, K. Bu, F. Huang, Metastable mos2: crystal structure, electronic band structure, synthetic approach and intriguing physical properties, chemistry – A, European Journal. 24 (2018) 15942–15954, https://doi.org/10.1002/CHEM.201801018.
[51] O. Samy, D. Birowosuto, A. El Moutaouakil, A short review on Molybdenum disulfide (MoS 2) applications and challenges, in: 2021 6th International Conference on Renewable Energy: Generation and Applications (ICREGA), IEEE, 2021: pp. 220–222. https://doi.org/10.1109/ICREGA50506.2021.9388220.
[52] Quanta Magazine (n.d.). accessed January 15, 2023 https://www.quantamagazine.org/physics-duo-finds-magic-in-two-dimensions-20220816/.
[53] M. Srivastava, S. Kumar, M. Yousuf, B. Kumar, P. Singh, S. Wazed Ali, Reaching high piezoelectric performance with rotating directional-field-aligned pvdf–mos 2 piezo-polymer applicable for large-area flexible electronics, Macromol Rapid Commun. 2300315 (2023) 1–10, https://doi.org/10.1002/marc.202300315.
[54] M. Kim, S.H. Kim, M.U. Park, ChangJun Lee, M. Kim, Y. Yi, K.-H. Yoo, MoS2 triboelectric nanogenerators based on depletion layers, Nano Energy 65 (2019) 104079.
[55] Y. Xie, T.-M. Chou, W. Yang, M. He, Y. Zhao, N. Li, Z.-H. Lin, Flexible thermoelectric nanogenerator based on the MoS2/graphene nanocomposite and its application for a self-powered temperature sensor, Semicond Sci Technol. 32 (4) (2017) 044003.
[56] W. Gu, Y. Yan, C. Zhang, C. Ding, Y. Xian, One-step synthesis of water-soluble mos2 quantum dots via a hydrothermal method as a fluorescent probe for hyaluronidase detection, ACS Appl Mater Interfaces. 8 (2016) 11272–11279, https://doi.org/10.1021/ACSAMI.6B01166.

[57] K. Bazaka, I. Levchenko, J.W.M. Lim, O. Baranov, C. Corbella, S. Xu, M. Keidar, MoS 2 -based nanostructures: synthesis and applications in medicine, J Phys D Appl Phys. 52 (18) (2019) 183001.

[58] M.R. Vazirisereshk, A. Martini, D.A. Strubbe, M.Z. Baykara, Solid lubrication with MoS2: a Review, Lubricants. 7 (2019) 57, https://doi.org/10.3390/lubricants7070057.

[59] N. Izyumskaya, D.O. Demchenko, V. Avrutin, Ü. Özgür, H. Morkoç, Two-dimensional MoS_2 as a new material for electronic devices, Journals. Tubitak. Gov. Tr. 38 (2014) 478–496.

[60] C.L.C. Rodriguez, M.A.B.S. Nunes, P.S. Garcia, G.J.M. Fechine, Molybdenum disulfide as a filler for a polymeric matrix at an ultralow content: polystyrene case, Polym Test. 93 (2021), 106882, https://doi.org/10.1016/j.polymertesting.2020.106882.

[61] R.F. Sebenik, A.R. Burkin, R.R. Dorfler, J.M. Laferty, G. Leichtfried, H. Meyer-Grünow, P.C.H. Mitchell, M.S. Vukasovich, D.A. Church, G.G. Van Riper, J. C. Gilliland, S.A. Thielke, Molybdenum and molybdenum compounds, ullmann's encyclopedia of industrial, Chemistry (2000), https://doi.org/10.1002/14356007.A16_655.

[62] Z. He, W. Que, Molybdenum disulfide nanomaterials: Structures, properties, synthesis and recent progress on hydrogen evolution reaction, Appl Mater Today. 3 (2016) 23–56, https://doi.org/10.1016/j.apmt.2016.02.001.

[63] J.R. Jaleel UC, M. R, S. Devi K R, D. Pinheiro, M.K. Mohan, Morphological and optical properties of mos2-based materials for photocatalytic degradation of organic dye, Photochem. 2 (3) (2022) 628–650.

[64] Y.-C. Lin, D.O. Dumcenco, Y.-S. Huang, K. Suenaga, Atomic mechanism of the semiconducting-to-metallic phase transition in single-layered MoS2, Nat Nanotechnol. 9 (2014) 391–396, https://doi.org/10.1038/nnano.2014.64.

[65] C. Ataca, M. Topsakal, E. Aktürk, S. Ciraci, A comparative study of lattice dynamics of three- and two-dimensional MoS2, J. Phys. Chem. C 115 (2011) 16354–16361, https://doi.org/10.1021/JP205116X.

[66] I. Song, C. Park, H.C.-R. Advances, undefined 2015, Synthesis and properties of molybdenum disulphide: from bulk to atomic layers, Pubs.Rsc.OrgI Song, C Park, HC ChoiRsc Advances, 2015•pubs.Rsc.Org. (n.d.). https://pubs.rsc.org/en/content/articlehtml/2014/ra/c4ra11852a (accessed November 25, 2023).

[67] R. Khalil, F. Hussain, A. Rana, … M.I.-P.E.L., undefined 2019, Comparative study of polytype 2H-MoS2 and 3R-MoS2 systems by employing DFT, Elsevier. (n.d.). https://www.sciencedirect.com/science/article/pii/S1386947718305332?casa_token=sn94X2-r-IoAAAAA:MR8E1oS1gOWOoRJxwxdLTTfgRbWjmOGytY3mchI6kr69YmCXb25JYd0EY-lwaymBpVNJhZ3ABw (accessed November 25, 2023).

[68] R. Hinchet, U. Khan, C. Falconi, S.W. Kim, Piezoelectric properties in two-dimensional materials: simulations and experiments, Mater. Today 21 (2018) 611–630, https://doi.org/10.1016/J.MATTOD.2018.01.031.

[69] K.F. Mak, C. Lee, J. Hone, J. Shan, T.F. Heinz, Atomically thin <math display="inline"> <msub> <mi>MoS</mi> <mn>2</mn> </msub> </math> : A new direct-gap semiconductor, Phys Rev Lett. 105 (2010), 136805, https://doi.org/10.1103/PhysRevLett.105.136805.

[70] J.A. Wilson, A.D. Yoffe, The transition metal dichalcogenides discussion and interpretation of the observed optical, electrical and structural properties, Adv Phys. 18 (1969) 193–335, https://doi.org/10.1080/00018736900101307.

[71] O. Samy, S. Zeng, M.D. Birowosuto, A. el Moutaouakil, A review on mos2 properties, synthesis, sensing applications and challenges, Crystals (basel). 11 (2021) 355, https://doi.org/10.3390/cryst11040355.

[72] O. Lopez-Sanchez, D. Lembke, M. Kayci, A. Radenovic, A. Kis, Ultrasensitive photodetectors based on monolayer MoS 2, Nat Nanotechnol. 8 (2013) 497–501, https://doi.org/10.1038/nnano.2013.100.

[73] S.W. Han, W.S. Yun, H. Kim, Y. Kim, D. Kim, C.W. Ahn, S. Ryu, Hole doping effect of MoS2 via electron capture of He+ ion irradiation, Sci Rep. 11 (2021) 23590, https://doi.org/10.1038/s41598-021-02932-6.

[74] S.S. Ding, W.Q. Huang, Y.C. Yang, B.X. Zhou, W.Y. Hu, M.Q. Long, P. Peng, G.F. Huang, Dual role of monolayer MoS2 in enhanced photocatalytic performance of hybrid MoS2/SnO2 nanocomposite, J Appl Phys. 119 (2016). https://doi.org/10.1063/1.4952377.

[75] S. Lebègue, O. Eriksson, Electronic structure of two-dimensional crystals from ab initio theory, Phys Rev B Condens Matter Mater Phys. 79 (2009), https://doi.org/10.1103/PHYSREVB.79.115409.

[76] A. Splendiani, L. Sun, Y. Zhang, T. Li, J. Kim, C.-Y. Chim, G. Galli, F. Wang, Emerging photoluminescence in monolayer MoS 2, Nano Lett. 10 (2010) 1271–1275, https://doi.org/10.1021/nl903868w.

[77] J. Xiao, M. Zhao, Y. Wang, X. Zhang, Excitons in atomically thin 2D semiconductors and their applications, Nanophotonics. 6 (2017) 1309–1328, https://doi.org/10.1515/NANOPH-2016-0160/HTML.

[78] M. Sang, J. Shin, K. Kim, K. Yu, Electronic and thermal properties of graphene and recent advances in graphene based electronics applications, Nanomaterials 9 (2019) 374, https://doi.org/10.3390/nano9030374.

[79] E. Scalise, M. Houssa, G. Pourtois, V. Afanas'ev, A. Stesmans, Strain-induced semiconductor to metal transition in the two-dimensional honeycomb structure of MoS2, Nano Res. 5 (1) (2012) 43–48.

[80] M. Shahbazi, M.R. Khanlary, A. Taherkhani, Enhancement of optical, morphological and electronic properties of MoS2 thin film by annealing to improve the performance of silicon solar cells, J. Mater. Sci. Mater. Electron. 34 (2023) 1–11, https://doi.org/10.1007/S10854-022-09538-2/TABLES/3.

[81] W. Li, T. Wang, X. Dai, X. Wang, C. Zhai, Y. Ma, S. Chang, Y. Tang, Electric field modulation of the band structure in MoS2/WS2 van der waals heterostructure, Solid State Commun. 250 (2017) 9–13, https://doi.org/10.1016/j.ssc.2016.11.006.

[82] X.D. Li, S.Q. Wu, Z.Z. Zhu, Band gap control and transformation of monolayer-MoS 2 -based hetero-bilayers, J Mater Chem C Mater. 3 (2015) 9403–9411, https://doi.org/10.1039/C5TC01584G.

[83] I.N. Yakovkin, Interlayer interaction and screening in MoS 2, Surf. Rev. Lett. 21 (2014) 1450039, https://doi.org/10.1142/S0218625X14500395.

[84] J. Pu, Y. Yomogida, K.K. Liu, L.J. Li, Y. Iwasa, T. Takenobu, Highly flexible MoS 2 thin-film transistors with ion gel dielectrics, Nano Lett. 12 (2012) 4013–4017, https://doi.org/10.1021/NL301335Q.

[85] A. Taube, J. Judek, A. Łapińska, M. Zdrojek, Temperature-dependent thermal properties of supported mos 2 monolayers, ACS Appl Mater Interfaces. 7 (2015) 5061–5065, https://doi.org/10.1021/acsami.5b00690.

[86] S. Zhang, J. Liu, M.M. Kirchner, H. Wang, Y. Ren, W. Lei, Two-dimensional heterostructures and their device applications: progress, challenges and opportunities—review, J Phys D Appl Phys. 54 (43) (2021) 433001.

[87] S. Bertolazzi, J. Brivio, A. Kis, Stretching and breaking of ultrathin MoS 2, ACS Nano 5 (2011) 9703–9709, https://doi.org/10.1021/NN203879F.

[88] R.C. Cooper, C. Lee, C.A. Marianetti, X. Wei, J. Hone, J.W. Kysar, Nonlinear elastic behavior of two-dimensional molybdenum disulfide, Phys Rev B Condens Matter Mater Phys. 87 (2013), https://doi.org/10.1103/PHYSREVB.87.035423.

[89] K. Liu, Q. Yan, M. Chen, W. Fan, Y. Sun, J. Suh, D. Fu, S. Lee, J. Zhou, S. Tongay, J. Ji, J.B. Neaton, J. Wu, Elastic properties of chemical-vapor-deposited monolayer MoS2, WS2, and their bilayer heterostructures, Nano Lett. 14 (2014) 5097–5103, https://doi.org/10.1021/NL501793A.

[90] Y. Wang, Z. Shi, Y. Huang, Y. Ma, C. Wang, M. Chen, Y. Chen, Supercapacitor devices based on graphene materials, J. Phys. Chem. C 113 (2009) 13103–13107, https://doi.org/10.1021/JP902214F.

[91] M.B. Khan, R. Jan, A. Habib, A.N. Khan, Evaluating Mechanical Properties of Few Layers MoS2 Nanosheets-Polymer Composites, Adv. Mater. Sci. Eng. 2017 (2017) 1–6.

[92] P. Tao, H. Guo, T. Yang, Z. Zhang, Strain-induced magnetism in MoS2 monolayer with defects, J Appl Phys. 115 (2014). https://doi.org/10.1063/1.4864015.

[93] J.-W. Jiang, Z. Qi, H.S. Park, T. Rabczuk, Elastic bending modulus of single-layer molybdenum disulfide (MoS 2): finite thickness effect, Nanotechnology 24 (43) (2013) 435705.

[94] S. Reich, J. Maultzsch, C. Thomsen, P. Ordejón, Tight-binding description of graphene, Phys Rev B Condens Matter Mater Phys. 66 (2002) 354121–354125, https://doi.org/10.1103/PHYSREVB.66.035412.

[95] V.M. Pereira, A.H. Castro Neto, N.M.R. Peres, Tight-binding approach to uniaxial strain in graphene, Phys Rev B Condens Matter Mater Phys. 80 (2009), https://doi.org/10.1103/PHYSREVB.80.045401.

[96] F. Guinea, M.I. Katsnelson, A.K. Geim, Energy gaps and a zero-field quantum Hall effect in graphene by strain engineering, Nat Phys. 6 (2010) 30–33, https://doi.org/10.1038/nphys1420.

[97] K. Nakada, M. Fujita, G. Dresselhaus, M.S. Dresselhaus, Edge state in graphene ribbons: Nanometer size effect and edge shape dependence, Phys Rev B Condens Matter Mater Phys. 54 (1996) 17954–17961, https://doi.org/10.1103/PHYSREVB.54.17954.

[98] K.K. Kam, B.A. Parkinson, Detailed photocurrent spectroscopy of the semiconducting group VI transition metal dichalcogenides, J. Phys. Chem. 86 (1982) 463–467, https://doi.org/10.1021/J100393A010.

[99] T. Eknapakul, P.D.C. King, M. Asakawa, P. Buaphet, R.H. He, S.K. Mo, H. Takagi, K.M. Shen, F. Baumberger, T. Sasagawa, S. Jungthawan, W. Meevasana, Electronic structure of a quasi-freestanding MoS2 monolayer, Nano Lett. 14 (2014) 1312–1316, https://doi.org/10.1021/NL4042824.

[100] J.W. Jiang, The buckling of single-layer MoS 2 under uniaxial compression, Nanotechnology 25 (35) (2014) 355402.

[101] I. Kaur, R.L. Mahajan, P. Singh, Generalized correlation for effective thermal conductivity of high porosity architectured materials and metal foams, Int J Heat Mass Transf. 200 (2023), 123512, https://doi.org/10.1016/J.IJHEATMASSTRANSFER.2022.123512.

[102] S. Sahoo, A.P.S. Gaur, M. Ahmadi, J.-F. Guinel, R.S. Katiyar, Temperature-Dependent Raman Studies and Thermal Conductivity of Few-Layer MoS2, ACS Publications. 117 (2013) 117–9042, https://doi.org/10.1021/jp402509w.

[103] M. Damnjanović, E. Dobardžić, I. Milošević, M. Viršek, M. Remškar, Phonons in MoS2 and WS2 nanotubes, Mater. Manuf. Process. 23 (2008) 579–582, https://doi.org/10.1080/10426910802160361.

[104] H. Wang, Y. Wang, X. Cao, M. Feng, G. Lan, Vibrational properties of graphene and graphene layers, J. Raman Spectrosc. 40 (2009) 1791–1796, https://doi.org/10.1002/jrs.2321.

[105] S. Balendhran, S. Walia, H. Nili, J. Zhen Ou, S. Zhuiykov, R.B. Kaner, S. Sriram, M. Bhaskaran, K. Kalantar-Zadeh, Two-dimensional molybdenum trioxide and dichalcogenides, Wiley Online, Library 23 (2013) 3952–3970, https://doi.org/10.1002/adfm.201300125.

[106] C. Lee, X. Wei, J.W. Kysar, J. Hone, Measurement of the elastic properties and intrinsic strength of monolayer graphene, Science 321 (2008) (1979) 385–388, https://doi.org/10.1126/SCIENCE.1157996.

[107] E. Cadelano, P.L. Palla, S. Giordano, L. Colombo, Nonlinear elasticity of monolayer graphene, Phys Rev Lett. 102 (2009), https://doi.org/10.1103/PHYSREVLETT.102.235502.

[108] C. Damodara Reddy, S. Rajendran, K.M. Liew, C.D. Reddy, S. Rajendran, Equilibrium configuration and continuum elastic properties of finite sized graphene, Iopscience. Iop. Org. 17 (2006) 864–870, https://doi.org/10.1088/0957-4484/17/3/042.

[109] X. Liu, G. Zhang, Q.-X. Pei, Y.-W. Zhang, Phonon thermal conductivity of monolayer MoS 2 sheet and nanoribbons, Appl Phys Lett. 103 (13) (2013) 133113.

[110] J.-W. Jiang, H.S. Park, T. Rabczuk, Molecular dynamics simulations of single-layer molybdenum disulphide (MoS 2): Stillinger-Weber parametrization, mechanical properties, and thermal conductivity, J Appl Phys. 114 (2013) 064307. https://doi.org/10.1063/1.4818414.
[111] N. Abid, A.M. Khan, S. Shujait, K. Chaudhary, M. Ikram, M. Imran, J. Haider, M. Khan, Q. Khan, M. Maqbool, Synthesis of nanomaterials using various top-down and bottom-up approaches, influencing factors, advantages, and disadvantages: A review, Adv Colloid Interface Sci. 300 (2022), 102597, https://doi.org/10.1016/j.cis.2021.102597.
[112] L. Seravalli, M. Bosi, A Review on Chemical Vapour Deposition of Two-Dimensional MoS2 Flakes, Materials. 14 (2021) 7590, https://doi.org/10.3390/ma14247590.
[113] A.K. Singh, P. Kumar, D. Late, A. Kumar, S. Patel, J. Singh, 2D layered transition metal dichalcogenides (MoS2): Synthesis, applications and theoretical aspects, Appl Mater Today. 13 (2018) 242–270, https://doi.org/10.1016/j.apmt.2018.09.003.
[114] J. Pal Singh, M. Kumar, A. Sharma, G. Pandey, K. Chae, S. Lee, Bottom-Up and Top-Down Approaches for MgO, in, in: S. Karakuş (Ed.), Sonochemical Reactions, IntechOpen, 2020.
[115] Y. Yan, F.Z. Nashath, S. Chen, S. Manickam, S.S. Lim, H. Zhao, E. Lester, T. Wu, C. H. Pang, Synthesis of graphene: Potential carbon precursors and approaches, Nanotechnol Rev. 9 (2020) 1284–1314, https://doi.org/10.1515/NTREV-2020-0100/HTML.
[116] C.C. Mayorga-Martinez, A. Ambrosi, A.Y.S. Eng, Z. Sofer, M. Pumera, Transition metal dichalcogenides (MoS2, MoSe2, WS2 and WSe2) exfoliation technique has strong influence upon their capacitance, Electrochem Commun. 56 (2015) 24–28, https://doi.org/10.1016/j.elecom.2015.03.017.
[117] B. Radisavljevic, A. Radenovic, J. Brivio, V. Giacometti, A. Kis, Single-layer MoS2 transistors, Nature. Com. 6 (3) (2011) 147–150.
[118] S. Joseph, J. Mohan, S. Lakshmy, S. Thomas, B. Chakraborty, S. Thomas, N. Kalarikkal, A review of the synthesis, properties, and applications of 2D transition metal dichalcogenides and their heterostructures, Mater Chem Phys. 297 (2023), 127332, https://doi.org/10.1016/J.MATCHEMPHYS.2023.127332.
[119] Y. Xu, H. Cao, Y. Xue, B. Li, W. Cai, Liquid-Phase Exfoliation of Graphene: An Overview on Exfoliation Media, Techniques, and Challenges, Nanomaterials. 8 (2018) 942, https://doi.org/10.3390/nano8110942.
[120] V. Forsberg, R. Zhang, J. Bäckström, C. Dahlström, B. Andres, M. Norgren, M. Andersson, M. Hummelgård, H. Olin, V. Bansal, Exfoliated MoS2 in water without additives, PLoS One 11 (4) (2016) e0154522.
[121] J.N. Coleman, M. Lotya, A. O'Neill, S.D. Bergin, P.J. King, U. Khan, K. Young, A. Gaucher, S. De, R.J. Smith, I.V. Shvets, S.K. Arora, G. Stanton, H.Y. Kim, K. Lee, G.T. Kim, G.S. Duesberg, T. Hallam, J.J. Boland, J.J. Wang, J.F. Donegan, J. C. Grunlan, G. Moriarty, A. Shmeliov, R.J. Nicholls, J.M. Perkins, E.M. Grieveson, K. Theuwissen, D.W. McComb, P.D. Nellist, V. Nicolosi, Two-dimensional nanosheets produced by liquid exfoliation of layered materials, Science 331 (2011) (1979) 568–571, https://doi.org/10.1126/SCIENCE.1194975.
[122] R.J. Smith, P.J. King, M. Lotya, C. Wirtz, U. Khan, S. De, A. O'Neill, G.S. Duesberg, J.C. Grunlan, G. Moriarty, J. Chen, J. Wang, A.I. Minett, V. Nicolosi, J. N. Coleman, Large-scale exfoliation of inorganic layered compounds in aqueous surfactant solutions, Wiley Online, Library 23 (2011) 3944–3948, https://doi.org/10.1002/adma.201102584.
[123] K. Lee, H.Y. Kim, M. Lotya, J.N. Coleman, G.T. Kim, G.S. Duesberg, Electrical characteristics of molybdenum disulfide flakes produced by liquid exfoliation, Adv. Mater. 23 (2011) 4178–4182, https://doi.org/10.1002/ADMA.201101013.
[124] A. Ambrosi, Z. Sofer, M. Pumera, 2H → 1T phase transition and hydrogen evolution activity of MoS 2, MoSe 2, WS 2 and WSe 2 strongly depends on the MX 2 composition, Chem. Commun. 51 (2015) 8450–8453, https://doi.org/10.1039/C5CC00803D.
[125] B. Pal, A. Singh, P. Mahale, A. Kumar, S. Thirupathaiah, H. Sezen, M. Amati, L. Gregoratti, U. V Waghmare, D.D. Sarma, Chemical exfoliation of MoS2 leads to semiconducting 1T'phase and not the metallic 1T phase, Arxiv.Org. (n.d.). https://arxiv.org/abs/1703.00772 (accessed January 17, 2023).
[126] X. Gu, Y. Zhao, K. Sun, C.L.Z. Vieira, Z. Jia, C. Cui, Z. Wang, A. Walsh, S. Huang, Method of ultrasound-assisted liquid-phase exfoliation to prepare graphene, Ultrason Sonochem. 58 (2019), 104630, https://doi.org/10.1016/j.ultsonch.2019.104630.
[127] A. Jawaid, D. Nepal, K. Park, M. Jespersen, A. Qualley, P. Mirau, L.F. Drummy, R. A. Vaia, Mechanism for liquid phase exfoliation of mos2, Chem. Mater. 28 (2016) 337–348, https://doi.org/10.1021/ACS.CHEMMATER.5B04224.
[128] G. Eda, H. Yamaguchi, D. Voiry, T. Fujita, M. Chen, M. Chhowalla, Photoluminescence from chemically exfoliated MoS 2, Nano Lett. 11 (2011) 5111–5116, https://doi.org/10.1021/NL201874W.
[129] F. Wypych, R.S.-J. of the C. Society, U. Chemical, U. 1992, 1T-MoS 2, a new metallic modification of molybdenum disulfide, J Chem Soc Chem Commun. 19 (1992) 1386–1388. https://pubs.rsc.org/en/content/articlehtml/1992/c3/c39920001386?casa_token=5d4iet5r-QMAAAAA:3iDPex7xF46CQSPjON9m5VHlWEAVo61_51YrgFCZ_N6v2mAI-itqsgbzU3b-voJ7_T6mm5sealZikQ (accessed January 17, 2023).
[130] Z. Wang, A. Von Dem Bussche, Y. Qiu, T.M. Valentin, K. Gion, A.B. Kane, R. H. Hurt, Chemical dissolution pathways of mos2 nanosheets in biological and environmental media, Environ Sci Technol. 50 (2016) 7208–7217, https://doi.org/10.1021/ACS.EST.6B01881.
[131] M. Chhowalla, H.S. Shin, G. Eda, L.-J. Li, K.P. Loh, H. Zhang, The chemistry of two-dimensional layered transition metal dichalcogenide nanosheets, Nature. Com. 5 (4) (2013) 263–275.
[132] H. Lin, J. Wang, Q. Luo, H. Peng, C. Luo, R. Qi, R. Huang, J. Travas-Sejdic, C.-G. Duan, Rapid and highly efficient chemical exfoliation of layered MoS 2 and WS 2, J Alloys Compd. 699 (2017) 222–229, https://doi.org/10.1016/j.jallcom.2016.12.388.
[133] R. Goeke, P. Kotula, S. Prasad, T. Scharf, Synthesis of MoS2-Au nanocomposite films by sputter deposition., (2012). https://www.osti.gov/servlets/purl/1055586 (accessed January 17, 2023).
[134] S. Hussain, J. Singh, D. Vikraman, A.K. Singh, M.Z. Iqbal, M.F. Khan, P. Kumar, D. C. Choi, W. Song, K.S. An, J. Eom, W.G. Lee, J. Jung, Large-area, continuous and high electrical performances of bilayer to few layers MoS2 fabricated by RF sputtering via post-deposition annealing method, Sci Rep. 6 (2016), https://doi.org/10.1038/SREP30791.
[135] T.F. Jaramillo, K.P. Jørgensen, J. Bonde, J.H. Nielsen, S. Horch, I. Chorkendorff, Identification of active edge sites for electrochemical H2 evolution from MoS2 nanocatalysts, Science 317 (2007) (1979) 100–102, https://doi.org/10.1126/SCIENCE.1141483.
[136] C. Gong, C. Huang, J. Miller, L. Cheng, Y. Hao, D. Cobden, J. Kim, R.S. Ruoff, R. M. Wallace, K. Cho, X. Xu, Y.J. Chabal, Metal contacts on physical vapor deposited monolayer MoS2, ACS Nano 7 (2013) 11350–11357, https://doi.org/10.1021/NN4052138.
[137] T. Spalvins, Morphological and frictional behavior of sputtered MoS2 films, Thin Solid Films 96 (1982) 17–24, https://doi.org/10.1016/0040-6090(82)90208-5.
[138] M. Audronis, A. Leyland, P.J. Kelly, A. Matthews, Composition and structure-property relationships of chromium-diboride/ molybdenum-disulphide PVD nanocomposite hard coatings deposited by pulsed magnetron sputtering, Appl Phys A Mater Sci Process. 91 (2008) 77–86, https://doi.org/10.1007/S00339-007-4362-5/METRICS.
[139] N. Baig, I. Kammakakam, W. Falath, I. Kammakakam, Nanomaterials: A review of synthesis methods, properties, recent progress, and challenges, Mater Adv. 2 (2021) 1821–1871, https://doi.org/10.1039/D0MA00807A.
[140] M. Chhowalla, G.A.J. Amaratunga, Thin films of fullerene-like MoS2 nanoparticles with ultra-low friction and wear, Nature 407 (2000) 164–167, https://doi.org/10.1038/35025020.
[141] J. Hu, J. Bultman, J.S. Zabinski, Inorganic Fullerene-Like Nanoparticles Produced by Arc Discharge in Water with Potential Lubricating Ability, Tribol Lett. 17 (2004) 543–546, https://doi.org/10.1023/B:TRIL.0000044502.93266.59.
[142] L. Rapoport, N. Fleischer, L. Rapoport, N. Fleischer, R. Tenne, Applications of WS 2 (MoS 2) inorganic nanotubes and fullerene-like nanoparticles for solid lubrication and for structural nanocomposites, Pubs. Rsc. Org. (2005), https://doi.org/10.1039/b417488g.
[143] I. Alexandrou, N. Sano, A. Burrows, R.R. Meyer, H. Wang, A.I. Kirkland, C. J. Kiely, G.A.J. Amaratunga, Structural investigation of MoS2 core–shell nanoparticles formed by an arc discharge in water, accessed January 17, 2023, Iopscience. Iop. Org. 14 (2003) 913–917, https://iopscience.iop.org/article/10.1088/0957-4484/14/8/313/meta.
[144] N. Sano, H. Wang, M. Chhowalla, I. Alexandrou, G.A.J. Amaratunga, M. Naito, T. Kanki, Fabrication of inorganic molybdenum disulfide fullerenes by arc in water, Chem Phys Lett. 368 (2003) 331–337, https://doi.org/10.1016/S0009-2614(02)01884-5.
[145] D.B. Chrisey, G.K. Hubler, Pulsed laser deposition of thin films, (1994) 3. https://pdfs.semanticscholar.org/9505/32a6afaa94d708fe680618eb6cf72f741f2b.pdf (accessed January 17, 2023).
[146] P.A. Parilla, A.C. Dillon, B.A. Parkinson, K.M. Jones, J. Alleman, G. Riker, D. S. Ginley, M.J. Heben, Formation of nanooctahedra in molybdenum disulfide and molybdenum diselenide using pulsed laser vaporization, ACS Publications. (2004), https://doi.org/10.1021/jp036202.
[147] M.I. Serna, S.H. Yoo, S. Moreno, Y. Xi, J.P. Oviedo, H. Choi, H.N. Alshareef, M. J. Kim, M. Minary-Jolandan, M.A. Quevedo-Lopez, Large-Area Deposition of MoS2 by Pulsed Laser Deposition with in Situ Thickness Control, ACS Nano 10 (2016) 6054–6061, https://doi.org/10.1021/ACSNANO.6B01636.
[148] R. Sahu, Two-Dimensional MoS2 and Heterostructure Growth by Pulsed Laser Deposition, Modern Concepts in Material Science. 2 (2019). https://doi.org/10.33552/MCMS.2019.02.000534.
[149] D. Vollath, D.V. Szabó, Synthesis of nanocrystalline MoS2 and WS2 in a microwave plasma, Mater Lett. 35 (1998) 236–244, https://doi.org/10.1016/S0167-577X(97)00247-4.
[150] N. Liu, X. Wang, W. Xu, H. Hu, J. Liang, J. Qiu, Microwave-assisted synthesis of MoS2/graphene nanocomposites for efficient hydrodesulfurization, Fuel 119 (2014) 163–169, https://doi.org/10.1016/j.fuel.2013.11.045.
[151] S. Reshmi, M.V. Akshaya, B. Satpati, A. Roy, P. Kumar Basu, K. Bhattacharjee, Tailored MoS 2 nanorods: a simple microwave assisted synthesis, Mater Res Express. 4 (2017), 115012, https://doi.org/10.1088/2053-1591/aa949c.
[152] S.Z. Mortazavi, P. Parvin, A. Reyhani, S. Mirershadi, R. Sadighi-Bonabi, Generation of various carbon nanostructures in water using IR/UV laser ablation, J Phys D Appl Phys. 46 (16) (2013) 165303.
[153] G. Pradhan Department of Physics, Indian Institute of Technology Guwahati , Guwahati 781039, India P.P. Dey Department of Physics, Indian Institute of Technology Guwahati , Guwahati 781039, India A. Khare Department of Physics, Indian Institute of Technology Guwahati , Guwahati 781039, India A.K. Sharma Department of Physics, Indian Institute of Technology Guwahati , Guwahati 781039, India Synthesis and size modulation of MoS2quantum dots by pulsed laser ablation in liquid for viable hydrogen generation J Appl Phys. 129 2 2021 2021 10.1063/5.0022833.
[154] F. Shahi, P. Parvin, S.Z. Mortazavi, A. Reyhani, B. Soltannia, M. Sadrzadeh, H. Moradi, A. Ojaghloo, A. Moafi, Synthesis, Characterization, and Typical Application of Nitrogen-Doped MoS2 Nanosheets Based on Pulsed Laser Ablation

in Liquid Nitrogen, Physica Status Solidi (A) Applications and Materials, Science 219 (14) (2022), https://doi.org/10.1002/PSSA.202100677.
[155] R.G. Dickinson, L. Pauling, The crystal structure of molybdenite, J Am Chem Soc. 45 (1923) 1466–1471, https://doi.org/10.1021/JA01659A020.
[156] A. Zak, Y. Feldman, V. Lyakhovitskaya, G. Leitus, R. Popovitz-Biro, E. Wachtel, H. Cohen, S. Reich, R. Tenne, Alkali Metal Intercalated Fullerene-Like MS2 (M = W, Mo) Nanoparticles and Their Properties, ACS Publications. 124 (2002) 4747–4758, https://doi.org/10.1021/ja012060q.
[157] O. Chusid, Y. Gofer, H. Gizbar, Y. Vestfrid, E. Levi, D. Aurbach, I. Riech, Solid-state rechargeable magnesium batteries, Adv. Mater. 15 (2003) 627–630, https://doi.org/10.1002/ADMA.200304415.
[158] X.L. Li, Y.D. Li, MoS2 nanostructures: Synthesis and electrochemical Mg 2+ intercalation, J. Phys. Chem. B 108 (2004) 13893–13900, https://doi.org/10.1021/JP0367575.
[159] N. Feng, R. Meng, L. Zu, Y. Feng, C. Peng, J. Huang, G. Liu, B. Chen, J. Yang, A polymer-direct-intercalation strategy for MoS 2 /carbon-derived heteroaerogels with ultrahigh pseudocapacitance, Nat Commun. 10 (2019), https://doi.org/10.1038/S41467-019-09384-7.
[160] R. Thiruvengadathan, V. Korampally, A. Ghosh, N. Chanda, K. Gangopadhyay, S. Gangopadhyay, Nanomaterial processing using self-assembly-bottom-up chemical and biological approaches, Rep. Prog. Phys. 76 (6) (2013) 066501.
[161] X. Wang, H. Feng, Y. Wu, L. Jiao, Controlled synthesis of highly crystalline MoS2 flakes by chemical vapor deposition, J Am Chem Soc. 135 (2013) 5304–5307, https://doi.org/10.1021/JA4013485.
[162] J. Yue, J. Jian, P. Dong, L. Luo, F. Chang, Growth of Single-Layer MoS 2 by Chemical Vapor Deposition on sapphire substrate, IOP Conf Ser Mater Sci Eng. 592 (1) (2019) 012044.
[163] M.A. Butt C. Tyszkiewicz P. Karasiński M. Zięba A. Kaźmierczak M. Zdończyk Ł. Duda M. Guzik J. Olszewski T. Martynkien A. Bachmatiuk R. Piramidowicz Optical Thin Films Fabrication Techniques—Towards a Low-Cost Solution for the Integrated Photonic Platform: A Review of the Current Status Materials 15 13 4591.
[164] N. Ali, J. Teixeira, A. Addali, M. Saeed, F. Al-Zubi, A. Sedaghat, H. Bahzad, Deposition of Stainless Steel Thin Films: An Electron Beam Physical Vapour Deposition Approach, Materials. 12 (2019) 571, https://doi.org/10.3390/ma12040571.
[165] S. Wu, C. Huang, G. Aivazian, J.S. Ross, D.H. Cobden, X. Xu, Vapor-Solid Growth of High Optical Quality MoS2 Monolayers with Near-Unity Valley Polarization, ACS Publications. 7 (2013) 2768–2772, https://doi.org/10.1021/nn4002038.
[166] X. Zhang, Y. Zhang, B.-B. Yu, X.-L. Yin, W.-J. Jiang, Y. Jiang, J.-S. Hu, L.-J. Wan, Physical vapor deposition of amorphous MoS 2 nanosheet arrays on carbon cloth for highly reproducible large-area electrocatalysts for the hydrogen evolution reaction, J Mater Chem A Mater. 3 (2015) 19277–19281, https://doi.org/10.1039/C5TA05793K.
[167] L.K. Tan, B. Liu, J.H. Teng, S. Guo, H.Y. Low, K.P. Loh, Atomic layer deposition of a MoS2 film, Nanoscale 6 (2014) 10584–10588, https://doi.org/10.1039/c4nr02451f.
[168] T. Jurca, M.J. Moody, A. Henning, J.D. Emery, B. Wang, J.M. Tan, T.L. Lohr, L. J. Lauhon, T.J. Marks, Low-Temperature Atomic Layer Deposition of MoS 2 Films, Angew. Chem. 129 (2017) 5073–5077, https://doi.org/10.1002/ange.201611838.
[169] Y. Huang, L. Liu, W. Zhao, Y. Chen, Preparation and characterization of molybdenum disulfide films obtained by one-step atomic layer deposition method, Thin Solid Films 624 (2017) 101–105, https://doi.org/10.1016/j.tsf.2017.01.015.
[170] H. Liao, Y. Wang, S. Zhang, Y. Qian, A solution low-temperature route to mos2 fiber, Chem. Mater. 13 (2001) 6–8, https://doi.org/10.1021/CM000602H.
[171] X. Li, W. Zhang, Y. Wu, C. Min, J. Fang, Solution-processed MoSx as an efficient anode buffer layer in organic solar cells, ACS Appl Mater Interfaces. 5 (2013) 8823–8827, https://doi.org/10.1021/AM402105D.
[172] K.K. Liu, W. Zhang, Y.H. Lee, Y.C. Lin, M.T. Chang, C.Y. Su, C.S. Chang, H. Li, Y. Shi, H. Zhang, C.S. Lai, L.J. Li, Growth of large-area and highly crystalline MoS 2 thin layers on insulating substrates, Nano Lett. 12 (2012) 1538–1544, https://doi.org/10.1021/NL2043612.
[173] I. Bezverkhy, P. Afanasiev, M. Lacroix, Aqueous preparation of highly dispersed molybdenum sulfide, Inorg Chem. 39 (2000) 5416–5417, https://doi.org/10.1021/IC000627I.
[174] P. Afanasiev, C. Geantet, C. Thomazeau, B. Jouget, Molybdenum polysulfide hollow microtubules grown at room temperature from solution, Chem. Commun. (2000) 1001–1002, https://doi.org/10.1039/b001406k.
[175] A.W. Maijenburg, M. Regis, A.N. Hattori, H. Tanaka, K.S. Choi, J.E. Ten Elshof, MoS2 nanocube structures as catalysts for electrochemical H 2 evolution from acidic aqueous solutions, ACS Appl Mater Interfaces. 6 (2014) 2003–2010, https://doi.org/10.1021/AM405075F.
[176] Q. Li, E.C. Walter, W.E. Van Der Veer, B.J. Murray, J.T. Newberg, E.W. Bohannan, J.A. Switzer, J.C. Hemminger, R.M. Penner, Molybdenum disulfide nanowires and nanoribbons by electrochemical/chemical synthesis, J. Phys. Chem. B 109 (2005) 3169–3182, https://doi.org/10.1021/JP045032D.
[177] J. Kibsgaard, Z. Chen, B.N. Reinecke, T.F. Jaramillo, Engineering the surface structure of MoS2 to preferentially expose active edge sites for electrocatalysis, Nat Mater. 11 (2012) 963–969, https://doi.org/10.1038/nmat3439.
[178] M. Nguyen, P.D. Tran, S.S. Pramana, R.L. Lee, S.K. Batabyal, N. Mathews, L. H. Wong, M. Graetzel, In situ photo-assisted deposition of MoS2 electrocatalyst onto zinc cadmium sulphide nanoparticle surfaces to construct an efficient photocatalyst for hydrogen generation, Nanoscale 5 (2013) 1479, https://doi.org/10.1039/c2nr34037b.
[179] J. Sun, X. Li, W. Guo, M. Zhao, X. Fan, Y. Dong, C. Xu, J. Deng, Y. Fu, Synthesis methods of two-dimensional MoS2: A brief review, Crystals (basel). 7 (7) (2017) 198.
[180] F. Wang, G. Li, J. Zheng, J. Ma, C. Yang, Q. Wang, Hydrothermal synthesis of flower-like molybdenum disulfide microspheres and their application in electrochemical supercapacitors, RSC Adv. 8 (2018) 38945–38954, https://doi.org/10.1039/C8RA04350G.
[181] S. Wang, G. Li, G. Du, X. Jiang, C. Feng, Z. Guo, S.-J. Kim, Hydrothermal Synthesis of Molybdenum Disulfide for Lithium Ion Battery Applications, Chin J Chem Eng. 18 (2010) 910–913, https://doi.org/10.1016/S1004-9541(09)60147-6.
[182] H. Liu, R. Wu, H. Zhang, M. Ma, Microwave Hydrothermal Synthesis of 1T@2H−MoS2 as an Excellent Photocatalyst, ChemCatChem 12 (2020) 893–902, https://doi.org/10.1002/CCTC.201901569.
[183] N. Liu, Y. Guo, X. Yang, H. Lin, L. Yang, Z. Shi, Z. Zhong, S. Wang, Y. Tang, Q. Gao, Microwave-Assisted Reactant-Protecting Strategy toward Efficient MoS2 Electrocatalysts in Hydrogen Evolution Reaction, ACS Appl Mater Interfaces. 7 (2015) 23741–23749, https://doi.org/10.1021/ACSAMI.5B08103.
[184] Y. Wang, X. Lia, C.W. Glasses, Synthesis and characterization of MoS2 nanocomposites by a high pressure hydrothermal method, accessed January 17, 2023, Journal of Non-Oxide Glasses. 9 (2017) 47–54, https://www.chalcogen.ro/47_WangY.pdf.
[185] M. Choucair, P. Thordarson, J.A. Stride, Gram-scale production of graphene based on solvothermal synthesis and sonication, Nat Nanotechnol. 4 (2009) 30–33, https://doi.org/10.1038/nnano.2008.365.
[186] Z. Ni, R.I. Masel, Rapid production of metal-organic frameworks via microwave-assisted solvothermal synthesis, J Am Chem Soc. 128 (2006) 12394–12395, https://doi.org/10.1021/JA0635231.
[187] F. Lu, W. Cai, Y. Zhang, ZnO Hierarchical Micro/Nanoarchitectures: Solvothermal Synthesis and Structurally Enhanced Photocatalytic Performance, Adv Funct Mater. 18 (2008) 1047–1056, https://doi.org/10.1002/adfm.200700973.
[188] R. Wang, C. Xu, M. Du, J. Sun, L. Gao, P. Zhang, H. Yao, C. Lin, Solvothermal-Induced Self-Assembly of Fe2O3/GS Aerogels for High Li-Storage and Excellent Stability, Wiley Online, Library 10 (2014) 2260–2269, https://doi.org/10.1002/smll.201303371.
[189] S.-M. Jung, E.K. Lee, M. Choi, D. Shin, I.-Y. Jeon, J.-M. Seo, H.Y. Jeong, N. Park, J. H. Oh, J.-B. Baek, Direct Solvothermal Synthesis of B/N-Doped Graphene, Angew. Chem. 126 (2014) 2430–2433, https://doi.org/10.1002/ANGE.201310260.
[190] Z. He, W. Que, Surface scattering and reflecting: the effect on light absorption or photocatalytic activity of TiO2 scattering microspheres, PCCP 15 (2013) 16768, https://doi.org/10.1039/c3cp52570h.
[191] Z. He, W. Que, X. Yin, Y. He, Hydrogen titanium oxide hydrate: Excellent performance on degradation of methyl blue in aqueous solutions, RSC Adv. 4 (2014) 39678–39683, https://doi.org/10.1039/C4RA04010D.
[192] Z. He, W. Que, Y. He, Enhanced photocatalytic performance of sensitized mesoporous TiO 2 nanoparticles by carbon mesostructures, RSC Adv. 4 (2014) 3332–3339, https://doi.org/10.1039/C3RA46389C.
[193] Z. He, W. Que, J. Chen, Y. He, G. Wang, Surface chemical analysis on the carbon-doped mesoporous TiO2 photocatalysts after post-thermal treatment: XPS and FTIR characterization, J. Phys. Chem. Solid 74 (2013) 924–928, https://doi.org/10.1016/j.jpcs.2013.02.001.
[194] Z. He, W. Que, Y. He, J. Chen, H. Xie, G. Wang, Nanosphere assembled mesoporous titanium dioxide with advanced photocatalystic activity using absorbent cotton as template, J Mater Sci. 47 (2012) 7210–7216, https://doi.org/10.1007/S10853-012-6667-9.
[195] Z. He, W. Que, J. Chen, X. Yin, Y. He, J. Ren, Photocatalytic Degradation of Methyl Orange over Nitrogen-Fluorine Codoped TiO 2 Nanobelts Prepared by Solvothermal Synthesis, ACS Appl Mater Interfaces. 4 (2012) 6816–6826, https://doi.org/10.1021/am3019965.
[196] Z. Zhu, Z. He, J. Li, J. Zhou, N. Wei, D. Liu, Two-step template-free route for synthesis of TiO2 hollow spheres, J Mater Sci. 46 (2011) 931–937, https://doi.org/10.1007/S10853-010-4837-1.
[197] Z. He, Z. Zhu, J. Li, J. Zhou, N. Wei, Characterization and activity of mesoporous titanium dioxide beads with high surface areas and controllable pore sizes, J Hazard Mater. 190 (2011) 133–139, https://doi.org/10.1016/j.jhazmat.2011.03.011.
[198] Z.F. Zhu, Z.L. He, J.Q. Li, D.G. Liu, N. Wei, Synthesis and characterisation of fluorinated TiO 2 microspheres with novel structure by sonochemical–microwave hydrothermal treatment, Mater. Res. Innov. 14 (2010) 426–430, https://doi.org/10.1179/143307510X12820854749277.
[199] J. Kibsgaard, J.V. Lauritsen, E. Lægsgaard, B.S. Clausen, H. Topsøe, F. Besenbacher, Cluster-support interactions and morphology of MoS2 nanoclusters in a graphite-supported hydrotreating model catalyst, J Am Chem Soc. 128 (2006) 13950–13958, https://doi.org/10.1021/JA0651106.
[200] K.-J. Huang, L. Wang, J. Li, Y.-M. Liu, Electrochemical sensing based on layered MoS2–graphene composites, Sens Actuators B Chem. 178 (2013) 671–677, https://doi.org/10.1016/j.snb.2013.01.028.
[201] V.G. Pol, S.V. Pol, P.P. George, A. Gedanken, Combining MoS2 or MoSe2 nanoflakes with carbon by reacting Mo(CO)6 with S or Se under their autogenic pressure at elevated temperature, J Mater Sci. 43 (2008) 1966–1973, https://doi.org/10.1007/S10853-008-2462-Z.
[202] V.G. Pol, S.V. Pol, A. Gedanken, Micro to nano conversion: A one-step, environmentally friendly, solid state, bulk fabrication of WS2 and MoS2 nanoplates, Cryst Growth Des. 8 (2008) 1126–1132, https://doi.org/10.1021/CG0700972.
[203] T.S. Sreeprasad, P. Nguyen, N. Kim, V. Berry, Controlled, Defect-Guided, Metal-Nanoparticle Incorporation onto MoS 2 via Chemical and Microwave Routes:

Electrical, Thermal, and Structural Properties, Nano Lett. 13 (2013) 4434–4441, https://doi.org/10.1021/nl402278y.
[204] L. Chang, H. Yang, W. Fu, J. Zhang, Q. Yu, H. Zhu, J. Chen, R. Wei, Y. Sui, X. Pang, G. Zou, Simple synthesis of MoS2 inorganic fullerene-like nanomaterials from MoS2 amorphous nanoparticles, Mater Res Bull. 43 (2008) 2427–2433, https://doi.org/10.1016/j.materresbull.2007.07.043.
[205] Z. He, W. Que, Y. Dang, Y. He, Z. Hou, Characterization and adsorption characteristics of mesoporous molybdenum sulfide microspheres, Mater Lett. 120 (2014) 58–61, https://doi.org/10.1016/j.matlet.2014.01.007.
[206] N.A. Dhas, K.S. Suslick, Sonochemical preparation of hollow nanospheres and hollow nanocrystals, J Am Chem Soc. 127 (2005) 2368–2369, https://doi.org/10.1021/JA049494G.
[207] M.M. Mdleleni, T. Hyeon, K.S. Suslick, Sonochemical Synthesis of Nanostructured Molybdenum Sulfide, J Am Chem Soc. 120 (1998) 6189–6190, https://doi.org/10.1021/ja9800333.
[208] Y. Mastai M. Homyonfer A.g., Room Temperature Sonoelectrochemical Synthesis of Molybdenum Sulfide Fullerene-Like Nanoparticles, Wiley Online Library. 11 1999 1010 1013 https://doi.org/https://doi.org/10.1002/(SICI)1521-4095(199908)11:12<1010::AID-ADMA1010>3.0.CO;2-%23.
[209] K. Wang, J. Wang, J. Fan, M. Lotya, A. O'Neill, D. Fox, Y. Feng, X. Zhang, B. Jiang, Q. Zhao, H. Zhang, J.N. Coleman, L. Zhang, W.J. Blau, Ultrafast saturable absorption of two-dimensional MoS2 nanosheets, ACS Nano 7 (2013) 9260–9267, https://doi.org/10.1021/NN403886T.
[210] A. Cho, S.H. Moon, Development of highly active Co(Ni)Mo catalysts for the hydrodesulfurization of dibenzothiophene compounds, Catal. Surv. Asia 14 (2010) 64–74, https://doi.org/10.1007/S10563-010-9088-2.
[211] I. Uzcanga, I. Bezverkhyy, P. Afanasiev, C. Scott, M. Vrinat, Sonochemical preparation of MoS2 in aqueous solution: Replication of the cavitation bubbles in an inorganic material morphology, Chem. Mater. 17 (2005) 3575–3577, https://doi.org/10.1021/CM0501766.
[212] S.E. Skrabalak, K.S. Suslick, Porous MoS2 synthesized by ultrasonic spray pyrolysis, J Am Chem Soc. 127 (2005) 9990–9991, https://doi.org/10.1021/JA051654G.
[213] D. Mahajan, C.L. Marshall, N. Castagnola, J.C. Hanson, Sono synthesis and characterization of nano-phase molybdenum-based materials for catalytic hydrodesulfurization, Appl Catal A Gen. 258 (2004) 83–91, https://doi.org/10.1016/J.APCATA.2003.08.014.
[214] J. Zhang, T. Liu, L. Fu, G. Ye, Synthesis of nanosized ultrathin MoS2 on montmorillonite nanosheets by CVD method, Chem Phys Lett. 781 (2021), 138972, https://doi.org/10.1016/J.CPLETT.2021.138972.
[215] Y.D. Liu, L. Ren, X. Qi, L.W. Yang, G.L. Hao, J. Li, X.L. Wei, J.X. Zhong, Preparation, characterization and photoelectrochemical property of ultrathin MoS2 nanosheets via hydrothermal intercalation and exfoliation route, J Alloys Compd. 571 (2013) 37–42, https://doi.org/10.1016/J.JALLCOM.2013.03.031.
[216] J. Xu, H. Tang, G. Tang, C.L.-C. Letters, U. 2014, FACILE SYNTHESIS AND CHARACTERIZATION OF FLOWER-LIKE MoS2 MICROSPHERES., Search. Ebscohost.Com. 11 (2014) 265–270. https://search.ebscohost.com/login.aspx?direct=true&profile=ehost&scope=site&authtype=crawler&jrnl=18414834&AN=96536120&h=oHToSOSEvMQGpPZ9TDuDQz%2Bi3oZV0iW7HCnuvF8C1J1IaWyvm1VMiCoCKMRGxNnCgv5gSjCfvgUH%2BfWdy8ecyQ%3D%3D&crl=c (accessed March 1, 2023).
[217] S.V.P. Vattikuti, C. Byon, C.V. Reddy, J. Shim, B. Venkatesh, Co-precipitation synthesis and characterization of faceted MoS2 nanorods with controllable morphologies, Appl Phys A Mater Sci Process. 119 (2015) 813–823, https://doi.org/10.1007/S00339-015-9163-7/FIGURES/11.
[218] H.S. Lee, S.W. Min, Y.G. Chang, M.K. Park, T. Nam, H. Kim, J.H. Kim, S. Ryu, S. Im, MoS 2 nanosheet phototransistors with thickness-modulated optical energy gap, Nano Lett. 12 (2012) 3695–3700, https://doi.org/10.1021/NL301485Q.
[219] A. Castellanos-Gomez, M. Poot, G.A. Steele, H.S.J. van der Zant, N. Agraït, G. Rubio-Bollinger, Elastic Properties of Freely Suspended MoS 2 Nanosheets, Adv. Mater. 24 (2012) 772–775, https://doi.org/10.1002/adma.201103965.
[220] Z. Wu, B. Fang, Z. Wang, C. Wang, Z. Liu, F. Liu, W. Wang, A. Alfantazi, D. Wang, D.P. Wilkinson, MoS2 nanosheets: A designed structure with high active site density for the hydrogen evolution reaction, ACS Catal. 3 (2013) 2101–2107, https://doi.org/10.1021/CS400384H.
[221] D. Lembke, A. Kis, Breakdown of high-performance monolayer MoS2 transistors, ACS Nano 6 (2012) 10070–10075, https://doi.org/10.1021/NN303772B.
[222] F.A. Frame, F.E. Osterloh, CdSe-MoS2: A quantum size-confined photocatalyst for hydrogen evolution from water under visible light, J. Phys. Chem. C 114 (2010) 10628–10633, https://doi.org/10.1021/JP101308E.
[223] Lithium storage performance in ordered mesoporous MoS2 electrode material, Elsevier. (n.d.). https://www.sciencedirect.com/science/article/pii/S1387181111004707 (accessed January 17, 2023).
[224] Y. Shi, W. Zhou, A.Y. Lu, W. Fang, Y.H. Lee, A.L. Hsu, S.M. Kim, K.K. Kim, H. Y. Yang, L.J. Li, J.C. Idrobo, J. Kong, Van der Waals epitaxy of MoS 2 layers using graphene as growth templates, Nano Lett. 12 (2012) 2784–2791, https://doi.org/10.1021/NL204562J.
[225] F.K. Perkins, A.L. Friedman, E. Cobas, P.M. Campbell, G.G. Jernigan, B.T. Jonker, Chemical vapor sensing with monolayer MoS2, Nano Lett. 13 (2013) 668–673, https://doi.org/10.1021/NL3043079.
[226] D.J. Late, Y.K. Huang, B. Liu, J. Acharya, S.N. Shirodkar, J. Luo, A. Yan, D. Charles, U.V. Waghmare, V.P. Dravid, C.N.R. Rao, Sensing behavior of atomically thin-layered MoS2 transistors, ACS Nano 7 (2013) 4879–4891, https://doi.org/10.1021/NN400026U.
[227] Gate-tunable memristive phenomena mediated by grain boundaries in single-layer MoS2, Nature.Com. (n.d.). https://www.nature.com/articles/nnano.2015.56 (accessed January 17, 2023).
[228] S. Bairagi, Shahid-ul-Islam, M. Shahadat, D.M. Mulvihill, W. Ali, Mechanical energy harvesting and self-powered electronic applications of textile-based piezoelectric nanogenerators: a systematic review, Nano Energy 111 (2023) 108414.
[229] N. Sezer, M.K.-N. Energy, undefined 2021, A comprehensive review on the state-of-the-art of piezoelectric energy harvesting, Elsevier. (n.d.). https://www.sciencedirect.com/science/article/pii/S2211285520311411 (accessed November 25, 2022).
[230] R. Bagherzadeh, S. Abrishami, … A.S.-M.T., undefined 2022, Wearable and flexible electrodes in nanogenerators for energy harvesting, tactile sensors, and electronic textiles: Novel materials, recent advances, and, Elsevier. (n.d.). https://www.sciencedirect.com/science/article/pii/S2589234722001257?casa_token=TElUPpezMlcAAAAA:WJzMzXIAhsc0ZN-g-L3YPWW1OJXACUh7yQdF-GEy6oE4LD5B511evwx6UFVKAKQJhmRb3EL_AQ (accessed November 25, 2023).
[231] W. Wu, L. Wang, Y. Li, F. Zhang, L. Lin, S. Niu, D. Chenet, X. Zhang, Y. Hao, T. F. Heinz, J. Hone, Z.L. Wang, Piezoelectricity of single-atomic-layer MoS2 for energy conversion and piezotronics, Nature 514 (2014) 470–474, https://doi.org/10.1038/nature13792.
[232] A. Piasecki M. Kotkowiak F. Ilie A.-C. Cristescu A study on the tribological behavior of molybdenum disulfide particles as additives Mdpi. ComF Ilie, AC CristescuCoatings 2022•mdpi.Com. (2022). 10.3390/coatings12091244.
[233] Y. Wu, S. Kuang, H. Li, H. Wang, R. Yang, Y. Zhai, G. Zhu, Z. Lin Wang, Y. Wu, Y. Zhai, S. Kuang, H. Li, H. Wang, G. Zhu, Z.L. Wang, R. Yang, Triboelectric–thermoelectric hybrid nanogenerator for harvesting energy from ambient environments, Wiley Online Library 3 (2018), https://doi.org/10.1002/admt.201800166.
[234] Ashraf Forsberg Mattsson Thungström Thermoelectric Properties of n-Type Molybdenum Disulfide (MoS2) Thin Film by Using a Simple Measurement Method Materials 12 21 3521.
[235] S.P. Muduli, S. Veeralingam, S. Badhulika, Interface induced high-performance piezoelectric nanogenerator based on a electrospun three-phase composite nanofiber for wearable applications, ACS Appl Energy Mater. 4 (2021) 12593–12603, https://doi.org/10.1021/ACSAEM.1C02371.
[236] M.N. Islam, R.H. Rupom, P.R. Adhikari, Z. Demchuk, I. Popov, A.P. Sokolov, H. F. Wu, R.C. Advincula, N. Dahotre, Y. Jiang, W. Choi, Boosting piezoelectricity by 3d printing pvdf-mos 2 composite as a conformal and high-sensitivity piezoelectric sensor, Adv Funct Mater. 33 (42) (2023), https://doi.org/10.1002/adfm.202302946.
[237] C. Sharma, A.K. Srivastava, M.K. Gupta, Unusual nanoscale piezoelectricity-driven high current generation from a self S-defect-neutralised few-layered MoS 2 nanosheet-based flexible nanogenerator, Nanoscale 14 (2022) 12885–12897, https://doi.org/10.1039/D2NR02347D.
[238] D. Bhattacharya, S. Bayan, R.K. Mitra, S.K. Ray, Flexible biomechanical energy harvesters with colossal piezoelectric output (~2.07 V/kPa) based on transition metal dichalcogenides-poly(vinylidene fluoride) nanocomposites, ACS Appl Electron Mater. 2 (2020) 3327–3335, https://doi.org/10.1021/acsaelm.0c00632.
[239] C. Zhang, W. Fan, S. Wang, Q. Wang, Y. Zhang, K. Dong, Recent progress of wearable piezoelectric nanogenerators, ACS Appl Electron Mater. 3 (2021) 2449–2467, https://doi.org/10.1021/ACSAELM.1C00165.
[240] H. Zhu, Y. Wang, J. Xiao, M. Liu, S. Xiong, Z.J. Wong, Z. Ye, Y. Ye, X. Yin, X. Zhang, Observation of piezoelectricity in free-standing monolayer MoS2, Nat Nanotechnol. 10 (2015) 151–155, https://doi.org/10.1038/NNANO.2014.309.
[241] J.H. Kang, D.K. Jeong, S.W. Ryu, Transparent, flexible piezoelectric nanogenerator based on gan membrane using electrochemical lift-off, ACS Appl Mater Interfaces. 9 (2017) 10637–10642, https://doi.org/10.1021/ACSAMI.6B15587.
[242] M. Ghosh, S. Ghosh, M. Seibt, K.Y. Rao, P. Peretzki, G. Mohan Rao, Ferroelectric origin in one-dimensional undoped ZnO towards high electromechanical response, CrstEngComm 18 (2016) 622–630, https://doi.org/10.1039/C5CE02262B.
[243] S.H. Shin, S.Y. Choi, M.H. Lee, J. Nah, High-performance piezoelectric nanogenerators via imprinted sol-gel batio3 nanopillar array, ACS Appl Mater Interfaces. 9 (2017) 41099–41103, https://doi.org/10.1021/ACSAMI.7B11773.
[244] S. Liu, D. Zou, X. Yu, Z. Wang, Z. Yang, Transfer-free pzt thin films for flexible nanogenerators derived from a single-step modified sol-gel process on 2d mica, ACS Appl Mater Interfaces. 12 (2020) 54991–54999, https://doi.org/10.1021/ACSAMI.0C16973.
[245] P. Manchi, S.A. Graham, B. Dudem, H. Patnam, J.S. Yu, Improved performance of nanogenerator via synergetic piezo/triboelectric effects of lithium niobate microparticles embedded composite films, Compos Sci Technol. 201 (2021), 108540, https://doi.org/10.1016/j.compscitech.2020.108540.
[246] L. Jin, L. Li, Quantum simulation of ZnO nanowire piezotronics, Nano Energy 15 (2015) 776–781, https://doi.org/10.1016/j.nanoen.2015.06.002.
[247] C. Pan, J. Zhai, Z.L. Wang, Piezotronics and piezo-phototronics of third generation semiconductor nanowires, Chem Rev. 119 (2019) 9303–9359, https://doi.org/10.1021/ACS.CHEMREV.8B00599.
[248] W. Ouyang Department of Materials Science, Fudan University 1 , Shanghai 200433, People's Republic of China MOE Key Laboratory of Materials Physics and Chemistry under Extraordinary Conditions and Shaanxi Key Laboratory of Condensed Matter Structures and Properties, School of Physical Science and Technology, Northwestern Polytechnical University 2 , Xi'an 710072, People's Republic of China J. Chen Department of Materials Science, Fudan University 1 ,

Shanghai 200433, People's Republic of China Z. Shi Key Laboratory of Materials Physics of Ministry of Education, School of Physics and Microelectronics, Zhengzhou University 3 , Zhengzhou 450052, People's Republic of China X. Fang Department of Materials Science, Fudan University 1 , Shanghai 200433, People's Republic of China Self-powered UV photodetectors based on ZnO nanomaterials Appl Phys Rev. 8 3 2021 2021 031315 10.1063/5.0058482.

[249] K.Z. Milowska, J.A. Majewski, Graphene-based sensors: theoretical study, J. Phys. Chem. C 118 (2014) 17395–17401, https://doi.org/10.1021/JP504199R.

[250] S. Yu K. Eshun H. Zhu Q. Li Novel Two-Dimensional Mechano-Electric Generators and Sensors Based on Transition Metal Dichalcogenides Sci Rep 5 1.

[251] P. Cui, J. Wang, J. Xiong, S. Li, W. Zhang, X. Liu, G. Gu, J. Guo, B. Zhang, G. Cheng, Z. Du, Meter-scale fabrication of water-driven triboelectric nanogenerator based on in-situ grown layered double hydroxides through a bottom-up approach, Nano Energy 71 (2020), 104646, https://doi.org/10.1016/j.nanoen.2020.104646.

[252] S. Imani Yengejeh, W. Wen, Y. Wang, Mechanical properties of lateral transition metal dichalcogenide heterostructures, Front Phys (beijing) 16 (2021) 1–7, https://doi.org/10.1007/S11467-020-1001-5/METRICS.

[253] K. Xu, Y. Wang, Y. Zhao, Y. Chai, Modulation doping of transition metal dichalcogenide/oxide heterostructures, J Mater Chem C Mater. 5 (2017) 376–381, https://doi.org/10.1039/C6TC04640A.

[254] P. Hess, Bonding, structure, and mechanical stability of 2D materials: the predictive power of the periodic table, Nanoscale Horiz. 6 (2021) 856–892, https://doi.org/10.1039/D1NH00113B.

[255] K.A.N. Duerloo, M.T. Ong, E.J. Reed, Intrinsic piezoelectricity in two-dimensional materials, J. Phys. Chem. Lett. 3 (2012) 2871–2876, https://doi.org/10.1021/JZ3012436.

[256] L. Xu, L. Zhao, Y. Wang, M. Zou, Q. Zhang, A. Cao, Analysis of photoluminescence behavior of high-quality single-layer MoS2, Nano Res. 12 (2019) 1619–1624, https://doi.org/10.1007/s12274-019-2401-0.

[257] S. Imani Yengejeh, J. Liu, S.A. Kazemi, W. Wen, Y. Wang, Effect of Structural Phases on Mechanical Properties of Molybdenum Disulfide, ACS, Omega 5 (2020) 5994–6002, https://doi.org/10.1021/ACSOMEGA.9B04360.

[258] Y. Huang Jiangsu Key Laboratory for Design and Manufacture of Micro-Nano Biomedical Instruments, School of Mechanical Engineering, Southeast University , Nanjing 211189, People's Republic of China L. Liu Jiangsu Key Laboratory for Design and Manufacture of Micro-Nano Biomedical Instruments, School of Mechanical Engineering, Southeast University , Nanjing 211189, People's Republic of China J. Sha Jiangsu Key Laboratory for Design and Manufacture of Micro-Nano Biomedical Instruments, School of Mechanical Engineering, Southeast University , Nanjing 211189, People's Republic of China Y. Chen Jiangsu Key Laboratory for Design and Manufacture of Micro-Nano Biomedical Instruments, School of Mechanical Engineering, Southeast University , Nanjing 211189, People's Republic of China Size-dependent piezoelectricity of molybdenum disulfide (MoS2) films obtained by atomic layer deposition (ALD) Appl Phys Lett. 111 6 2017 2017 10.1063/1.4998447.

[259] K. Maity, B. Mahanty, T.K. Sinha, S. Garain, A. Biswas, S.K. Ghosh, S. Manna, S. K. Ray, D. Mandal, Two-Dimensional Piezoelectric MoS2-Modulated Nanogenerator and Nanosensor Made of Poly(vinlydine Fluoride) Nanofiber Webs for Self-Powered Electronics and Robotics, Energy, Technology 5 (2017) 234–243, https://doi.org/10.1002/ENTE.201600419.

[260] S.A. Han, T.H. Kim, S.K. Kim, K.H. Lee, H.J. Park, J.H. Lee, S.W. Kim, Point-Defect-Passivated MoS2 Nanosheet-Based High Performance Piezoelectric Nanogenerator, Adv. Mater. 30 (2018), https://doi.org/10.1002/ADMA.201800342.

[261] B. Bagchi, N.A. Hoque, N. Janowicz, S. Das, M.K. Tiwari, Re-usable self-poled piezoelectric/piezocatalytic films with exceptional energy harvesting and water remediation capability, Nano Energy 78 (2020) 105339.

[262] J. Arunguvai, P. Lakshmi, Influence of ZrO2 and TiO2 nano particles in P(VDF-TrFE) composite for energy harvesting application, J. Mater. Sci. Mater. Electron. 32 (2021) 12223–12231, https://doi.org/10.1007/S10854-021-05851-4.

[263] P. Sahatiya, S. Kannan, S. Badhulika, Few layer MoS2 and in situ poled PVDF nanofibers on low cost paper substrate as high performance piezo-triboelectric hybrid nanogenerator: Energy harvesting from handwriting and human touch, Appl Mater Today. 13 (2018) 91–99, https://doi.org/10.1016/j.apmt.2018.08.009.

[264] M. Xu, T. Wu, Y. Song, M. Jiang, Z. Shi, C. Xiong, Q. Yang, Achieving high-performance energy harvesting and self-powered sensing in a flexible cellulose nanofibril/MoS 2 /BaTiO 3 composite piezoelectric nanogenerator, J Mater Chem C Mater. 9 (2021) 15552–15565, https://doi.org/10.1039/D1TC03886A.

[265] M. Faraz, H.H. Singh, N. Khare, A progressive strategy for harvesting mechanical energy using flexible PVDF-rGO-MoS2 nanocomposites film-based piezoelectric nanogenerator, J Alloys Compd. 890 (2022), 161840, https://doi.org/10.1016/j.jallcom.2021.161840.

[266] S. Cao, H. Zou, B. Jiang, M. Li, Q. Yuan, Incorporation of ZnO encapsulated MoS2 to fabricate flexible piezoelectric nanogenerator and sensor, Nano Energy 102 (2022) 107635.

[267] D. Zhang, Z. Yang, P. Li, M. Pang, Q. Xue, Flexible self-powered high-performance ammonia sensor based on Au-decorated MoSe2 nanoflowers driven by single layer MoS2-flake piezoelectric nanogenerator, Nano Energy 65 (2019) 103974.

[268] Y. Liu, H. Khanbareh, M.A. Halim, A. Feeney, X. Zhang, H. Heidari, R. Ghannam, Piezoelectric energy harvesting for self-powered wearable upper limb applications, Nano Select. 2 (2021) 1459–1479, https://doi.org/10.1002/NANO.202000242.

[269] J. Arunguvai, P. Lakshmi, Flexible piezoelectric mos2/p(vdf-trfe) nanocomposite film for vibration energy harvesting, J Electron Mater. 50 (2021) 6870–6880, https://doi.org/10.1007/S11664-021-09204-Z/TABLES/4.

[270] S. Chen, J. Li, Y. Song, Q. Yang, Z. Shi, C. Xiong, Flexible and environment-friendly regenerated cellulose/MoS2 nanosheet nanogenerators with high piezoelectricity and output performance, Cellul. 28 (2021) 6513–6522, https://doi.org/10.1007/s10570-021-03962-z.

[271] D. Enescu, Thermoelectric energy harvesting: basic principles and applications, in: D. Enescu (Ed.), Green Energy Advances, IntechOpen, 2019.

[272] A. Nozariasbmarz, H. Collins, K. Dsouza, M.H. Polash, M. Hosseini, M. Hyland, J. Liu, A. Malhotra, F.M. Ortiz, F. Mohaddes, V.P. Ramesh, Y. Sargolzaeiaval, N. Snouwaert, M.C. Özturk, D. Vashaee, Review of wearable thermoelectric energy harvesting: from body temperature to electronic systems, Appl Energy. 258 (2020), 114069, https://doi.org/10.1016/j.apenergy.2019.114069.

[273] M. Otsuka, H. Terakado, R. Homma, al -, J. Lim, J. Hyeok Choi, G. Lim, Technical feasibility evaluation on the use of a Peltier thermoelectric module to recover automobile exhaust heat, Iopscience.Iop.Org. 953 (2018) 12090. https://doi.org/10.1088/1742-6596/953/1/012090.

[274] M. He, Y.-J. Lin, C.-M. Chiu, W. Yang, B. Zhang, D. Yun, Y. Xie, Z.-H. Lin, A flexible photo-thermoelectric nanogenerator based on mos2/pu photothermal layer for infrared light harvesting minghui, Nano Energy 49 (2018) 588–595.

[275] M. Buscema, M. Barkelid, V. Zwiller, H.S.J. Van Der Zant, G.A. Steele, A. Castellanos-Gomez, Large and tunable photothermoelectric effect in single-layer MoS 2, Nano Lett. 13 (2013) 358–363, https://doi.org/10.1021/nl303321g.

[276] J. Wu, H. Schmidt, K.K. Amara, X. Xu, G. Eda, B. Özyilmaz, Large thermoelectricity via variable range hopping in chemical vapor deposition grown single-layer MoS2, Nano Lett. 14 (2014) 2730–2734, https://doi.org/10.1021/nl500666m.

[277] S. Kim, C. Lee, Y.S. Lim, J.H. Shim, Investigation for thermoelectric properties of the mos2monolayer-graphene heterostructure: density functional theory calculations and electrical transport measurements, ACS Omega 6 (2021) 278–283, https://doi.org/10.1021/acsomega.0c04488.

[278] F.R. Fan, W. Wu, Emerging devices based on two-dimensional monolayer materials for energy harvesting, Research 2019 (2019) 1–16, https://doi.org/10.34133/2019/7367828.

[279] M. Seol, S. Kim, Y. Cho, K.E. Byun, H. Kim, J. Kim, S.K. Kim, S.W. Kim, H.J. Shin, S. Park, Triboelectric Series of 2D Layered Materials, Adv. Mater. 30 (2018), https://doi.org/10.1002/adma.201801210.

[280] G. Xue, Y. Xu, T. Ding, J. Li, J. Yin, W. Fei, Y. Cao, J. Yu, L. Yuan, L. Gong, J. Chen, S. Deng, J. Zhou, W. Guo, Water-evaporation-induced electricity with nanostructured carbon materials, Nat Nanotechnol. 12 (2017) 317–321, https://doi.org/10.1038/nnano.2016.300.

[281] L. Huang, S. Lin, Z. Xu, H. Zhou, J. Duan, B. Hu, J. Zhou, Fiber-based energy conversion devices for human-body energy harvesting, Adv. Mater. 32 (2020) 1902034, https://doi.org/10.1002/adma.201902034.

[282] S. Karmakar, R. Sarkar, C.S. Tiwary, P. Kumbhakar, Synthesis of bilayer MoS2 nanosheets by green chemistry approach and its application in triboelectric and catalytic energy harvesting, J Alloys Compd. 844 (2020), 155690, https://doi.org/10.1016/j.jallcom.2020.155690.

[283] J. Liu, A. Goswami, K. Jiang, F. Khan, S. Kim, R. McGee, Z. Li, Z. Hu, J. Lee, T. Thundat, Direct-current triboelectricity generation by a sliding Schottky nanocontact on MoS2 multilayers, Nat Nanotechnol. 13 (2018) 112–116, https://doi.org/10.1038/s41565-017-0019-5.

[284] S. Park, J. Park, Y.-G. Kim, S. Bae, T.-W. Kim, K.-I. Park, B.H. Hong, C.K. Jeong, S.-K. Lee, Laser-directed synthesis of strain-induced crumpled MoS2 structure for enhanced triboelectrification toward haptic sensors, Nano Energy 78 (2020) 105266.

[285] K. Shrestha, S. Sharma, G.B. Pradhan, T. Bhatta, P. Maharjan, S.S. Rana, S. Lee, S. Seonu, Y. Shin, J.Y. Park, A siloxene/ecoflex nanocomposite-based triboelectric nanogenerator with enhanced charge retention by mos2/lig for self-powered touchless sensor applications, Adv Funct Mater. 32 (2022), https://doi.org/10.1002/adfm.202113005.

[286] S.Y. Kim, S. Jang, K.N. Kim, S. Lee, H. Chang, S. Yim, W. Song, S. Lee, J. Lim, S. Myung, Multilayered mos 2 sphere-based triboelectric–flexoelectric nanogenerators as self-powered mechanical sensors for human motion detection, ACS Appl. Nano Mater. 5 (10) (2022) 15192–15200.

[287] B. Hedau, B.C. Kang, T.J. Ha, Enhanced triboelectric effects of self-poled mos2-embedded pvdf hybrid nanocomposite films for bar-printed wearable triboelectric nanogenerators, ACS Nano 16 (2022) 18355–18365, https://doi.org/10.1021/ACSNANO.2C06257.

[288] S. Tremmel, X. Luo, B. Rothammer, A. Seynstahl, B. Wang, A. Rosenkranz, M. Marian, L. Zhu, Evaluation of DLC, MoS2, and Ti3C2Tx thin films for triboelectric nanogenerators, Nano Energy 97 (2022), 107185, https://doi.org/10.1016/j.nanoen.2022.107185.

[289] K. Zhao, W. Sun, X. Zhang, J. Meng, M. Zhong, L. Qiang, M.-J. Liu, B.-N. Gu, C.-C. Chung, M. Liu, F. Yu, Y.-L. Chueh, High-performance and long-cycle life of triboelectric nanogenerator using PVC/MoS2 composite membranes for wind energy scavenging application, Nano Energy 91 (2022), 106649, https://doi.org/10.1016/j.nanoen.2021.106649.

[290] C. Sun, G. Zu, Y. Wei, X. Song, X. Yang, Flexible triboelectric nanogenerators based on electrospun poly(vinylidene fluoride) with mos2/carbon nanotube composite nanofibers, Langmuir 38 (2022) 1479–1487, https://doi.org/10.1021/acs.langmuir.1c02785.

[291] M. Kim, C.J. Lee, S.H. Kim, M.U. Park, J. Yang, Y. Yi, K.H. Yoo, Tribodiffusion-driven triboelectric nanogenerators based on MoS2, J Mater Chem A Mater. 9 (2021) 10316–10325, https://doi.org/10.1039/d1ta01233a.

[292] C. Wu, T.W. Kim, J.H. Park, H. An, J. Shao, X. Chen, Z.L. Wang, Enhanced triboelectric nanogenerators based on mos2 monolayer nanocomposites acting as electron-acceptor layers, ACS Nano 11 (8) (2017) 8356–8363.
[293] M. Kim, D. Park, M.M. Alam, S. Lee, P. Park, J. Nah, Remarkable output power density enhancement of triboelectric nanogenerators via polarized ferroelectric polymers and bulk mos 2 composites, ACS Nano 13 (2019) 4640–4646, https://doi.org/10.1021/acsnano.9b00750.
[294] V. Singh, D. Meena, H. Sharma, A. Trivedi, B. Singh, Investigating the role of chalcogen atom in the piezoelectric performance of PVDF/TMDCs based flexible nanogenerator, Energy 239 (2022), 122125, https://doi.org/10.1016/j.energy.2021.122125.
[295] S.S. Kwak, S. Lin, J.H. Lee, H. Ryu, T.Y. Kim, H. Zhong, H. Chen, S.W. Kim, Triboelectrification-induced large electric power generation from a single moving droplet on graphene/polytetrafluoroethylene, ACS Nano 10 (2016) 7297–7302, https://doi.org/10.1021/ACSNANO.6B03032.
[296] D. Park, S. Won, K.-S. Kim, J.-Y. Jung, J.-Y. Choi, J. Nah, The influence of substrate-dependent triboelectric charging of graphene on the electric potential generation by the flow of electrolyte droplets, Nano Energy 54 (2018) 66–72, https://doi.org/10.1016/j.nanoen.2018.09.054.
[297] S. Yang, Y. Su, Y. Xu, Q. Wu, Y. Zhang, M.B. Raschke, M. Ren, Y. Chen, J. Wang, W. Guo, Y. Ron Shen, C. Tian, mechanism of electric power generation from ionic droplet motion on polymer supported graphene, J Am Chem Soc. 140 (2018) 13746–13752, https://doi.org/10.1021/JACS.8B07778.
[298] H.J. Li, D. Zhang, H. Wang, Z. Chen, N. Ou, P. Wang, D. Wang, X. Wang, J. Yang, Molecule-driven nanoenergy generator, Small 15 (2019), https://doi.org/10.1002/SMLL.201804146.
[299] A.S. Aji, R. Nishi, H. Ago, Y. Ohno, High output voltage generation of over 5 V from liquid motion on single-layer MoS2, Nano Energy 68 (2020), https://doi.org/10.1016/J.NANOEN.2019.104370.
[300] Y. Yang, Y. Zhou, J.M. Wu, Z.L. Wang, Single micro/nanowire pyroelectric nanogenerators as self-powered temperature sensors, ACS Nano 6 (2012) 8456–8461, https://doi.org/10.1021/NN303414U.
[301] A.J. Minnich, M.S. Dresselhaus, Z.F. Ren, G. Chen, Bulk nanostructured thermoelectric materials: current research and future prospects, Energy Environ Sci. 2 (2009) 466, https://doi.org/10.1039/b822664b.
[302] D.D. Fan Wuhan University 1 Key Laboratory of Artificial Micro- and Nano-Structures of Ministry of Education and School of Physics and Technology, , Wuhan 430072, China H.J. Liu Wuhan University 1 Key Laboratory of Artificial Micro- and Nano-Structures of Ministry of Education and School of Physics and Technology, , Wuhan 430072, China L. Cheng Wuhan University 1 Key Laboratory of Artificial Micro- and Nano-Structures of Ministry of Education and School of Physics and Technology, , Wuhan 430072, China P.H. Jiang Wuhan University 1 Key Laboratory of Artificial Micro- and Nano-Structures of Ministry of Education and School of Physics and Technology, , Wuhan 430072, China J. Shi Wuhan University 1 Key Laboratory of Artificial Micro- and Nano-Structures of Ministry of Education and School of Physics and Technology, , Wuhan 430072, China X.F. Tang Wuhan University of Technology 2 State Key Laboratory of Advanced Technology for Materials Synthesis and Processing, , Wuhan 430070, China MoS2 nanoribbons as promising thermoelectric materials Appl Phys Lett. 105 13 2014 2014 10.1063/1.4897349.
[303] D. Wickramaratne University of California 1 Department of Electrical Engineering, , Riverside, California 92521-0204, USA F. Zahid The University of Hong Kong 2 Department of Physics and the Center of Theoretical and Computational Physics, , Pokfulam Road, Hong Kong SAR, China R.K. Lake University of California 1 Department of Electrical Engineering, , Riverside, California 92521-0204, USA Electronic and thermoelectric properties of few-layer transition metal dichalcogenides Journal of Chemical Physics. 140 12 2014 2014 10.1063/1.4869142.
[304] Y. Xu, Z. Li, W. Duan, Thermal and thermoelectric properties of graphene, Small 10 (2014) 2182–2199, https://doi.org/10.1002/SMLL.201303701.
[305] P. Dollfus, V.H. Nguyen, J. Saint-Martin, Thermoelectric effects in graphene nanostructures, Iopscience.Iop.Org. (n.d.). https://iopscience.iop.org/article/10.1088/0953-8984/27/13/133204/meta (accessed January 18, 2023).
[306] M.S. Dresselhaus, G. Chen, M.Y. Tang, R. Yang, H. Lee, D. Wang, Z. Ren, J. P. Fleurial, P. Gogna, New directions for low-dimensional thermoelectric materials, Adv. Mater. 19 (2007) 1043–1053, https://doi.org/10.1002/ADMA.200600527.
[307] Y. Yang, W. Guo, K.C. Pradel, G. Zhu, Y. Zhou, Y. Zhang, Y. Hu, L. Lin, Z.L. Wang, Pyroelectric nanogenerators for harvesting thermoelectric energy, Nano Lett. 12 (2012) 2833–2838, https://doi.org/10.1021/NL3003039.
[308] A. Ahangar, M. Hedayati, M. Maleki, … H.G.-R., undefined 2023, A hydrophilic carbon foam/molybdenum disulfide composite as a self-floating solar evaporator, Pubs.Rsc.Org. (n.d.). https://pubs.rsc.org/en/content/articlehtml/2023/ra/d2ra07810d (accessed November 25, 2023).
[309] A. Gautam, M. Faraz, N.K.-J. of A. and Compounds, undefined 2020, Enhanced thermoelectric properties of MoS2 with the incorporation of reduced graphene oxide (RGO), Elsevier. (n.d.). https://www.sciencedirect.com/science/article/pii/S0925838820320375?casa_token=MK6SXNV81pMAAAAA:8ErZwgSmZFPgCeJ4AXMNTFoL1OFTDE_shJu2BmDU6BsufWJ3uRd63IdW9y95jVXkjnVc1DQ9YA (accessed November 25, 2023).
[310] S.S. Chou, B. Kaehr, J. Kim, B.M. Foley, M. De, P.E. Hopkins, J. Huang, C. J. Brinker, V.P. Dravid, Chemically exfoliated MoS2 as near-infrared photothermal agents, Angewandte Chemie - International Edition. 52 (2013) 4160–4164, https://doi.org/10.1002/ANIE.201209229.
[311] L. Cheng, J. Liu, X. Gu, H. Gong, X. Shi, T. Liu, C. Wang, X. Wang, G. Liu, H. Xing, W. Bu, B. Sun, Z. Liu, PEGylated WS2 nanosheets as a multifunctional theranostic agent for in vivo dual-modal CT/photoacoustic imaging guided photothermal therapy, Adv. Mater. 26 (2014) 1886–1893, https://doi.org/10.1002/ADMA.201304497.
[312] X. Li, H. Zhu, Two-dimensional MoS2: properties, preparation, and applications, J. Materiomics 1 (2015) 33–44, https://doi.org/10.1016/j.jmat.2015.03.003.
[313] M. Hassan, G. Abbas, N. Li, A. Afzal, Z. Haider, S. Ahmed, X. Xu, C. Pan, Z. Peng, Significance of flexible substrates for wearable and implantable devices: recent advances and perspectives, Adv Mater Technol. 7 (2022), https://doi.org/10.1002/ADMT.202100773.
[314] Y. Wang, T. Li, Y. Li, R. Yang, G. Zhang, 2D-materials-based wearable biosensor systems, Biosensors (basel). 12 (2022) 1–19, https://doi.org/10.3390/bios12110936.
[315] S.S. Nardekar, K. Krishnamoorthy, P. Pazhamalai, S. Sahoo, S. Jae Kim, MoS2 quantum sheets-PVDF nanocomposite film based self-poled piezoelectric nanogenerators and photovoltaically self-charging power cell, Nano Energy 93 (2022), 106869, https://doi.org/10.1016/j.nanoen.2021.106869.
[316] M.A. Lukowski, A.S. Daniel, F. Meng, A. Forticaux, L. Li, S. Jin, Enhanced hydrogen evolution catalysis from chemically exfoliated metallic MoS2 nanosheets, J Am Chem Soc. 135 (2013) 10274–10277, https://doi.org/10.1021/JA404523S.
[317] J.M. Evans, K.S. Lee, E.X. Yan, A.C. Thompson, M.B. Morla, M.C. Meier, Z. P. Ifkovits, A.I. Carim, N.S. Lewis, Demonstration of a sensitive and stable chemical gas sensor based on covalently functionalized mos2, ACS Mater Lett. 4 (2022) 1475–1480, https://doi.org/10.1021/ACSMATERIALSLETT.2C00372.
[318] C. Roxlo, Optical absorption and catalytic activity of molybdenum sulfide edge surfaces, J Catal. 100 (1986) 176–184, https://doi.org/10.1016/0021-9517(86)90083-7.
[319] M. Daage, R.R. Chianelli, Structure-function relations in molybdenum sulfide catalysts: the "rim-edge" model, J Catal. 149 (1994) 414–427, https://doi.org/10.1006/jcat.1994.1308.
[320] H. Yang, C. Fairbridge, Z. Ring, Adsorption of dibenzothiophene derivatives over a mos 2 nanoclustera density functional theory study of structure−reactivity relations, Energy Fuel 17 (2003) 387–398, https://doi.org/10.1021/ef020171k.
[321] J. V. Lauritsen, M. Nyberg, R.T. Vang, M. V. Bollinger, B.S. Clausen, H. Topsøe, K. W. Jacobsen, E. Lægsgaard, J.K. Nørskov, F. Besenbacher, Chemistry of one-dimensional metallic edge states in MoS2 nanoclusters, Nanotechnology. 14 (2003) 385. https://doi.org/10.1088/0957-4484/14/3/306.
[322] M. Mahdavi, S. Kimiagar, F. Abrinaei, Preparation of few-layered wide bandgap MoS2 with nanometer lateral dimensions by applying laser irradiation, Crystals (basel). 10 (3) (2020) 164.
[323] M. Zhang, R.C.T. Howe, R.I. Woodward, E.J.R. Kelleher, F. Torrisi, G. Hu, S. V. Popov, J.R. Taylor, T. Hasan, Solution processed MoS2-PVA composite for sub-bandgap mode-locking of a wideband tunable ultrafast Er:fiber laser, Nano Res. 8 (2015) 1522–1534, https://doi.org/10.1007/s12274-014-0637-2.
[324] E. Singh, P. Singh, K.S. Kim, G.Y. Yeom, H.S. Nalwa, Flexible molybdenum disulfide (mos 2) atomic layers for wearable electronics and optoelectronics, ACS Appl Mater Interfaces. 11 (2019) 11061–11105, https://doi.org/10.1021/ACSAMI.8B19859.
[325] M. Shrivastava, R. Kumari, M. Parra, P.P.-O. Materials, undefined 2017, Electrochemical synthesis of MoS2 quantum dots embedded nanostructured porous silicon with enhanced electroluminescence property, Elsevier. (n.d.). https://www.sciencedirect.com/science/article/pii/S0925346717305906?casa_token=h-0eYEPM6zoAAAAA:2ZqzkRFdpkPNvYQMb7IxQQQUtrD7n7mPpurzwmpXTjNuZgeNu2ZPPClbB6AQf9JAHYnQIOt3XQ (accessed November 25, 2023).
[326] H.J. Conley, B. Wang, J.I. Ziegler, R.F. Haglund, S.T. Pantelides, K.I. Bolotin, Bandgap engineering of strained monolayer and bilayer MoS2, Nano Lett. 13 (8) (2013) 3626–3630.
[327] T. Cheiwchanchamnangij, W.R.L. Lambrecht, Y. Song, H. Dery, Strain effects on the spin-orbit-induced band structure splittings in monolayer MoS <math display="inline"> <msub> <mrow/> <mn>2</mn> </msub> </math> and graphene, Phys Rev b. 88 (2013), 155404, https://doi.org/10.1103/PhysRevB.88.155404.
[328] N. Masurkar, N. Thangavel, … S.Y.-B. and, undefined 2021, Reliable and highly sensitive biosensor from suspended MoS2 atomic layer on nano-gap electrodes, Elsevier. (n.d.). https://www.sciencedirect.com/science/article/pii/S0956566320307120?casa_token=LDJJ8YXuSHgAAAAA:iwmG0dvKU3tMiAuSp2C-TRdX3z0_UAeNxiXUno988sksUPb0bX3m0-3fDck5wTf7KNlNFlO8tA (accessed November 25, 2023).
[329] M. Pourmadadi, A. Tajiki, S. Hosseini, … A.S.-J. of D.D., undefined 2022, A comprehensive review of synthesis, structure, properties, and functionalization of MoS2; emphasis on drug delivery, photothermal therapy, and tissue, Elsevier. (n.d.). https://www.sciencedirect.com/science/article/pii/S1773224722006785?casa_token=t1p0mNBXVMMAAAAA:tyL4QLnoE-9zB8jYws-j2IrOB7II1ZNTZiGkaGgjE6MmdGI5EDpvqFteeXV_0WGqPqO1Zfor6A (accessed November 27, 2023).
[330] X. Chen Y.J. Park M. Kang S.-K. Kang J. Koo S.M. Shinde J. Shin S. Jeon G. Park Y. Yan M.R. MacEwan W.Z. Ray K.-M. Lee J.A. Rogers J.-H. Ahn CVD-grown monolayer MoS2 in bioabsorbable electronics and biosensors Nat Commun 9 1.
[331] Z. Sobanska, L. Zapor, M. Szparaga, M. Stepnik, Biological effects of molybdenum compounds in nanosized forms under *in vitro* and *in vivo* conditions, Int J Occup Med Environ Health. 33 (2020) 1–19, https://doi.org/10.13075/ijomeh.1896.01411.

[332] S. Catalán-Gómez, M. Briones, S. Cortijo-Campos, T. García-Mendiola, A. de Andrés, S. Garg, P. Kung, E. Lorenzo, J.L. Pau, A. Redondo-Cubero, Breast cancer biomarker detection through the photoluminescence of epitaxial monolayer MoS2 flakes, Sci Rep. 10 (2020) 16039, https://doi.org/10.1038/s41598-020-73029-9.
[333] Y. Huang, Y. Shi, H.Y. Yang, Y. Ai, A novel single-layered MoS2 nanosheet based microfluidic biosensor for ultrasensitive detection of DNA, Nanoscale 7 (2015) 2245–2249, https://doi.org/10.1039/C4NR07162J.
[334] A. Barati Farimani, M. Heiranian, N.R. Aluru, Identification of amino acids with sensitive nanoporous MoS2: towards machine learning-based prediction, NPJ 2D Mater Appl. 2 (2018) 14, https://doi.org/10.1038/s41699-018-0060-8.
[335] C. Zheng, X. Jin, Y. Li, J. Mei, Y. Sun, M. Xiao, H. Zhang, Z. Zhang, G.J. Zhang, Sensitive molybdenum disulfide based field effect transistor sensor for real-time monitoring of hydrogen peroxide, Sci Rep. 9 (2019), https://doi.org/10.1038/S41598-018-36752-Y.
[336] E.E. Benson, H. Zhang, S.A. Schuman, S.U. Nanayakkara, N.D. Bronstein, S. Ferrere, J.L. Blackburn, E.M. Miller, Balancing the hydrogen evolution reaction, surface energetics, and stability of metallic mos2 nanosheets via covalent functionalization, J Am Chem Soc. 140 (2018) 441–450, https://doi.org/10.1021/JACS.7B11242.
[337] H. Wang, C. Li, P. Fang, Z. Zhang, J.Z. Zhang, Synthesis, properties, and optoelectronic applications of two-dimensional MoS 2 and MoS 2 -based heterostructures, Chem Soc Rev. 47 (2018) 6101–6127, https://doi.org/10.1039/C8CS00314A.
[338] Y. Arora, A.P. Shah, S. Battu, C.B. Maliakkal, S. Haram, A. Bhattacharya, D. Khushalani, Nanostructured MoS2/BiVO4 composites for energy storage applications, Sci Rep. 6 (2016) 36294, https://doi.org/10.1038/srep36294.
[339] O. Samy, A. El Moutaouakil, K. Mutta, S.J. Ray, A review on mos2 energy applications: recent developments and challenges, Mdpi. Com. (2021), https://doi.org/10.3390/en14154586.
[340] A. Stroud, P.A. Derosa, G. Leuty, C. Muratore, R. Berry, C. Muratory, Effects of impurities and lattice imperfections on the conductive properties of MoS2, in, in: 2015 IEEE 15th International Conference on Nanotechnology (IEEE-NANO), IEEE, 2015, pp. 613–616, https://doi.org/10.1109/NANO.2015.7388679.
[341] P. Kumar, J.P. Horwath, A.C. Foucher, C.C. Price, N. Acero, V.B. Shenoy, E. A. Stach, D. Jariwala, Direct visualization of out-of-equilibrium structural transformations in atomically thin chalcogenides, NPJ 2D Mater Appl. 4 (2020) 16, https://doi.org/10.1038/s41699-020-0150-2.
[342] K. Kang, S. Xie, L. Huang, Y. Han, P. Huang, K.M.- Nature, undefined 2015, High-mobility three-atom-thick semiconducting films with wafer-scale homogeneity, Nature.ComK Kang, S Xie, L Huang, Y Han, PY Huang, KF Mak, CJ Kim, D Muller, J ParkNature, 2015•nature.Com. (n.d.). https://idp.nature.com/authorize/casa?redirect_uri=https://www.nature.com/articles/nature14417&casa_token=X38Ra9GzGZ8AAAAA:sdClXkmEoC1VFoADF4X0O7FBZa2j5MAA8Gbu4ubaKWRNaxO0WRtisf9_lKCPbcTDU4c6N_6doBOT0PWvzQ (accessed November 25, 2023).
[343] A. Sohn, C. Kim, J.H. Jung, J.H. Kim, K.E. Byun, Y. Cho, P. Zhao, S.W. Kim, M. Seol, Z. Lee, S.W. Kim, H.J. Shin, Precise layer control and electronic state modulation of a transition metal dichalcogenide via phase-transition-induced growth, Adv. Mater. 34 (2022), https://doi.org/10.1002/ADMA.202103286.
[344] S. Kumar, A. Sharma, V. Gupta, M. Tomar, Development of novel MoS2 hydrovoltaic nanogenerators for electricity generation from moving NaCl droplet, J Alloys Compd. 884 (2021), 161058, https://doi.org/10.1016/j.jallcom.2021.161058.
[345] E. Delgado-Alvarado, E.A. Elvira-Hernández, J. Hernández-Hernández, J. Huerta-Chua, H. Vázquez-Leal, J. Martínez-Castillo, P.J. García-Ramírez, A.L. Herrera-May, Recent progress of nanogenerators for green energy harvesting: performance, Applications, and Challenges, Nanomaterials. 12 (2022) 2549, https://doi.org/10.3390/nano12152549.